The Geological Society of America
Field Guide 55

A river is born: Highlights of the geologic evolution of the Colorado River extensional corridor and its river: A field guide honoring the life and legacy of Warren Hamilton

Keith A. Howard*
U.S. Geological Survey, Geology, Minerals, Energy, and Geophysics Science Center, Menlo Park, California 94025, USA

P. Kyle House*
U.S. Geological Survey, Geology, Minerals, Energy, and Geophysics Science Center, Flagstaff, Arizona 86001, USA

Barbara E. John*
Department of Geology & Geophysics, University of Wyoming, Laramie, Wyoming 82071, USA

Ryan S. Crow*
U.S. Geological Survey, Geology, Minerals, Energy, and Geophysics Science Center, Flagstaff, Arizona 86001, USA

Philip A. Pearthree*
Arizona Geological Survey, University of Arizona, Tucson, Arizona 85701, USA

ABSTRACT

The Colorado River extensional corridor, which stretched by a factor of 2 in the Miocene, left a series of lowland basins and intervening bedrock ranges that, at the dawn of the Pliocene, were flooded by Colorado River water newly diverted from the Colorado Plateau through Grand Canyon. This water and subsequent sediment gave birth, through a series of overflowing lakes, to an integrated Colorado River flowing to the newly opened Gulf of California. Topock Gorge, which the river now follows between the Chemehuevi and Mohave Mountains, is a major focus of this field guide, as it very nicely exposes structural, stratigraphic, and magmatic aspects of the Miocene extensional corridor, a core complex, and detachment faults as well as a pre-Cenozoic batholith. Topock Gorge also is the inferred site of a paleodivide between early Pliocene basins of newly arrived Colorado River water. Overspilling of its upstream lake breached the divide and led the river southward. The Bouse Formation in this and other basins records the pre–river integration water bodies. Younger riverlaid deposits including the Bullhead Alluvium (Pliocene) and the Chemehuevi Formation (Pleistocene) record subsequent evolution of the Colorado River through a succession of aggradational and re-incision stages. Their stratigraphic record

*khoward@usgs.gov, khouse@usgs.gov, bjohn@uwyo.edu, rcrow@usgs.gov, pearthre@email.arizona.edu

Howard, K.A., House, P.K., John, B.E., Crow, R.S., and Pearthree, P.A., 2019, A river is born: Highlights of the geologic evolution of the Colorado River extensional corridor and its river: A field guide honoring the life and legacy of Warren Hamilton, *in* Pearthree, P.A., ed., Geologic Excursions in Southwestern North America: Geological Society of America Field Guide 55, p. 61–113, https://doi.org/10.1130/2019.0055(03).

provides evidence of local basin deepening after river inception, but little deformation on a regional scale of the river valley in the last 4 m.y. except in the Lake Mead area. There, faults interrupt both the paleoriver grade and incision rates, and are interpreted to record 100's of m of true uplift of the Colorado Plateau. Warren Hamilton's insightful work beginning in the 1950s helped set the stage for interpretation of Mesozoic orogeny and Cenozoic extension in this region, as well as the record of the Bouse Formation.

INTRODUCTION

This field guide explores scenery and geology along and near the lower Colorado River between Laughlin, Nevada, and Blythe, California (Fig. 1). Sites along this reach document critical stages in the structural evolution of the Miocene Colorado River extensional corridor (CREC) and the later inception and 5-m.y. evolution of the lower Colorado River. This guide addresses bedrock and structural geology, fluvial stratigraphy, and geomorphology. It explores metamorphic core complexes and progressive extension as revealed by intrusions and by deposits from eruptions and rock avalanches. It also reveals a record of overspilling lakes and deltas giving birth to a continental-scale river, that river's subsequent evolution through aggradational and downcutting cycles, and the role of fluvial history in assessing Colorado Plateau uplift. This report celebrates the life of Warren Hamilton (1925–2018) and his enormous contributions to Earth science, including his discoveries and insights in the lower Colorado River region.

The present guide makes extensive use of earlier geologic guides and maps of this region, which provide further background and critical field sites (Howard et al., 1987, 1994, 2013; John and Howard, 1994; House et al., 2005, 2008, 2018; Pearthree and House, 2014). A geologic river guide to Topock Gorge accompanies this guide (GSA Data Repository[1]).

A Note on the Colorado River

The Colorado River drains 260,000 mi^2 (675,000 km^2) of the western United States and links strikingly diverse terrains and climates. Its watershed spans the high alpine terrain of the Rocky Mountains, extensive tablelands and canyons of the Colorado Plateau, and parts of three American deserts, including some of the lowest and warmest desert terrain in the western hemisphere (Fig. 1B). Today, this unique snowmelt-fed desert river, the 'American Nile,' conveys a water resource that is essential to sustaining the needs of more than 35 million people through elaborate water and power distribution networks.

The lower Colorado River was a very different fluvial system before the last century when it became an essential source of water and power. Imagine the spectacle of it brimming with snowmelt, flowing out of the high mountains and into the stark canyon country of the Colorado Plateau, exiting the plateau through the iconic depths of Grand Canyon, and finally through a series of rocky canyons and broad, parched desert valleys. In the lower alluvial reaches, floods would rip through the canyons into the valleys and relentlessly reshape the river's channel and floodplain. Evidence for the river's dynamic character is as clear in those floodplains as in the canyons. Accounts of early explorers and scientists, maps, and aerial photos of the lower Colorado predating its regulated era reveal miles-wide shifting channels and elaborate cross-cutting tracts of braiding and meandering flowpaths, all interspersed with desert riparian forests and active strips and fields of eolian dunes. As noted by Ives (1861) and re-emphasized by LaRue (1925, p. 81), "The rapidity and extent of the changes in the position of the Colorado can scarcely be imagined by one who has not witnessed them." The river's final stretch to its terminal delta transects some of the driest desert land in North America to reach its only desert sea, the Gulf of California—except when it wouldn't. Because, given a relatively minor channel excursion on the low-lying delta floodplain, the river at times would flow instead into an even lower-lying searing desert to fill a huge lake in the Salton trough.

This guide focuses on the central part of the Colorado River's lower, desert reach between Grand Canyon and the Gulf of California. The lower river corridor begins at the eastern edge of the Basin and Range province, and passes through a chain of alluvial valleys separated by bedrock canyons cut through rugged desert mountains. Our focus area will be between the cities of Laughlin, Nevada, and Blythe, California.

A Note on the Climate

The best times for geologic fieldwork in the lower Colorado River valley are early spring, late fall, or winter. For a September field visit, it is imperative to drink lots of water and shield yourself from the sun as much as possible. In 1876, Lt. Eric Bergland graphically described summer challenges for the Wheeler Survey's fieldwork:

> The climate in the Colorado Valley during the hot months is not one which a sane person would select in which to spend the summer. From the middle of June to the 1st of October panting humanity finds no relief from the heat. As soon as the sun appears above the horizon its heat is

[1]GSA Data Repository Item 2019318, Topock Gorge Geologic River Guide, is available at www.geosociety.org/datarepository/2019/, or on request from editing@geosociety.org or Documents Secretary, GSA, P.O. Box 9140, Boulder, CO 80301-9140, USA.

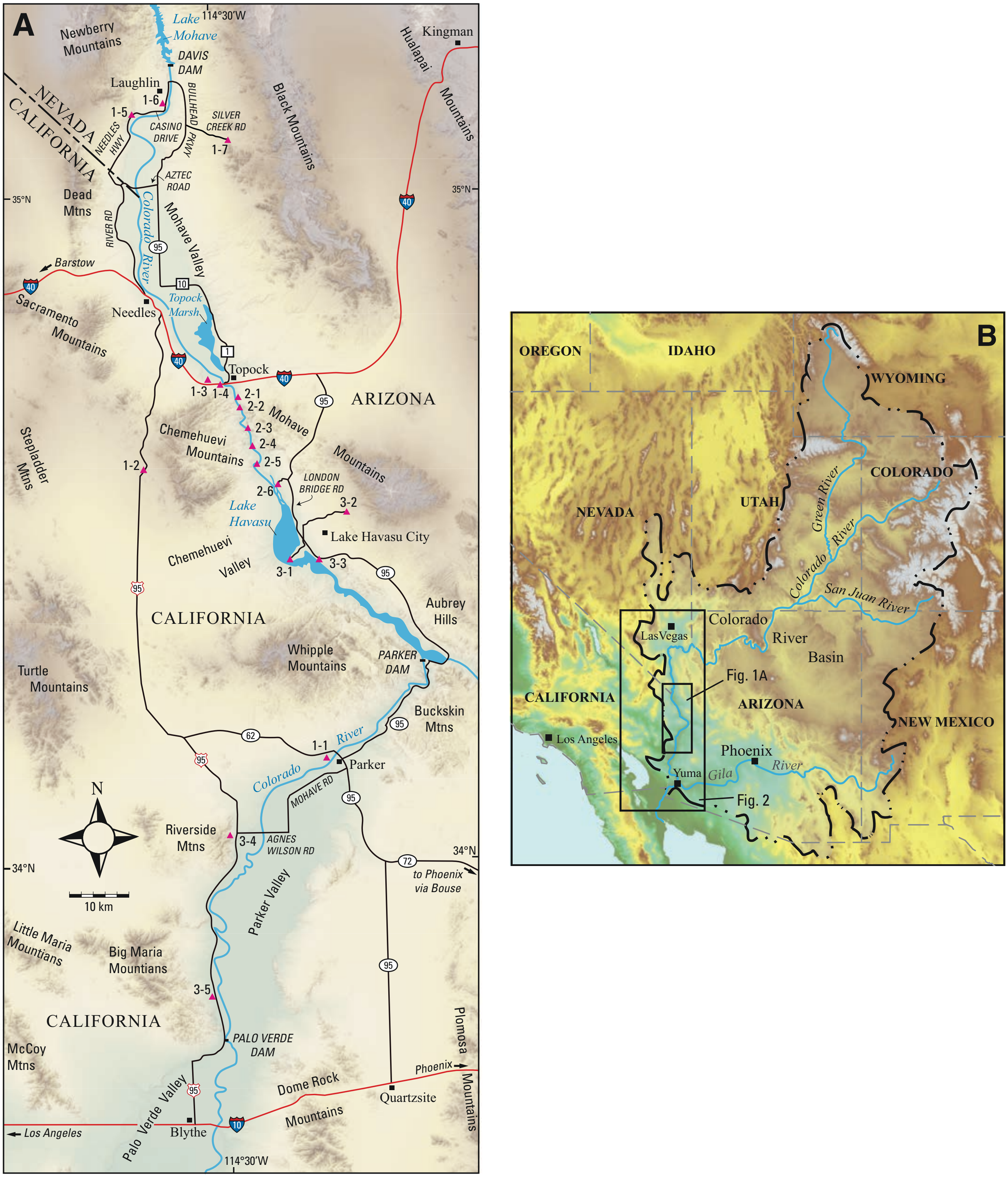

Figure 1. (A) Map of field-trip area, showing location of all stops. (B) Regional setting relative to the northern Basin and Range of Nevada and Utah north of Las Vegas, and the Colorado River drainage basin (outlined). Note the physiographic trough the lower Colorado River occupies (south of Las Vegas).

felt, and this continues to increase until a maximum is reached about 3 o'clock in the afternoon after which the temperature falls slowly, and oftentimes very slowly, until sunrise. During the hottest part of the day, exertion of any kind is impossible; even while lying perfectly quiet the perspiration oozes from the skin and runs from the body in numerous streams. Everything feels hot to the touch, and metallic objects cannot be handled without producing blisters on the skin. The white sand reflects the heat and blinds the traveler by its glare. Rain scarcely ever falls during the summer months, and not more than 3 or 4 inches the year round. Cloud-bursts frequently occur in the mountains, and at times we saw heavy showers all around us, but not a drop fell along the river.

The atmosphere is so dry and evaporation so rapid that the water in our canteens, if the cover was kept moist, kept at a temperature of 30 degrees below that of the air; a most fortunate circumstance, as it obviates the necessity of using ice-water where it would be impossible to preserve ice. Great quantities of water are drank during these hot days, and no uncomfortable fullness is experienced. One gallon per man, and sometimes two, was the daily consumption.

Notwithstanding this excessive heat, no sunstrokes occurred, although we were at one time exposed in a narrow canyon to a temperature of 120[°] F. All of the party preserved good health during the summer. There is no danger of catching cold in this climate, even if wet to the skin three or four times during the day or night. No dew or moisture is deposited during the night, hence no covering is required. The hot wind which blows frequently from the south is the most disagreeable feature of the climate. No matter where you go, it is sure to find you out and give you the full benefit of a gust that feels as if it issued from a blast-furnace, and parches the skin and tongue in an instant. Then there is no recourse but to take copious draughts from the canteens to keep up the supply of moisture in the body. If water cannot be obtained, the delirium of thirst soon overpowers the unfortunate traveler, and he dies a horrible death. (Bergland, 1876, p. 124–125)

GEOLOGIC FRAMEWORK

Each canyon, valley, and bounding mountain range of the river corridor offers detailed records of the varied geologic processes that created the physical framework that would accommodate and chronicle the birth and evolution of the Colorado River and the older extensional corridor that the river follows.

Cenozoic extension has doubled the width of the Basin and Range province of western North America, with local amounts of extension up to factors of 3–4 (Hamilton and Myers, 1966; Wernicke et al., 1988). In contrast to the northern Basin and Range, where extensional faulting continues today and much of the region is hydrologically closed, the southern Basin and Range south of Las Vegas, Nevada, is lower in elevation, has fewer young faults, and may show low-magnitude distributed extension (Kreemer et al., 2010).

The CREC south of Las Vegas, Nevada, forms one of several subregions within the Basin and Range that experienced a high degree of Cenozoic extension (Fig. 1). The CREC exposes regional-scale gently dipping extensional faults, steeply tilted syntectonic volcanic and sedimentary deposits in shingled fault panels, and metamorphic core complexes that were tectonically unroofed and uplifted from midcrustal levels during Miocene extension. This region has long been the target of seismic, gravity, and other geophysical studies, as well as numerous structural, stratigraphic, petrologic, and thermochronologic studies. Superb exposure, a wealth of geologic and geophysical data, and structural juxtapositions that allow comparison of different crustal levels all make this an excellent place to study relationships between magmatism and continental extension.

Ultimately, the lower Colorado River entered and followed the extensional corridor for 400 km in the early Pliocene. This major geologic and hydrologic event of river integration connected drainage from the Rocky Mountains and the Colorado Plateau with the Gulf of California. The story of the river's arrival and evolution is intimately linked with the structural framework and terrain of the extensional corridor, and the river's ultimate connection to the global ocean was achieved due to the formation of the Gulf of California through transtensional rifting.

Well-exposed upper Cenozoic strata offer insightful evidence of the downward- and southward-directed integration and evolution of this continental-scale river. The lower Colorado River's birth is becoming better and better documented, even as details of the mechanisms of its integration from a precursor upstream of Grand Canyon remain speculative and debated (Karlstrom et al., 2014) (Fig. 2).

Pre-Cenozoic Framework

The region along the Colorado River in Nevada, California, and Arizona was part of the stable North American craton prior to Mesozoic time. The Mojave crustal province consists largely of 1.8–1.6 Ga Paleoproterozoic orthogneisses and granitoids, and supracrustal gneisses carrying detrital zircons as old as Archean (Fig. 3; Wooden and Miller, 1990; Wooden et al., 2012; Holland et al., 2018). Mesoproterozoic plutons (1.4 Ga) and diabase sheets (1.1 Ga) intrude the gneisses (Anderson and Bender, 1989; Hammond, 1990; Goodge and Vervoort, 2006). The commonly horizontal original orientation of the diabase sheets throughout a region at least 600 km wide in California and Arizona provides a useful structural reference to evaluate younger deformation in the basement rocks (Howard, 1991).

After uplift and long erosion, the formerly deep-seated Proterozoic rocks served as depositional basement for layers of Paleozoic shallow-marine continental platform strata that nonconformably overlie it (Stone et al., 1983), as exposed spectacularly as flat-lying layers in Grand Canyon. These strata were largely stripped from a region ~200 km across, centered on the lower Colorado River during post-Paleozoic orogeny and erosion. However, Warren Hamilton first recognized that the lower Colorado River area locally exposes highly contorted equivalents of this Paleozoic sequence, which had been deeply buried and metamorphosed (Hamilton, 1964, 1982, 1984, 1987a; Hamilton et al., 1987).

Active convergence along the west coast of southwestern North America by late Paleozoic time led to a succession of Mesozoic magmatic and orogenic events that mobilized the crust eastward as far as the margin of the relatively stable Colorado Plateau province. The Cordilleran frontal fold and thrust belt of Wyoming, Utah, and Nevada transitions south of Las Vegas to

Figure 2. Map of the Colorado River from the mouth of the Grand Canyon downstream through the Blythe basin to its broad, low-lying delta that expands southwestward from Yuma. Box shows area of Figure 1A. Locations and names of inferred paleo-divide dams (black bars) and associated Pliocene lakes and their approximate maximum elevations are indicated. The approximate limits of the Miocene Colorado River extensional corridor are also shown. Base map modified from House et al. (2008).

a deeper-seated terrain of Mesozoic basement–involved thrusts including metamorphosed and thinned Paleozoic strata (Burchfiel and Davis, 1975; Miller et al., 1982; Hamilton et al., 1987; Spencer and Reynolds, 1989; Fletcher and Karlstrom, 1990; Tosdal, 1990; Howard et al., 1995). A Jurassic magmatic arc was followed in the mid-Cretaceous by local plutonism, and then in the latest Cretaceous by high-flux plutonism and extension with rapid cooling related to low-angle subduction of an oceanic rise and the Laramide orogeny (Howard et al., 1987; John and Mukasa, 1990; Carl and Miller, 1991; Foster et al., 1991, 1992; Allen et al., 1995; Saleeby, 2003; Wells and Hoisch, 2008; Tosdal and Wooden, 2015). Reconstruction of the now-dismembered Chemehuevi

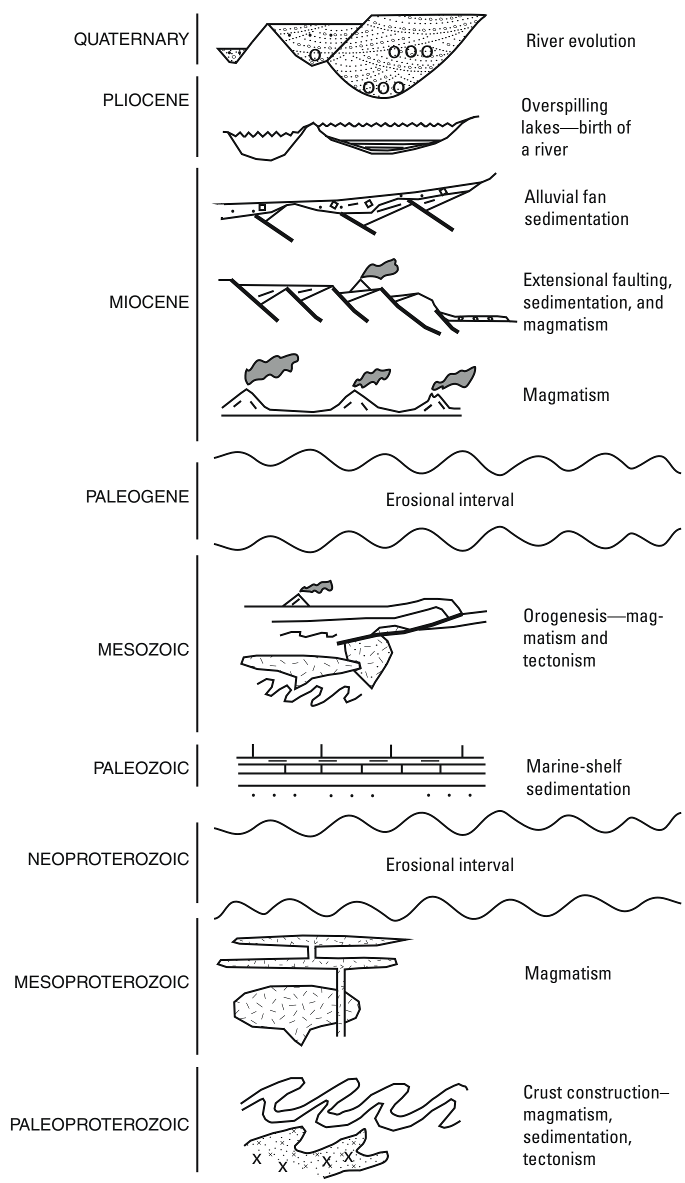

Figure 3. Schematic crustal history of the lower Colorado River region.

Mountains Plutonic Suite provides an example depth-section of a Late Cretaceous batholith, comparable to Hamilton and Myers's (1967) concept of flat-floored batholiths (Fig. 4).

Paleogene Erosion

The Paleogene was a time of gradual erosion and cooling of a highland in the former thrust and plutonic belt, in which Paleogene streams flowed northeastward toward the continental interior across the southwest margin of the Colorado Plateau province and also westward toward the coast (Elston and Young, 1991; J. Howard, 1996; Shulaker et al., 2019). The highland may have been a southern continuation of the Nevadoplano high plateau (DeCelles, 2004). Perhaps 3–7 km of crust may have been denuded before 23 Ma based on evidence of 70–150° of Paleogene cooling (Foster et al., 1991, 1992; Foster and John, 1999).

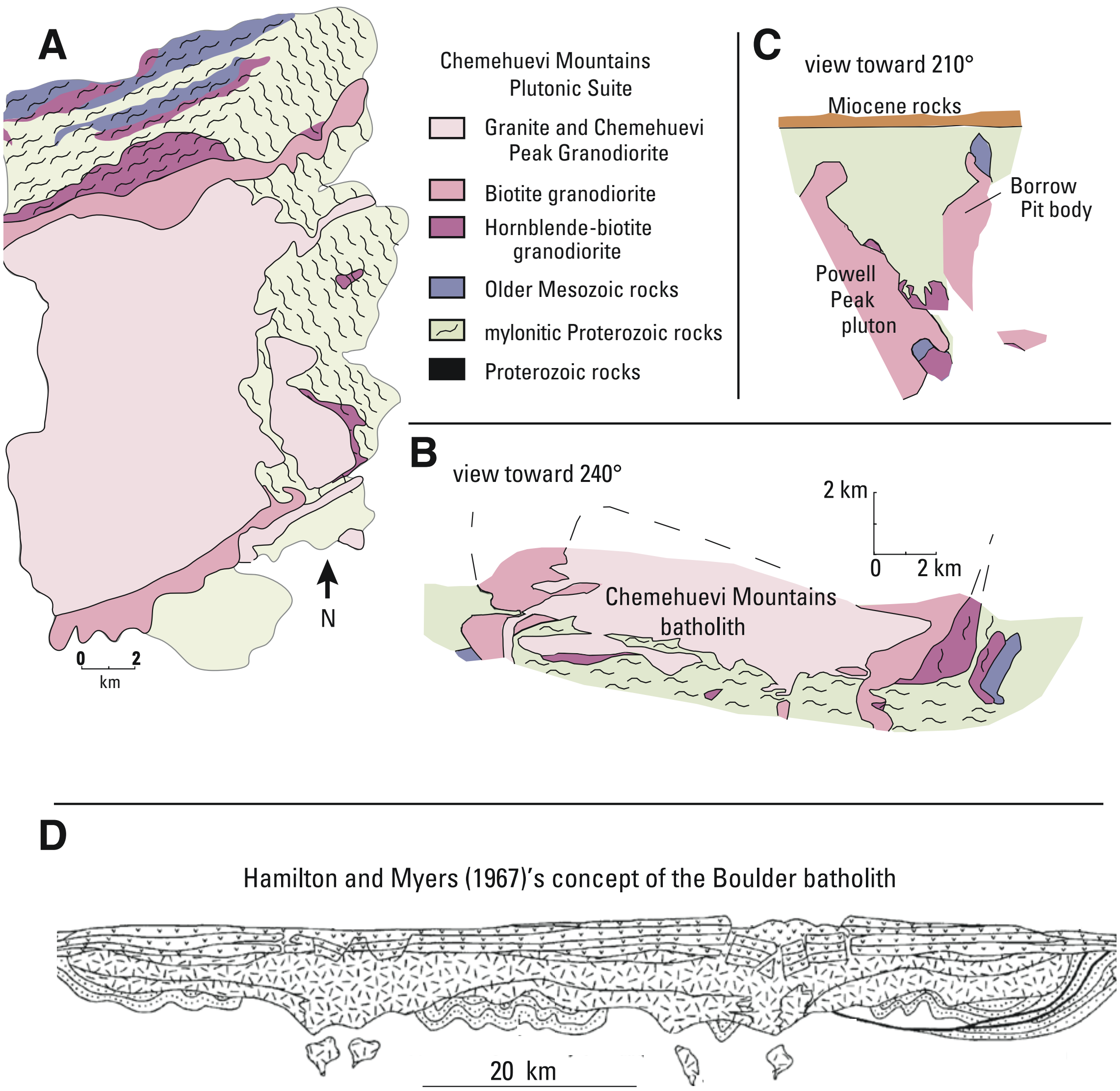

Figure 4. (A) Simplified map of the Chemehuevi Mountains footwall (below the Chemehuevi detachment fault) with Miocene faulting restored. (B) Down-structure view (Mackin, 1950) of the gently SW-dipping Chemehuevi Mountains Plutonic Suite (Late Cretaceous) exhibits its flat floor and a nested sequence of granitoid lithotypes. See John (1988) for more details about the plutonic suite. (C) Upper stories of the pre-Miocene cross section of the batholith expressed as restored plutonic bodies, after back-tilting and restoring fault offsets between three mapped, steeply tilted upper-plate blocks east of Topock Gorge, including the Tumarion and Jackpot blocks (Fig. 5A; Howard et al., 1999, 2013). This section restores to a central position above the batholith shown in B. A nonconformity at the base of the Miocene section records denudation of an unknown amount of cover before the Miocene. (D) Warren Hamilton's concept of a sill-like Boulder batholith (in Montana; Hamilton and Myers, 1967) for comparison with the Chemehuevi batholith. Extensive annotations decorate and further explain the original figure.

Neogene Setting

In the early Miocene, the margin of southwestern North America evolved from a convergent margin to a transform margin (Dickinson and Snyder, 1979; Severinghaus and Atwater, 1990; Ward, 1991). Subduction of zero-age crust on its eastern flank is believed to have resulted in a slab window under southern California at the latitude of the CREC at ca. 20 Ma (Atwater and Stock, 1998), coinciding with the onset of extension in the corridor. Magmatism and extension migrated northward through the southern Basin and Range province, coincident with the northward migration of the Mendocino triple junction and the slab window (Glazner and Supplee, 1982; Glazner and Bartley, 1984). As magmatism and extension migrated northward in the CREC, magmatism peaked slightly earlier than the highest rates of extensional faulting (Gans et al., 1989; Gans and Bohrson, 1998).

Syn-Extensional Stratigraphy

The early Miocene stratigraphy throughout the CREC and adjacent regions (Sherrod and Nielson, 1993) commonly begins with a basal arkose overlying deeply weathered pre-Tertiary crystalline rocks. It is followed in the central part of the corridor near Lake Havasu City by a lower volcanic section consisting of 100's of m of 23–18.8 Ma volcanic rocks, largely flows and breccias and interfingered sediments (Carr, 1991; Nielson and Beratan, 1995; Howard et al., 1999, 2013). This lower volcanic section is capped by a widespread rhyolitic ignimbrite, the 18.8 Ma Peach Spring Tuff (Ferguson et al., 2013). In and near the Chemehuevi Mountains, including Topock Gorge (Fig. 5), the eruption of the tuff marks a major transition from abundant magmatism to extensional faulting. Thick accumulations of syn-extensional alluvial-fan and landslide breccia deposits in local basins record progressive extensional faulting, tilting, and unroofing of metamorphic core complexes (Miller and John, 1988, 1999). Unconformities and fanning dips within dated Miocene sections show that faulting and tilting began ≥20 Ma and ended ≤12 Ma. Extension and magmatism both young northward in the extensional corridor. The thick lower volcanic section has younger compositional counterparts in northern parts of the extensional corridor, where they mostly overlie the Peach Spring Tuff.

Structural Framework of the Extensional Corridor

The extensional corridor is 50–100 km wide in the Parker-Laughlin region, and displays a common set of structural elements responsible for doubling its width (stretching factor beta = 2) (Fig. 6). They consist of a system of breakaway or headwall faults on the up-dip side of the fault system, numerous fault blocks tilted toward the breakaway, a central zone of domed metamorphic core complexes, and a distal zone where the fault system roots downdip under less deformed blocks. The CREC was originally defined as a domain of southwest to west stratal dips (Howard and John, 1987; Whipple tilt domain of Spencer and Reynolds, 1991); the CREC concept has since been broadened to include a northern domain of east stratal dips, between the area of Figure 1A and Lake Mead (Faulds et al., 1990). R.E. Anderson's (1971) seminal study on listric and low-angle normal faults in that northern part of the CREC recognized that the steep dips of slivered Miocene units meant they had tilted during extension, along with gently dipping normal faults that bound them. His analysis helped trigger a revolution in understanding extension in continental crust.

The great domal detachment faults are fundamental elements of the upper crustal structure in the CREC (Davis et al., 1980, 1982; John, 1987a; Davis and Lister, 1988; Lister and Davis, 1989). Mylonitic fabrics in the footwalls record ductile extensional shearing at deep crustal levels (Davis et al., 1980), and are overprinted in succession by cataclasite, breccia, and gouge, recording the progressive unroofing and doming of these fault systems (John, 1987a). This rise is recorded also in geobarometric and thermochronologic studies. For example, rocks exposed in the core of the Whipple Mountains rose from ~30 km depth in the Late Cretaceous through ~16 km depths in the latest Oligocene or early Miocene when extension began, and were tectonically unroofed in the middle Miocene (Anderson, 1988; Davis, 1988). The asymmetric shape and slip on the detachment fault system have been used to argue for a simple-shear model of crustal extension (Wernicke, 1985; Howard and John, 1987).

Geophysical measurements, on the other hand, suggest a crustal section that is more symmetrical, the deeper parts compatible with McKenzie's (1978) pure-shear model of crustal stretching. This symmetry is evident in elongate gravity and magnetic highs paralleling the axis of the core complex exposures today (Simpson et al., 1990; Mickus and James, 1991; Campbell and John, 1996), and by a seismically defined midcrustal body of moderate seismic velocity that thickens markedly under the up-domed core of the Whipple Mountains (Fig. 1; McCarthy et al., 1991; Wilson et al., 1991). The 10-km-deep midcrustal bulge shown by the top of this body conforms with structural and petrologic evidence that the core complexes were updomed 10–15 km during extension (Howard et al., 1982; Anderson, 1988). Rise of the bulge has been likened to diapirism and inward intracrustal flow as an isostatic response to tectonic unroofing during extension (Wilson et al., 1991; McCarthy et al., 1991; Spencer, 1984; Block and Royden, 1990). Heat-flow lows coincide with the core complexes here and elsewhere in the southern Basin and Range province, which provides evidence confirming that doming of the core complexes involved intracrustal flow rather than focused mantle upwelling (Lachenbruch et al., 1994).

McCarthy et al. (1991) demonstrated that the Moho is nearly flat and 26–30 km deep across this part of the Basin and Range (Fig. 6). Crustal thickness is therefore constant in this as in other parts of the Basin and Range province despite large geographic variations in magnitude of upper crustal extension, an observation consistent with lateral flow of ductile lower crust during pervasive crustal thinning (Gans, 1987) to compensate isostatic

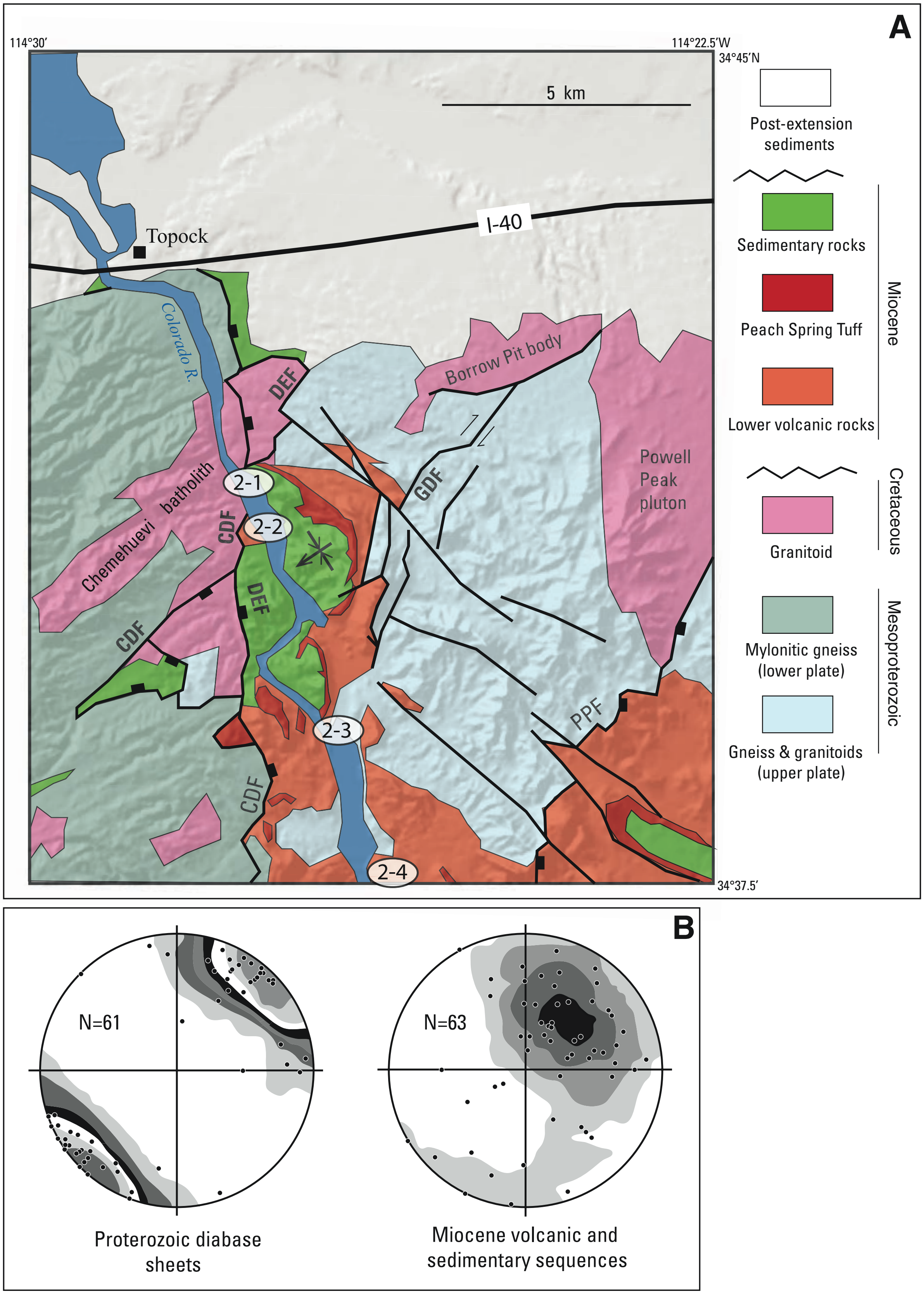
A
114°30′
114°22.5′W
34°45′N
5 km
Topock
I-40
Colorado R.
Borrow Pit body
DEF
GDF
Powell Peak pluton
Chemehuevi batholith
CDF
2-1
2-2
2-3
2-4
PPF
34°37.5′
Post-extension sediments
Sedimentary rocks
Peach Spring Tuff
Lower volcanic rocks
Miocene
Granitoid
Cretaceous
Mylonitic gneiss (lower plate)
Gneiss & granitoids (upper plate)
Mesoproterozoic
B
N=61
Proterozoic diabase sheets
N=63
Miocene volcanic and sedimentary sequences

Figure 5.

Figure 5. (A) Bedrock geologic sketch map of the Topock 7.5′ quadrangle showing most of the DAY 2 field-trip stops in Topock Gorge: CDF—Chemehuevi detachment fault; DEF—Devils Elbow fault; PPF—Powell Peak fault; GDF—Gold Dome fault zone (Howard et al., 2013). Boxes ornament the hanging walls of low-angle normal faults. (B) Lower hemisphere equal-area nets showing pole orientations in upper-plate tilted blocks in the Topock quadrangle of Mesoproterozoic diabase sheets intrusive into gneisses (left), and Miocene strata and volcanic rocks (right) (redrafted from John and Howard, 1994; 2-sigma contour interval by the Kamb method using Stereonet version 4.15 by R. Allmendiger). The Miocene rocks exhibit upward-fanning dips indicating progressive tilting during deposition. The diabase sheets within Proterozoic crystalline basement rocks are now subvertical, parallel to the lowest overlying Miocene strata, and are inferred to be tilted from originally subhorizontal orientations; they demonstrate that the large blocks tilted uniformly ~90° (Howard, 1991). The map views of the blocks thus reconstruct as cross sections, which help reconstruct the upper parts of the Chemehuevi batholith exposed in lower-plate position mostly west of this map area (Fig. 4C).

doming, where extensional faulting thins or removes the upper crust (Block and Royden, 1990; McCarthy et al., 1991; Wernicke, 1992; Fig. 6).

Many, perhaps most, low-angle extensional faults may have been rotated from originally steeper dips after the faults were active (Proffett, 1977; Spencer, 1984, 1985; Gans and Gentry, 2016). The rolling-hinge model postulates that as footwalls to moderately steep normal faults rebound isostatically in response to unloading, inactive portions of the faults arch to gentle dips (Buck, 1988; Wernicke and Axen, 1988; Hamilton, 1988). Geologic and thermochronologic relations have been used to argue that in some cases, including the Chemehuevi Mountains, the faults formed at dips much less than the moderately steep dips predicted by Anderson's (1951) theory of normal faulting (Wernicke et al., 1985; John and Foster, 1993; Miller and John, 1999; Pease et al., 1999).

Structural attenuation by faulting and tilting within the CREC has resulted in the exposure of a wide variety of crustal depth levels, thus allowing comparison of structures and igneous bodies formed at levels ranging from the surface to deep in the middle crust (e.g., Fig. 4). Tilted fault panels, now eroded, display oblique or upended cross sections revealing paleothicknesses as much as 15 km of Proterozoic, Cretaceous, and Tertiary crystalline rocks (Howard, 2011; Gans and Gentry, 2016).

Magmatism

Magmatism typically accompanies continental extension. Thermal softening by magmatic intrusion potentially can allow rapid stretching (Armstrong and Ward, 1991; Lister and Baldwin, 1993) and rise of domal core complexes (Brun et al., 1994). Magmatism may also influence the state of stress and therefore the mode and orientation of rock failure and faulting, potentially leading to low-angle normal fault initiation (Parsons and Thompson, 1993). Further, magmatic inflation by intrusion may accommodate crustal extension (Anderson, 1971; Parsons and Thompson, 1991), not dissimilar from the spreading of oceanic ridges.

The history of the CREC includes much magmatism during extension (Sherrod and Nielson, 1993; Fig. 7). Voluminous volcanism propagated northward through the CREC, as did brittle normal faulting ~1–4 m.y. later (Gans et al., 1989; Gans and Bohrson, 1998; Faulds et al., 1999). During and after the major extensional faulting, extrusive magmatism continued, but at much reduced rates (Howard and John, 1987; Gans and Bohrson, 1998; Miller and John, 1999; LaForge et al., 2017). This highlights a temporal and geographic pattern characteristic of active extension in the Basin and Range, consistent with magmatic crustal heating facilitating brittle failure of the upper and middle crust (Gans et al., 1989).

Miocene volcanism in the CREC evolved compositionally. The main magmatic pulse was preceded by initial low-volume

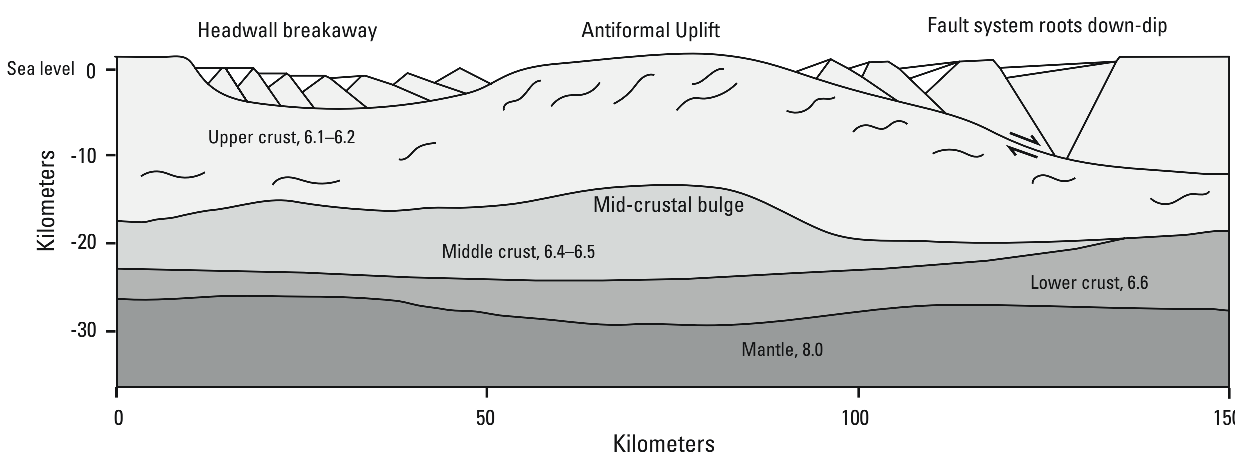

Figure 6. Schematic cross section of the Colorado River extensional corridor (redrafted and slightly modified from Howard et al., 1994). Seismic velocities are in km/s for a velocity model across the Whipple Mountains area (McCarthy et al., 1991). Alternative models can include secondary breakaway faults and multiple rooted faults (Spencer, 1985; Gans and Gentry, 2016).

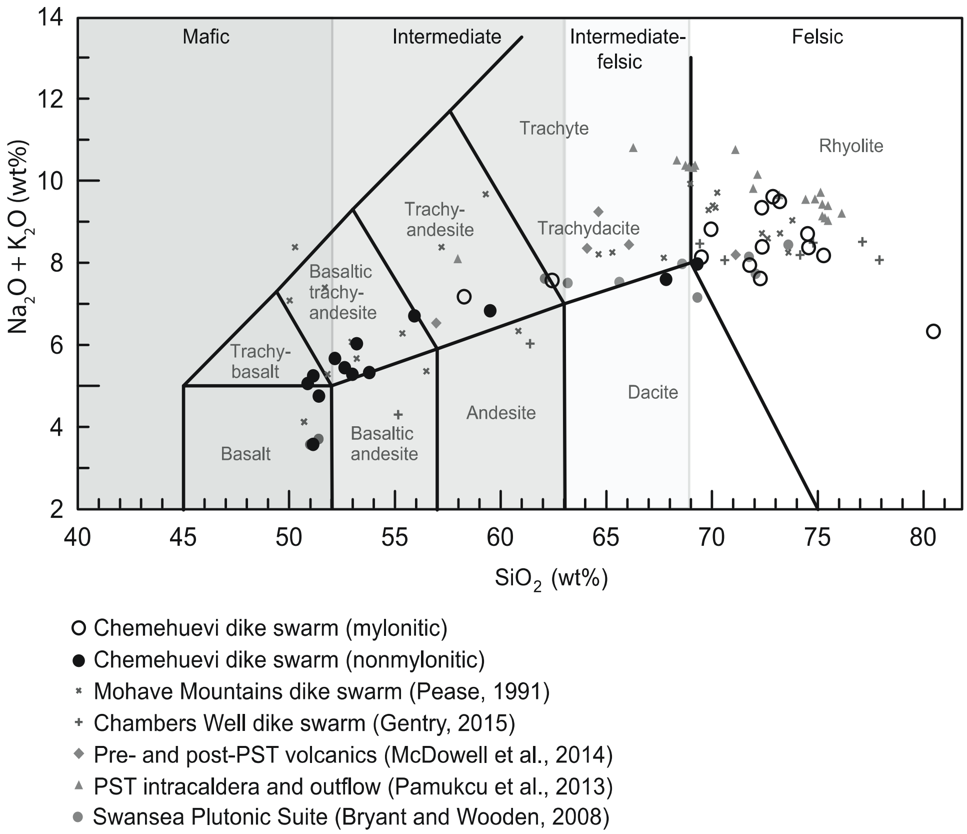

Figure 7. Total alkali versus silica plot showing representative Miocene igneous rock compositions, including dikes, lavas, and ash flow deposits in the Colorado River extensional corridor (compiled by LaForge et al., 2017), which span a broad range in composition from primitive basalt and trachybasalt to high-silica rhyolite. PST—Peach Spring Tuff.

eruption of early Miocene asthenosphere-derived basalts (Howard, 1993). The voluminous magmatism that then ensued involved eruption and intrusion of a heterogeneous suite of basaltic, intermediate, and minor felsic rocks, resembling intermediate suites in continental volcanic arcs (Smith et al., 1990). Following the peak of extension, as extension waned and rates of volcanism declined, the compositions became basaltic or bimodal (Suneson and Lucchitta, 1983; Bradshaw et al., 1993; Feuerbach et al., 1993; Gans and Bohrson, 1998; Foster and John, 1999).

Intrusive Rocks

Magmatic inflation of the crust by intrusion can accommodate significant extension (Gans and Bohrson, 1998). Mafic early Miocene intrusion under the core complexes was invoked to explain a gravity high that follows the corridor axis (Simpson et al., 1990; Campbell and John, 1996). The gravity high coincides in the southern Sacramento Mountains with small outcrops of early Miocene diorite, and was modeled as a large cumulative thickness of dikes that extend the crust by 5–18 km (10%–20% of the total extension), an inflation that would have preceded most of the extensional faulting (Campbell-Stone and John, 2002).

Early Miocene dike swarms in the CREC commonly strike perpendicular to extension directions (mostly NE) that are otherwise indicated by fault movements (Davis et al., 1982; Nakata, 1982; Campbell and John, 1996), but other dike swarms are parallel or oblique (Spencer, 1985; John and Foster, 1993; Campbell-Stone et al., 2000). In places, dike swarms are sheeted complexes occupying 15%–100% of the exposed rocks (Davis et al., 1982; Nakata, 1982; Spencer, 1985; Gans and Gentry, 2016).

In addition to the dikes, Miocene plutons ranging in composition from diorite to granite crop out in many ranges along the central part of the extensional corridor (Anderson, 1969; Anderson et al., 1972; Wright et al., 1987; Bryant and Wooden, 1989, 2008; Anderson and Cullers, 1990; Campbell and John, 1996; Howard et al., 1994; John and Foster, 1993). Some of the synextensional plutonic and dike rocks in the core complexes bear mylonitic fabrics, imprinted by extensional shear at midcrustal levels (Anderson and Cullers, 1990; Pease et al., 1999; Howard et al., 2013).

Peach Spring Tuff

This ignimbrite forms a critical stratigraphic and structural marker in the CREC. It covers an area now 400 km wide from Grand Canyon west to the central Mojave Desert, having originated in a supereruption from a caldera in the Black Mountains, Arizona, with dismembered caldera parts in the Sacramento Mountains, California (Figs. 1, 8; Ferguson et al., 2013). Detailed studies of the tuff and its crystals and related volcanics establish the stratified nature of the magma chamber from which it erupted, and igneous processes leading up to and following its eruption (Pamukcu et al., 2013; McDowell et al., 2014). Magnetic polarity measurements in the tuff documented vertical-axis

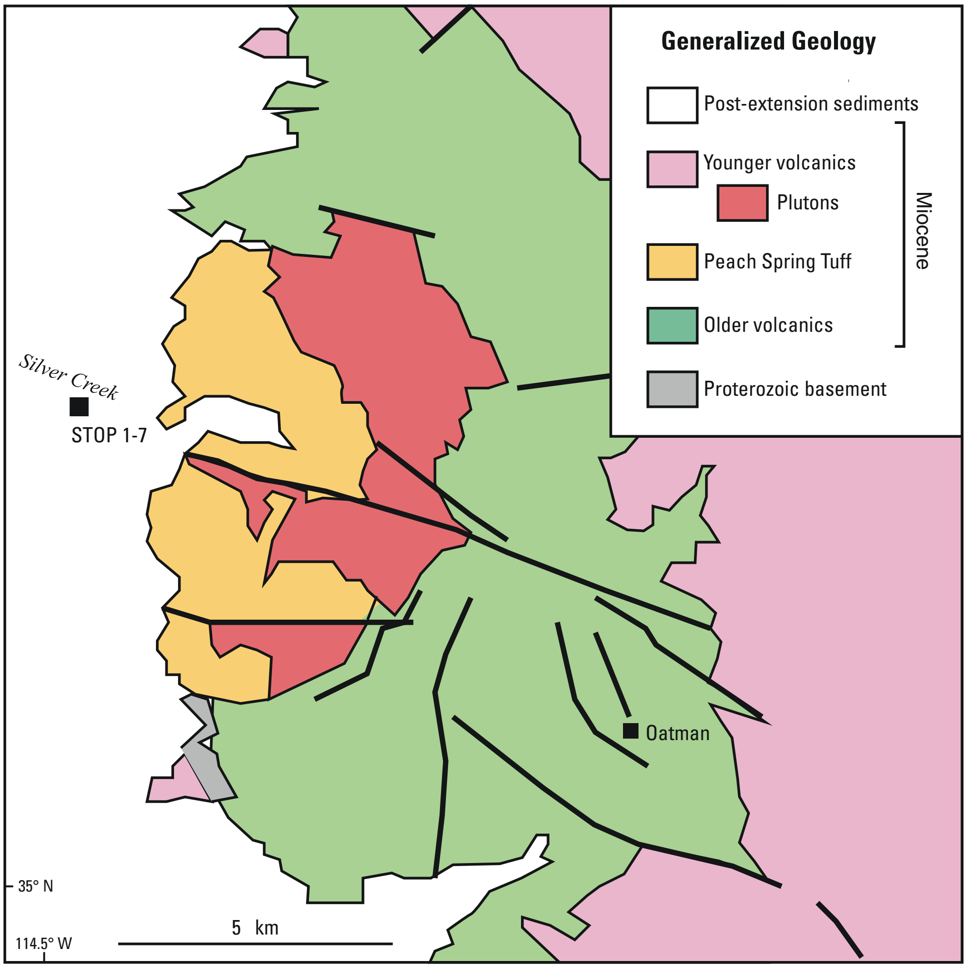

Figure 8. The Silver Creek caldera, outlined by caldera-fill Peach Spring Tuff and younger plutons, in the Black Mountains of Arizona (Ferguson et al., 2013). The caldera is the eruption site of the 18.8 Ma Peach Spring Tuff. Ferguson et al. (2013) recognized dismembered other parts of the caldera 40 km to the southwest in California's Sacramento Mountains.

rotations of various structural blocks in the CREC and helped point toward its eruptive source area (Wells and Hillhouse, 1989; Hillhouse and Wells, 1991).

Late Miocene Landscape Evolution—Setting the Stage for Arrival of Colorado River Waters

Upper Miocene alluvial fan deposits, rare playa deposits, and interbedded basalt flows younger than ca. 12–9 Ma unconformably overlie the highly extended and tilted sections, and document a marked decrease in extension. Some of these deposits perch high and project over subsequent valleys into which later initial Colorado River water emptied. Their configuration shows that when the extensional episode ended, a series of closed alluvial basins and intervening low bedrock ranges remained. Playa deposits accumulated in depocenters of individual valleys or sinks in multiple, linked valleys (House et al., 2008). The pre-river valleys, as recorded by younger stratigraphy, outline a discontinuous topographic trough, each basin in the chain being low compared to surrounding parts of the southern Basin and Range.

A major question, so far little addressed, is whether this troughlike feature resulted directly from the extensional corridor that it follows. Other aspects of how the post-extension late Miocene landscape evolved also remain poorly understood, including whether or how the basins that ultimately set the future course of the lower Colorado River were affected by the late Miocene to Pliocene southern San Andreas fault plate boundary and transtension in the northern Gulf of California and Salton trough (Oskin and Stock, 2003; Dorsey et al., 2007, 2011; Seiler et al., 2010; Bennett et al., 2013, 2016a, 2016b; Thacker et al., 2017, 2018; Pearthree et al., 2018). An apparent scarcity of post–10 Ma dextral slip upstream from the San Andreas fault system in the lower Colorado River corridor as compared to the now-active Eastern California Shear Zone (an inboard part of the plate boundary) suggests that any late Miocene shear in the lower Colorado River corridor may be subtly distributed and/or not yet recognized (Singleton, 2015; Bennett et al., 2016a; Thacker et al., 2017, 2018).

The Colorado River gravity high follows near the axis of the extensional corridor (Simpson et al., 1990), and Carr (1991) proposed that isostatic compensation of dense rocks along the gravity high may have sagged what became the river valley. Or, did the basins subside due to transtension along a distributed zone of dextral shear related to the Pacific–North American plate boundary? Did erosion remove material to unknown distal sinks? Did combinations of these processes operate to form a series of low depocenters? Cottonwood, Mohave, and Chemehuevi Valleys were apparently internally drained basins when Colorado River water first arrived less than 5.24 m.y. ago (see below), and Blythe basin downstream may have been internally drained as well. Younger stratigraphic evidence shows that at least Blythe and Mohave basins locally continued to subside after Colorado River integration (Metzger et al., 1973; Metzger and Loeltz, 1973; Pearthree and House, 2014; Howard et al., 2015).

The Bouse Formation and Integration of the Colorado River

Stratigraphic and geomorphic evidence in alluvial-valley parts of the river corridor, between bedrock divides (now canyons), shows that the modern topography of the valleys mirrors the paleotopography just before the river first arrived (House et al., 2008; Pearthree and House, 2014). Subsequent river aggradation packages and re-incision events have repeatedly partly filled and then exhumed valley shapes that approximate the original late pre-river valleys.

The Bouse Formation (Metzger, 1968) and the Bullhead Alluvium (Howard et al., 2015) preserve keys to understanding the early integration history of the lower Colorado River into and through the late Miocene extensional landscape. The Bouse Formation is the primordial deposit of the Colorado River and records the initial arrival of river's solute-rich water, followed by its sediment. It filled a succession of closed or restricted basins left over from Miocene extension with a characteristic facies assemblage that includes thin, landscape-coating basal limestones and wave-worked local sediments (the transgressive facies), overlain by a thick sequence of interbedded sand and mud (the fill facies). The transgressive facies lines the pre-inundation axes and margins of each valley and tracks changing water levels. The limestones, including marl, coquinas, and travertine-tufa, are iconic deposits of the Bouse Formation, but the interbedded siliciclastic-rich fill facies accounts for the majority of the formation's volume. The nearshore component of the transgressive sequence is least extensive, but is present in each valley. Locally, it can be several meters thick, including elaborately structured reworked local gravel and sand and interbedded travertine. In other locales, it is exceptionally thin limestone and often found sandwiched between alluvial fan deposits. Hamilton (1960) first recognized the nearshore inundation-facies along the margin of the Blythe basin, noting that "lime caps" and associated travertine, cross-bedded gravel, and coquina resemble beach rock. He recognized that the Blythe basin must have once contained a marine embayment or a large saline lake held by a natural dam at the southern end of the valley.

Lucchitta (1979) and Buising (1990) linked the Bouse Formation to the Colorado River, and postulated that interbedded siliciclastic deposits in the formation were marine delta deposits. Buising (1990) also recognized that shoreline gravels and carbonates along the perimeters of Bouse-holding basins reveal water-level history. The accumulation of hundreds of new mapped outcrops (summarized in Crow et al., 2018a) of the nearshore facies of the Bouse reinforces previous inferences that it has a distribution that steps up northward in elevation at each interbasin bedrock divide (summarized in House et al., 2008). This is consistent with the concept of Spencer and Patchett (1997) that the Bouse was deposited in lakes fed by the Colorado River. This stair-stepping stands in contrast to a steadily climbing ramp-like distribution that was once proposed as evidence for significant late Cenozoic tilt uplift of the region when the Bouse was assumed to be a sea-level datum (Lucchitta, 1979).

In upper basins, including Mohave and Chemehuevi Valleys where much of this field guide focuses, the characteristics and distribution of the Bouse Formation are consistent with it being lacustrine and deltaic (Spencer and Patchett, 1997; Poulson and John, 2003; House et al., 2005, 2008; Pearthree and House, 2014). In this model, the Bouse Formation is a facies association that records a downstream-directed, stepwise integration of the lower Colorado River through each of the valleys along the corridor. In this spilling-lakes interpretation, the association of basal carbonate and shoreline gravel overlain by Colorado River–sourced mud and sand records spilling of solute-rich water into successive lakes, followed by slower progradation of fluvial deltas. Thus the transgressive inundation facies records the initial spill of decanted water carrying little or no siliciclastic material from basin to basin resulting in the deposition of Bouse carbonate; carbonate deposition was accompanied by formation of rounded gravel at wave-washed shorelines. The fill facies records stepwise development and subsequent evisceration of lake-filling deltas that proceeded downstream as valleys filled with Colorado River sediment, erosion lowered spillover points, and lake areas and volumes diminished. At this point, the stored sediment was liberated into the succeeding valley at a rate commensurate with spillover lowering. This delta fill-and-spill model involves the temporary sequestration of fine Colorado River sediment up to a divide elevation threshold, followed by variably paced divide-lowering that forces evisceration of the old delta, and regurgitation into the new delta in the next valley downstream. The growth of the delta probably suppressed carbonate sedimentation where the siliciclastic input is heavy.

This process is illustrated schematically in Figure 9. Here, the 12-step diagram presented by Pearthree and House (2014) is distilled into 7 key steps:

1. Water fills Cottonwood basin upstream from Laughlin (to the right of the Pyramid divide).
2. Water spills south over low Pyramid divide into Mohave basin, depositing the Pyramid gravel flood deposit.
3. Mohave basin fills with water to a maximum elevation of ~550–560 m a.s.l. (above sea level), then decants

solute-rich water into Chemehuevi basin, depositing Bouse limestone. Deposits of the Colorado River delta accumulate in Mohave basin.

4. Delta wedge overtops the Topock divide at the southern end of Mohave basin. Colorado River incises its delta fill in the basin as the spillway lowers and builds delta in Chemehuevi basin. Delta plume of lacustrine mud flows into Blythe basin.
5. The Aubrey divide, separating Chemehuevi and Blythe basins, has been removed and Colorado River and its sediment begin incision through Chocolate Mountains divide.
6. Base level drops to sea level and culminates in graded profile of Colorado River, incising and truncating Bouse fill and underlying basin fills and bedrock.
7. Thick wedge of Bullhead Alluvium advances downstream as fluvial response to deep canyon-cutting and related landscape denudation in the drainage basin in response to the cumulative base-level drop.

Chronology of Integration

Dated ashes and magnetostratigraphy in playa deposits below the Bouse Formation in the upstream Cottonwood Valley constrain its age to less than 5.24 Ma (Crow et al., 2018c). Thus, Colorado River water arrived in the lower Colorado River region after 5.24 Ma. Downstream in the Blythe basin, the age and depositional environment of the Bouse Formation are more controversial. Conflicting lines of evidence there have been interpreted as either lacustrine (Spencer and Patchett, 1997; Spencer et al., 2013; Bright et al., 2016) and/or estuarine/marine (Smith, 1970; Buising, 1990; McDougall, 2008; McDougall and Miranda-Martinez, 2014; Crossey et al., 2015; O'Connell et al., 2017) depositional environments. The age of the Bouse Formation in the Blythe basin is also controversial. McDougall

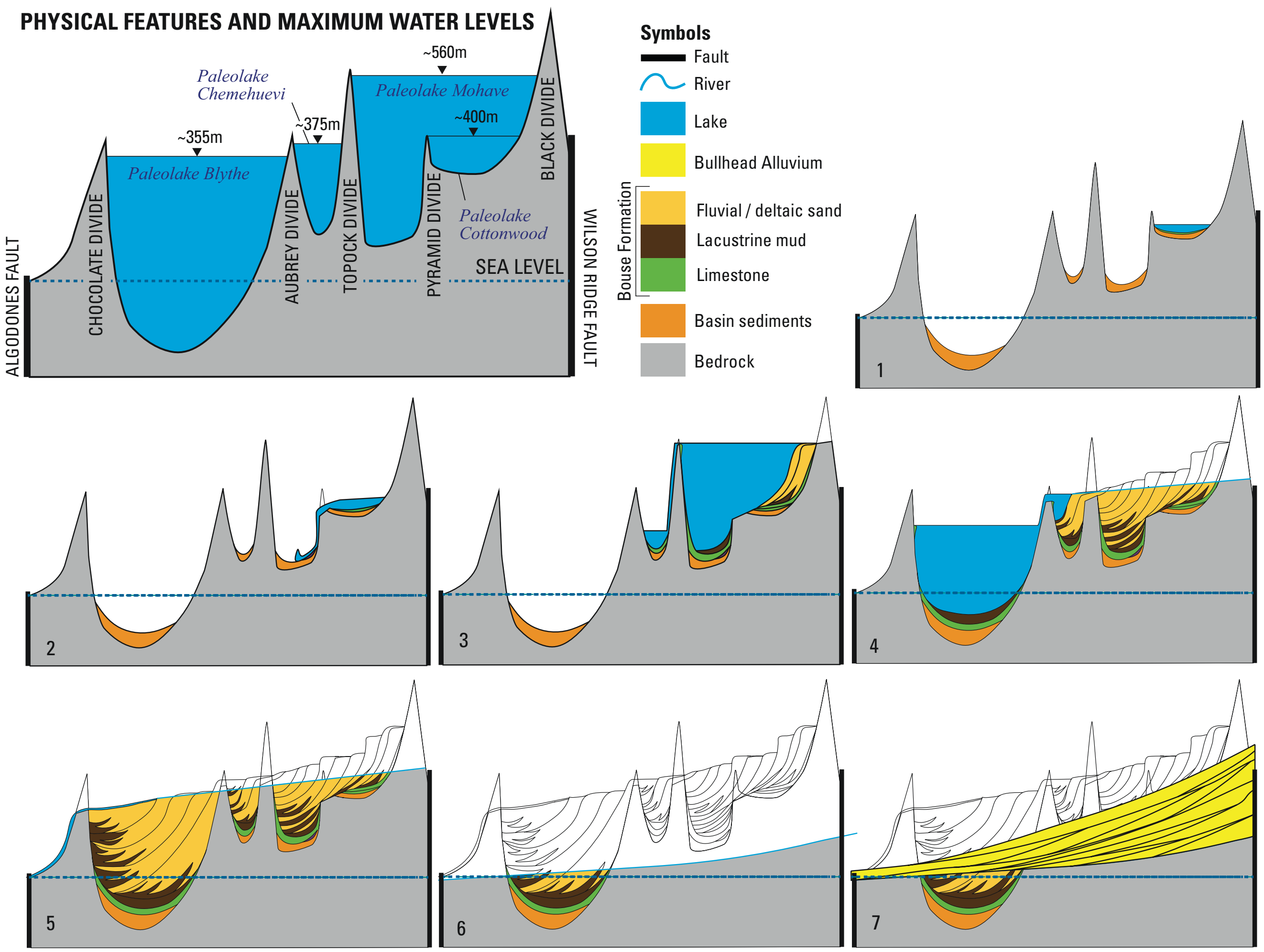

Figure 9. Schematic 7-step diagram illustrating the fill-and-spill model of the early development of the lower Colorado River through a series of closed basins (after Pearthree and House, 2014). Cottonwood basin is to the right of the Pyramid divide. *See text for additional explanation.*

and Miranda-Martinez (2014) suggested that the basal carbonates in the Blythe basin are older than 6 Ma, based on the global last occurrence date of a particular marine foraminifera species, implying that initial Bouse deposition there occurred well before the arrival of the waters of the Colorado River. At higher elevations in the Blythe basin, beds of the 4.9–4.8 Ma Lawlor Tuff are found interbedded with Bouse carbonate (Sarna-Wojcicki et al., 2011; Spencer et al., 2013; Harvey, 2014; Miller et al., 2014). Downstream, detrital sanidine dating in progress by R. Crow and colleagues (Crow et al., 2019, in press) in the Salton trough is providing evidence that Colorado River sands first arrived in the proto–Gulf of California half a million years or more later than an earlier magnetostratigraphic correlation age estimate of 5.3 Ma for this event (Dorsey et al., 2007).

River Evolution and Tectonic Implications

Shortly after integration with the proto–Gulf of California, the Colorado River established a smooth profile graded to sea level—the base of the Bullhead Alluvium (step 6 in Fig. 9). Increasing sediment load from the removal of divides, basin sediment fills, and especially by accelerated erosion on the Colorado Plateau led to rapid aggradation of sand and gravel in the lower Colorado River corridor as the 200–250-m-thick Bullhead Alluvium was deposited (Howard et al., 2015). A dated basalt flow interbedded in the Bullhead Alluvium in the Lake Mead area indicates that Bullhead Alluvium deposition was under way by ca. 4.5 Ma (Faulds et al., 2016). Ashes of known age in alluvial fans record the timing of piedmont response to Bullhead aggradation, and suggest that maximum levels of aggradation occurred shortly after 4.1 Ma; substantial post-Bullhead Colorado River incision had occurred by 3.3 Ma (House et al., 2008).

The top and base of the Bullhead Alluvium aggradation package each also serve as a datum to assess the amount of post-depositional vertical deformation (Howard et al., 2015; Crow et al., 2018b). In the lower Colorado River corridor, the highest Bullhead outcrops, generally on the flanks of the basins, define a mostly consistent upper Bullhead surface with a slope of 0.69 m/km (Fig. 10; Crow et al., 2018b). This slope of the top of the Bullhead Alluvium compares well with the 0.68 m/km slope of the top of a much younger river aggradational package, the 70-ka Chemehuevi Formation (Malmon et al., 2011). This coincident gradient for two very differently aged river aggradation packages is taken to indicate little tilting or offset of the ca. 4 Ma top of the Bullhead Alluvium regionally within most of the lower Colorado River corridor. Fault offsets occur in the central Lake Mead area where the top of the Bullhead Alluvium is offset ~200 m up to the east. Farther east and upriver, near the boundary with the Colorado Plateau, the top of ca. 6 Ma Hualapai Limestone is offset regionally another 130–165 m up-to-the-east across the Wheeler fault and associated folds (Howard and Bohannon, 2001; Crow et al., 2018b).

Mapping (summarized in Crow et al., 2018a) and subsurface studies (e.g., Metzger et al., 1973) allow for the identification of the base of the Bullhead Alluvium, which is below river level in the lower Colorado River corridor. In the center of some basins, this basal contact of the Bullhead Alluvium is significantly subsided by warping, faulting, and/or isostatic loading (Metzger et al., 1973; Howard et al., 2015; Thacker et al., 2017, 2018; Dorsey et al., 2017; Karlstrom et al., 2017). In the Blythe basin it is locally below sea level. However, in the divides between basins, the basal contact is only a few 10's of m below river level and projects toward Pliocene sea level, indicating little post–Bullhead incision, subsidence, or uplift. Although subsidence is documented in the center of some basins, regionally the gradient of uppermost Bullhead deposits in the lower Colorado River corridor suggests that the area has remained stable and not subsided or uplifted for the last 4–3 m.y. This leads to the interpretation that differential incision (Karlstrom et al., 2008; Crow et al., 2018b) across Lake Mead and Grand Canyon and fault offset of the top of the Bullhead Alluvium near the margin of the Colorado Plateau record a few hundred meters of uplift of the western Colorado Plateau area in the last 4 Ma (Howard et al., 2015; Crow et al., 2018b).

Geohydrological studies of the lower Colorado River valleys carried out by Metzger and Loeltz (1973), Metzger et al. (1973), and Olmstead et al. (1973) constitute a major achievement in characterizing the post-integration stratigraphy and regional distribution of the deposits of the lower Colorado River. These studies have richly informed all subsequent work. The post-integration evolution of the river involves the massive aggradation event of Bullhead Alluvium, followed by protracted phases of incision into the Bullhead, Bouse, and underlying deposits. A series of younger aggradation packages and other ancestral Colorado River deposits have been described including the Palo Verde alluvium (House, 2016; House et al., 2018), the facies of Santa Fe Railway (Howard et al., 2013; Reynolds et al., 2016), the boulder conglomerate of Bat Cave Wash (Howard et al., 2013), the Chemehuevi Formation (Malmon et al., 2011), the Riverside alluvium (House, 2016), and the Blythe alluvium (House, 2016; Block et al., 2018) (Fig. 11). Of these the 70 ka Chemehuevi Formation and the Holocene Blythe alluvium are the best studied. The Chemehuevi Formation records 100–150 m of fluvial aggradation (Malmon et al., 2011) before the river re-incised it and left flights of thin terraces lining the valleys. The Holocene Blythe alluvium (Block et al., 2018) records at least 35 m aggradation between 8 and 5 ka (Metzger et al., 1973; Howard et al., 2011).

Topock Gorge

Topock Gorge through the Chemehuevi (California side) and Mohave Mountains (Arizona side) cuts through one of the mountainous interbasin divides. In the early twentieth century, the constriction of this canyon (then called Mohave Canyon) was known to act as a hydraulic choke point that would hold back high stages of river flows and inundate bottom lands of Mohave Valley upstream (LaRue, 1925). The canyon was proposed in the

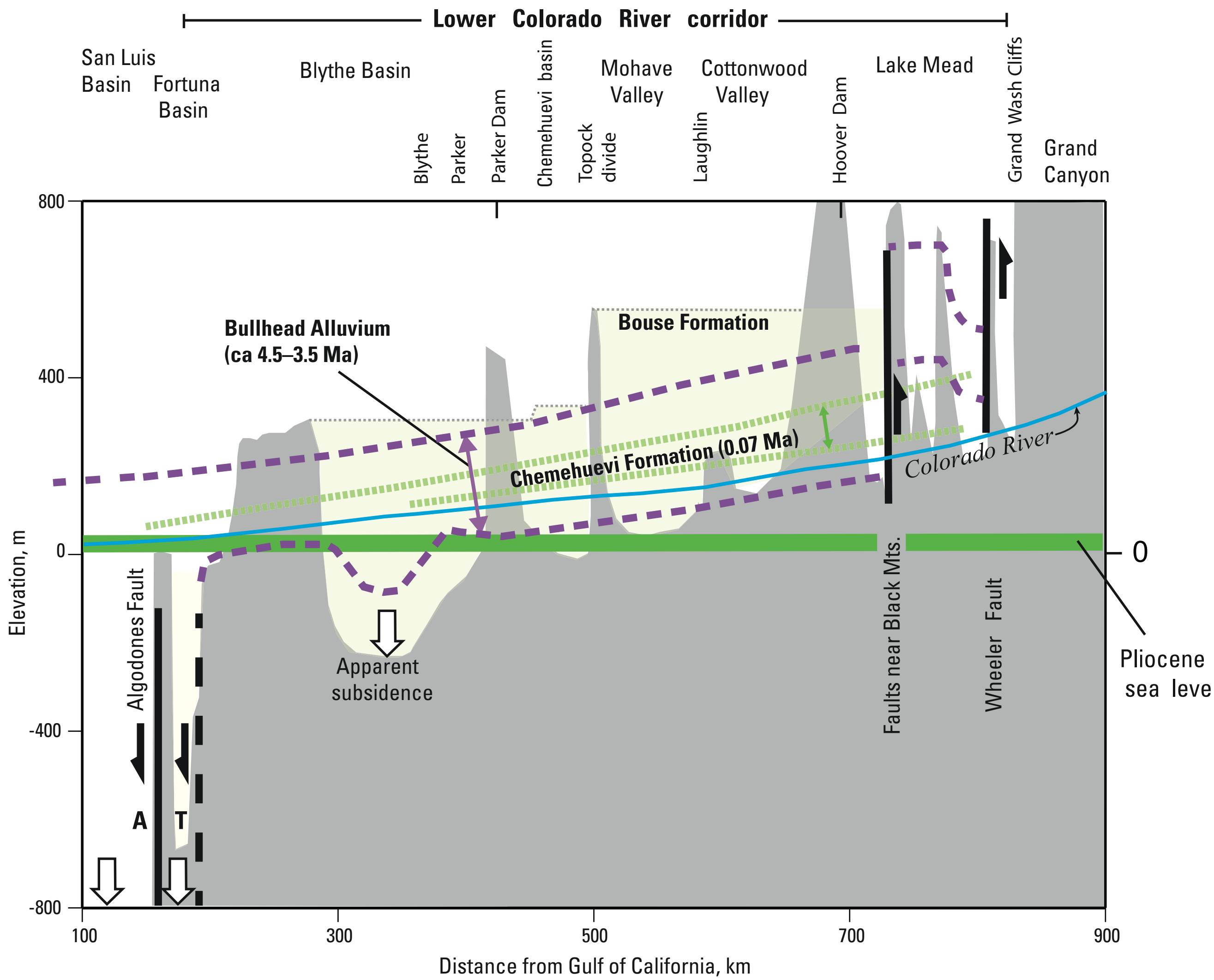

Figure 10. Sketched longitudinal profile of the ranges in elevation of the Bouse (pale green), Bullhead (dashed purple lines), and Chemehuevi (dashed green lines) Formations, from Grand Canyon downstream to the San Andreas plate-boundary zone at the Algodones fault. The modern river (blue), estimated range of Pliocene sea level, and pre–Colorado River topographic profile (gray background) are also shown (simplified after Howard et al., 2015). An expanded database of many more exposures further quantifies the elevation ranges of the formations (Crow et al., 2018a, 2018b).

early twentieth century as an optimal site to dam the river: "A dam built in this canyon would submerge the valleys … and form a reservoir with far greater storage capacity for a given height of dam than any other known site in the Colorado River basin" (LaRue, 1925, p. 84). That never happened, even though Parker Dam (at the next paleodivide downstream) and its Lake Havasu reservoir backfill the gorge and allowed a few meters of twentieth-century aggradation (Metzger and Loeltz, 1973). Most of Topock Gorge is now within the Havasu National Wildlife Refuge. The delta of the modern Colorado River building downstream into the Lake Havasu reservoir in the lower part of Topock Gorge hosts expanses of verdant, marshy wetlands.

The highest shoreline deposits of the Bouse Formation in Mohave Valley upstream (north) of Topock Gorge are 190–210 m higher[2] than the highest intact shoreline deposits south of the divide in Chemehuevi Valley. This difference is interpreted as recording separate Bouse lakes fed by the incipient lower Colorado River before the divide was eroded by overspilling and integration of the river (Pearthree and House, 2014).

The canyon is eroded along and near the gently east-dipping Chemehuevi detachment fault and its footwall of mylonitic granitoids and gneisses, on the west, separated from craggy upper-plate Miocene volcanic and sedimentary rocks and their nonconformably underlying crystalline basement on the east. As such,

[2]High value is the difference between intact shoreline deposits; lower value is the difference between the elevations of rare detrital clasts of likely Bouse travertine found in Quaternary alluvial fan deposits.

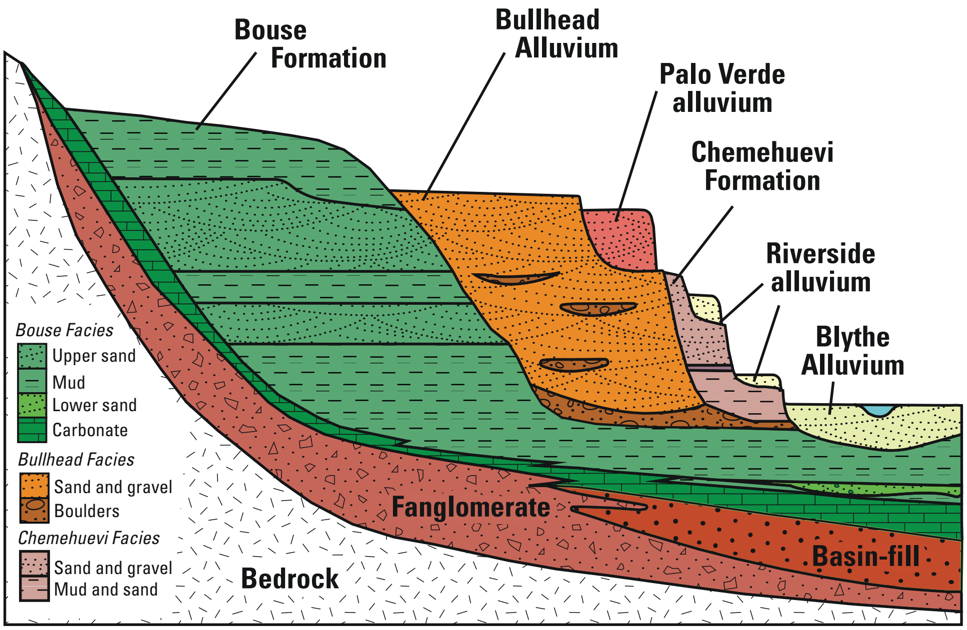

Figure 11. Generalized inset relations among Colorado River strata along the lower Colorado River strip (House, 2016).

the canyon reveals excellent exposures of the style and stratigraphic record of extensional deformation (John, 1987a; John and Howard, 1994; Howard and John, 1997; Miller and John, 1988, 1999; Howard et al., 2013). The gorge also exposes stratigraphic evidence of the Colorado River's post-Bouse evolution. A geologic river guide to Topock Gorge appears in the GSA Data Repository (see footnote 1).

In the early 1850s, the mountainous divide was encountered by Lt. A.W. Whipple's U.S. Army expedition to explore a transcontinental railway route. The expedition had already endured many difficulties crossing New Mexico Territory, but the terrain on the east side of Topock Gorge, south of The Needles, awed expedition member Lt. J.C. Tidball as "if possible, the worst yet. It was a confused mass of gorges, precipices, and serrated crests several thousand feet high ..." (Tidball, 2004, p. 124). Although exaggerating the magnitude of the relief, he captured its rugged nature.

The army's Colorado River expedition in the late 1850s under Lt. Joseph Christmas Ives surveyed the Colorado River for its navigability and natural history (Ives, 1861) (Fig. 12). Dr. John Strong Newberry, who later became G.K. Gilbert's mentor, was in charge of investigating the geology. Exploration was by a small steamboat built in Boston and sent by schooner to San Francisco, then back around Baja California by another ship to the Gulf of California and the mouth of the Colorado. Ives' (1861, p. 63–64) colorful impression of the approach into Topock Gorge ("Mojave Cañon") from the south was made before Lake Havasu flooded this valley behind Parker Dam:

> To-day has been perfectly serene, and the atmosphere indescribably soft and limpid. For several miles the river assumed a new aspect, being straight and broad, having high banks, and presenting a placid unbroken sheet of water—not a bar being visible above the surface. To one viewing the noble looking stream from the bank, it would have appeared navigable for vessels of the heaviest draught, but the depth of water was scarcely sufficient to enable the Explorer to pass without touching.
>
> Entering the foot hills of the Mojave range, the channel was again tortuous, and after traversing a narrow pass the Needles came in view directly in front. As we approached the mouth of the cañon through the Mojave mountains, a roaring noise ahead gave notice that we were coming to a rapid, and soon we reached the foot of a pebbly island, along either side of which the water was rushing, enveloped in a sheet of foam.
>
> After ascending few yards a harsh grating noise warned us that we were upon a rocky shoal, and Captain Robinson at once backed the Explorer out and went up in a skiff to reconnoiter…. There was danger that the after part of the boat in passing might catch upon a rock, and the bow be swung around by the rapid current against another with such violence as to knock a hole in the bottom. An anchor was carried to a point some distance up stream, and a line taken from it to the bow. This line was kept taut, while, with a high pressure of steam, the Explorer was forced up the rapids, once or twice trembling from stem to stern as she grazed upon a rock, but reaching the still water above without sustaining damage.
>
> A low purple gateway and a splendid corridor, with massive red walls, formed the entrance to the cañon. At the head of this avenue frowning mountains, piled one above the other, seemed to block the way. An abrupt run at the base of an apparent barrier revealed a cavern-like approach to the profound chasm beyond. A scene of such imposing grandeur as that which now presented itself I have never before witnessed. On either side majestic cliffs, hundreds of feet in height, rose perpendicularly from the water. As the river wound through the narrow enclosure every turn developed some sublime effect or startling novelty in the view. Brilliant tints of purple, green, brown, red, and white illuminated the stupendous surfaces and relieved their somber monotony. Far above, clear and distinct upon the narrow strip of sky, turrets, spires, jagged statue-like peaks and grotesque pinnacles overlooked the deep abyss.

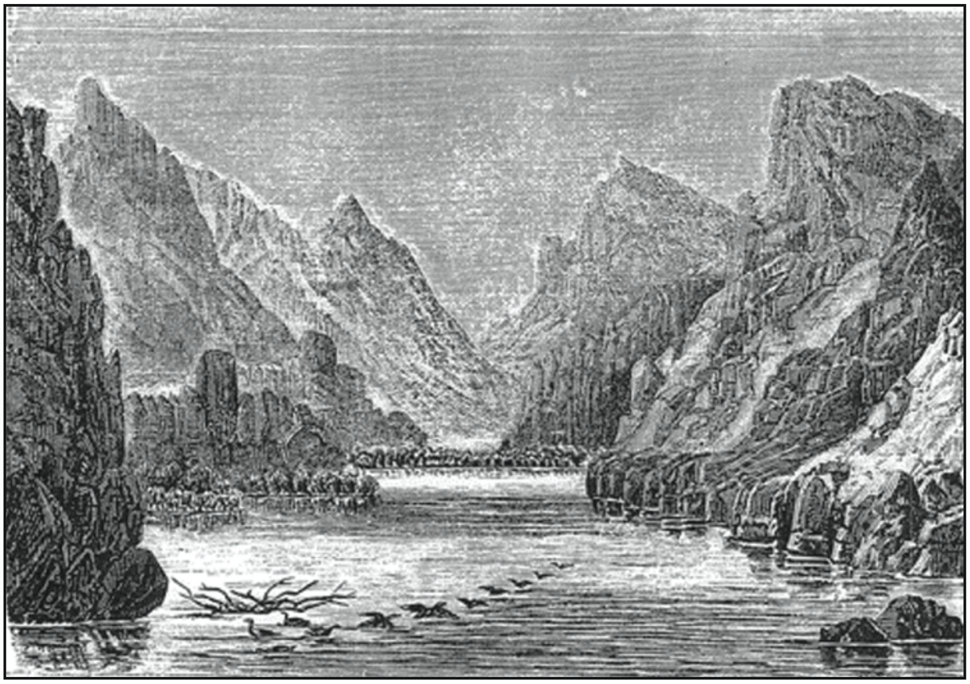

Figure 12. View downstream into Topock Gorge ("Head of Mojave Cañon") as pictured in the *Geological Report upon the Colorado River of the West* (Ives, 1861). Miocene rocks on the skyline dip steeply to the right (west) in hanging-wall blocks above the Chemehuevi detachment fault and Devils Elbow fault.

GUIDE AND ROAD LOG

This guide to field trip 21 of the Geological Society of America's 2019 Annual Meeting (Fig. 1) examines features that record the tectonic and magmatic evolution of the Colorado River extensional corridor and the subsequent birth and evolution of the lower Colorado River. Each day will examine features relevant to both the extensional corridor and the river's history. Day 1 explores features that record the Colorado River's earliest history in this region and its subsequent evolution, and the day introduces the Chemehuevi Mountains core complex. Day 2 by boat in Topock Gorge, reversing the route of the 1850s Ives expedition, examines the upper crust as dismembered by extensional faulting and tilting, and further explores records of the river's evolution. Day 3 addresses an upper-plate tilted block that exposes 15 km of crustal section, and finishes with a tribute to Warren Hamilton's field expertise and insights relating to both the complex tectonic history of the region and the evolution of the lower Colorado River.

DAY 0. Phoenix, Arizona, to Parker, Arizona

Drive west from Phoenix to Parker, Arizona, via I-10 westbound and Highway 95 (168 mi).

DAY 1. Parker, Arizona, to Laughlin, Nevada: Bouse Formation and Chemehuevi Mountains Core Complex

The road log (Fig. 1) begins in Parker, Arizona, adjacent to 'America's Nile,' the Colorado River (Fig. 13) and today ends in Laughlin, Nevada. Today, we gain an overview of the Colorado River extensional corridor (CREC) and of features that record the younger inception of the lower Colorado River. We cross into California and circle the Whipple and Chemehuevi Mountains core complexes spanning the central CREC. We continue a northward route to Mohave Valley and review evidence of overspilling lakes and their deltas, which integrated the Colorado River and its subsequent evolution.

Highlights on the Way to STOP 1-1

From the BlueWater Resort, drive south 1.4 mi on AZ 95 and turn right at the traffic light in Parker onto South California Avenue. In 1 mi, just across the Colorado River bridge, turn left on Rio Vista Drive to a parking area. We are on the outskirts of Earp, California, named for famed lawman Wyatt Earp, who lived part-time in the area beginning in 1906 and staked more than 100 copper and gold mining claims near the base of the Whipple Mountains (https://en.wikipedia.org/wiki/Wyatt_Earp).

STOP 1-1. Bouse Formation at Earp (34.1621° N, 114.3028° W)

The purpose of this stop is to introduce the geography of the river corridor and provide a first look at the Bouse Formation (upper Neogene) and discuss its role in understanding the integration of the Colorado River from Grand Canyon to the sea.

Here, we stand at the head of the Great Colorado Valley, named during the first government steamship exploration of this river in 1858–1859 (Ives, 1861). The Great Colorado Valley (GCV also known as the Blythe basin) extends south from Parker, Arizona, for 70 mi (113 km). The Colorado River floodplain is more than 9 mi wide in parts of the valley downstream

Figure 13. Photo of area by Warren Hamilton (inset) looking eastward over the Whipple Mountains, Colorado River, and the town of Parker (P). Dark hogbacks are SW-tilted Miocene rocks riding "nose-down" (a favorite Hamilton phrase) on light-toned footwall gneisses that form the footwall of the Whipple detachment fault. Parker sits within the large Blythe basin, a major depocenter first for water and then for sediments carried by the initial Colorado River and deposited as the Bouse Formation. East of Parker in the upper right of the photo is the Cactus Plain dune field. This large eolian complex is dominated by sand reworked from ancestral Colorado River deposits (Zimbelman and Williams, 2002; Muhs et al., 2003). Photos courtesy of Lawrence Hamilton.

Figure 14. Planar cross-bedded gravel interpreted as shoreline deposits interbedded with limestone of the Bouse Formation at STOP 1-1. Note the yellow oxidation of some of the sediments. This is a characteristic feature of sands and gravels in the Bouse that are or were capped by the Bouse limestone. Construction along the highway to Earp has made exposures in this area larger but even more dangerous to access here. If you are not driving, try to get a quick look at the new exposures.

and spans 435 mi^2. Most of the floodplain is cultivated. Historical aerial photos and early maps show that the active channel of the river was, in some places, more than 1 mile wide. Characteristic, easily discernible scroll bars, meander cutoffs, and paleochannel tracts are present across the floodplain, hinting that the river may have wandered the entirety of its floodplain width regularly—possibly in decades and almost certainly in centuries.

Three subdivisions of the GCV are delineated north to south by the modern and mostly engineered river position: Parker, Palo Verde, and Cibola Valleys. The narrowest span of the GCV is just over 3 mi wide ~30 mi south of our location. There (we will be passing through this point on Day 3), the southeastern tip of the Big Maria Mountains abuts the river on the California side, where its course begins to track obliquely across the floodplain for 8 mi toward the Arizona side to then follow the eastern floodplain margin near Ehrenberg, Arizona. This departure demarcates the boundary between Parker Valley on the north, where the floodplain is mostly in Arizona, and Palo Verde Valley to the south, where the floodplain is mostly in California. A major irrigation diversion structure, Palo Verde Dam, was built in 1958 at the upstream end of the departure of the Colorado River channel to the Arizona side of the floodplain. A structurally fortified westward bend of the river creates Cibola Valley, a small valley at the southern end of the GCV, most of which is in the Cibola National Wildlife Refuge.

The GCV occupies the Blythe basin, core of the largest basin to have stored the primordial waters of the Colorado River and possibly part of a marine estuary. High-standing Bouse Formation limestones and shoreline gravels are scattered along the perimeter of the GCV, and are known to extend into distal reaches as far as west as Amboy, California; as far east as Bouse, Arizona; and south to the flanks of the Chocolate Mountains (Miller et al., 2014; Spencer et al., 2014).

At this site, we see Bouse Formation limestone overlying deposits of weakly to moderately wave-worked gravel, winnowed from alluvial-fan deposits of the Osborne Wash Formation of Davis et al. (1980) (Fig. 14). This association of wave-worked gravel and limestone is the transgressive nearshore facies association in the Bouse. The highest remnants of this facies association are interpreted as evidence for lake highstands in each valley. A previously long-lived subaerial environment of alluvial fans and playas is inferred to have been rapidly inundated by water enriched in carbonate. The basal carbonate of the Bouse is the most common transgressive facies. Many of its outcroppings include conspicuously white layers of limestone, travertine, or calcareous mudstone forming intricate drapes over individual clasts on alluvial fan surfaces, colluvial slopes, or irregular bedrock surfaces. In some areas such as here near Earp, the carbonate rocks are found interbedded with cross-bedded shoreline gravel composed of subrounded gravels derived from underlying units, including bedrock.

Each valley along the lower Colorado River corridor contains this association, indicating rapid inundation of a dry desert landscape by waters rich in solutes and starved of sediment at progressively higher elevations above sea level toward the valley margins. Moreover, the highest remnants of this association in each valley are found to generally occur at consistent elevations through the length of the valley, recording a surface that we interpret as water level dammed by topographic divides.

Highlights on the Way to STOP 1-2

Return to the paved highway, turn left, and pass roadcuts in Bouse Formation a short distance to a stop sign. Turn left and follow highway CA 62 west for 23.2 mi. We are driving along the southern flank of the domal Whipple Mountains metamorphic core complex. Highly faulted dark Miocene volcanic and sedimentary rocks are structurally superposed onto middle crust Proterozoic and Cretaceous gneisses along the Whipple Mountains detachment fault (Davis et al., 1980; Carr, 1991). The core complex and faulting resulted from extreme Miocene extension that doubled the 50 km width of the CREC, as the gneissic footwall rose relatively southwestward from under a collapsing upper crust (Howard and John, 1987). Dark Savahia Peak to the northwest represents the most conspicuous extensional klippe of Miocene rocks above gray to greenish footwall gneisses. Gans and Gentry (2016) reinterpreted western exposures of crystalline rocks as nonconformably below rather than faulted against Miocene volcanic deposits, and interpreted the now subhorizontal Whipple detachment fault in that area as initiated as a normal fault dipping 50–60° northeast. Using that information and a fanning of Miocene dikes, which are progressively steeper eastward in dip in more eastern locations in the footwall, it is easy to imagine that the fault and its footwall have been domed upward and flexed, although a variety of alternative explanations have been offered (Gans and Gentry, 2016).

At Vidal Junction, turn right on U.S. 95 northward and proceed for 31 mi. At just past 6 mi, there are some limited outcrops of Bouse Formation basal carbonate on the east (right) side of the road that overlie alluvial fan deposits derived from the Whipple Mountains to the north. These and more extensive basal carbonate deposits to the northeast were draped over a ca. 5 Ma alluvial piedmont whose general configuration was very similar to the modern landscape. Proceeding to the west and then north, we pass between the Whipple Mountains on the right (east) and the Mopah Range and more distant Turtle Mountains on the left (west). The Turtle Mountains and adjacent Mopah Range host modestly faulted and tilted Miocene volcanic deposits nonconformable on Proterozoic basement gneisses (Carr et al., 1980); Hazlett, 1990; Nielson and Turner, 1986). They are interpreted as part of the breakaway zone for the CREC faults (Davis et al., 1980; Howard and John, 1987; Gans and Gentry, 2016).

About 25 mi north of Vidal Junction, a hill of light-toned Cretaceous granodiorite on the right side of the road, cut by numerous dark and rusty-colored dikes, is the southwestern-most exposure of the Late Cretaceous Chemehuevi Mountains Plutonic Suite (John and Wooden, 1990). The suite, along with similar dike swarms, makes up much of the footwall to the Chemehuevi Mountains core complex, ahead on the right (Fig. 15). The

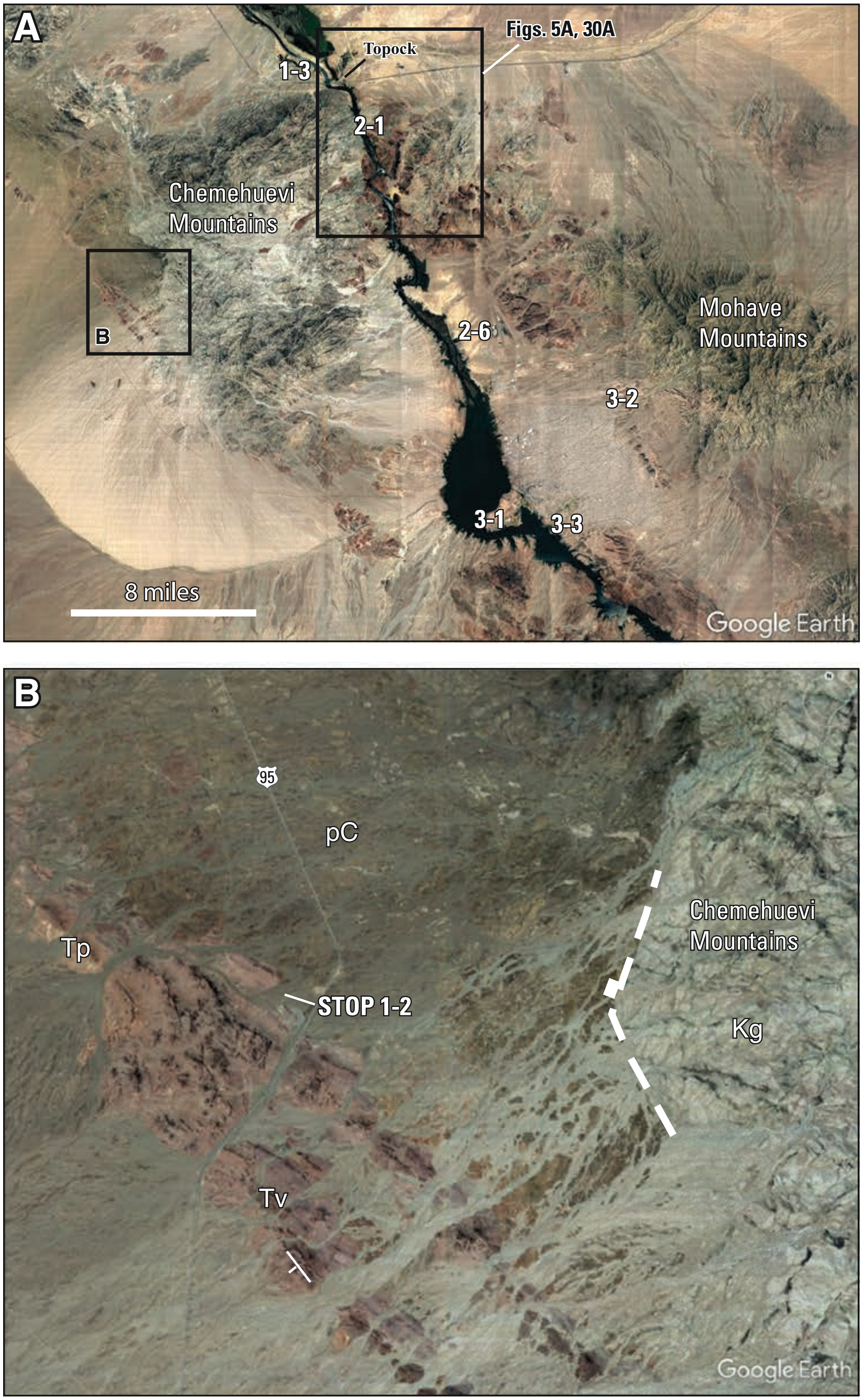

Figure 15. (A) Google Earth view of the Chemehuevi Mountains area showing selected field-trip stops. Box shows the location of 15B and STOP 1-2. Light-toned rocks making up the Chemehuevi Mountains core are granitoids and gneisses in the lower plate of the Chemehuevi detachment fault, and are mostly encircled by varicolored volcanics, sedimentary rocks, and gneisses above that fault. The Colorado River follows Topock Gorge between Topock and STOP 2-6, where it widens into a main part of Lake Havasu reservoir. (B) The area around STOP 1-2 at Snaggletooth. Tp—Peach Spring Tuff; Tv—older Miocene volcanics (repeated by normal faulting) in the Sawtooth Range; pC—their substrate of Proterozoic gneiss and granite; Kg—Chemehuevi Mountains Plutonic Suite (along with dark cross-cutting dikes) in the lower plate of the (dashed) Chemehuevi detachment fault.

granite here yielded a ^{40}Ar-^{39}Ar biotite cooling age of 66.5 ± 0.4 Ma, interpreted as rapid cooling following emplacement in the uppermost mid-crust (~4 kb; John and Wooden, 1990; John and Foster, 1993). We will see more of the core complex tomorrow. Study of piedmont alluvial fans, using ^{10}Be and ^{26}Al isotopes, adjacent to the western Chemehuevi Mountains and the Stepladder Mountains to the west yielded estimated bedrock erosion rates between ~40 and 10 mm ky^{-1} for the adjacent mountains (Nichols et al., 2005).

At ~31 mi past Vidal Junction, we will cross the Sawtooth Range at Snaggletooth pinnacle and pull off to the left to park.

STOP 1-2. The Chemehuevi Mountains Core Complex and Miocene Volcanic Rocks at Snaggletooth (34.5928° N, 114.6360° W)

The purpose of this stop is to introduce the Chemehuevi Mountains core complex and Miocene volcanic succession that lies in the hanging wall to the detachment fault system, and erupted early in the development of the CREC (Fig. 15).

Snaggletooth pinnacle and the Sawtooth Range are made of SW-tilted and fault-repeated early Miocene volcanic rocks (Fig. 15B). A dacitic rock near Snaggletooth was dated by U-Pb on zircon as 20.3 ± 0.9 Ma (Chapman et al., 2018). The 18.8 Ma Peach Spring Tuff lies at the top of the section here. The volcanic sequence rests nonconformably on Proterozoic gneiss, granite, and steeply dipping diabase sheets. To the northeast in the Chemehuevi Mountains, dark Proterozoic granitic rocks of this basement substrate can be seen prominently superposed along the Chemehuevi detachment fault onto light-toned Cretaceous rocks of the Chemehuevi Mountains Plutonic Suite. The gently west-dipping fault cuts out many kilometers of crustal section, as its hanging wall represents the upper crust in the early Miocene, and its footwall of Cretaceous granitoids and dark dikes have been exhumed from the middle crust. The Chemehuevi detachment fault nearly encircles the range (John, 1987a, 1987b). A seismic reflection profile has been interpreted by D. Okaya and E. Frost to indicate other southwest-tilted fault blocks, and one or more breakaway faults to the southwest of here (Frost and Okaya, 1986; Pridmore and Frost, 1992).

Introduction to the Chemehuevi Mountains

The Chemehuevi Mountains lie in the center of the CREC in the region of maximum crustal extension. All rock types in the range older than small young Miocene basaltic dikes and plugs were deformed during extension. The deformation produced three brittle low-angle normal faults, separating four plates. The footwall of the Chemehuevi Mountains includes the structurally deepest exposed rocks in the range, below the lowest exposed and small displacement (<2 km) Mohave Wash fault. This fault is structurally overlain and cut by the large-displacement (>15 km) Chemehuevi detachment fault, in turn overlain by the structurally higher Devils Elbow fault (John, 1987a, 1987b). The two structurally deepest faults are exposed a distance of more than 23 km in a down-dip direction, across a total area greater than 350 km^2.

Slip on each of the low-angle normal faults resulted in NE transport of successive hanging walls. At outcrop scale, each of the faults is planar, but when viewed at map scale, both the Mohave Wash and Chemehuevi faults are corrugated parallel to the northeastward slip direction. Dips on each fault vary from very gently inclined along the crests or troughs of corrugations, to as much as 40° parallel to the steeper flanks, or strike slip portions, of the faults (John, 1987a). Orthogonal to and superimposed on these corrugations are broad N-NW–striking antiformal and synformal undulations of the fault surfaces. Regionally, the Chemehuevi and Mohave Wash faults dip gently (10–15°) southwest along the western flank of the range, and gently toward the northeast (2–15°) on the eastern flank near Topock Gorge (Day 2).

The footwall to the Chemehuevi detachment fault crops out as a domal exposure of igneous and metamorphic rocks in the central part of the range (Fig. 15). These crystalline rocks include mylonitized Proterozoic layered gneisses and migmatites, the voluminous Late Cretaceous Chemehuevi Mountains Plutonic Suite (73 ± 8 Ma; John, 1988; John and Mukasa, 1990; John and Wooden, 1990), and a swarm of younger Cretaceous (?) and Miocene dikes.

The Chemehuevi Mountains Plutonic Suite forms a compositionally zoned, calc-alkaline sill- or laccolith-like body. The magma chamber associated with the body evidently grew laterally in stages, with each pulse more fractionated than the previous one (summarized in Fig. 4; John, 1988). The reconstructed shape of the body shows a flat floor for the lower part of the suite, intruded by at least three feeder dikes that fed the chamber. This floor is characterized by *lit-par-lit* intrusions into subhorizontally foliated mylonitic gneisses (Day 2). The roof is unexposed in the Chemehuevi Mountains, but apparent cupolas (Fig. 4C) occur in steeply tilted allochthons to the east in the Mohave Mountains, where granitoids correlated to the suite discordantly intrude Proterozoic gneisses (Fig. 5; Howard et al., 2013).

As viewed from STOP 1-2, erosion has carved a window through the domed detachment fault system, exposing the light-colored footwall. The domed fault crops out also in the eastern Chemehuevi Mountains and Topock Gorge (Day 2, STOPS 2-2 and 2-3). The dark weathering dikes that cut the footwall are part of a voluminous dike swarm that intrude rocks above, below, and along the Chemehuevi detachment fault in the western, southern, and central parts of the range (John and Foster, 1993; LaForge et al., 2017). Dikes in the west-central footwall are hosted by the isotropic Chemehuevi Mountains Plutonic Suite, and form two roughly orthogonal sets, striking WNW and SSW with moderate to steep dips. In the central and northern parts of the range, dikes intrude older plutonic rocks and Proterozoic country rocks; the dominant strike changes to ENE (subvertical dip). In contrast, dikes in the structurally deepest exposed part of the footwall strike ENE, dip gently SE, and commonly host a mylonitic fabric.

The dikes range in composition from mafic to felsic, and are of several generations. The swarm is subdivided, based on mineralogy, texture, and whole-rock geochemistry, into progressively younger types: altered, xenolith-bearing hornblende diorite, diabase and lamprophyre, basalt, trachybasalt, basaltic trachyandesite, trachyandesite, trachydacite, dacite, and rhyolite (50.9–80.5 wt% SiO_2; LaForge et al., 2017). Geographically, mafic to intermediate-felsic dikes are present throughout the footwall to the detachment system. In contrast, dikes having >70% SiO_2 are characteristic of and restricted to the northeasternmost footwall.

The dike swarm is similar in major element chemistry to Miocene dikes hosted in the adjacent Whipple and Mohave Mountains, and to pre–Peach Spring Tuff volcanic deposits, the Swansea Plutonic Suite in the Buckskin Mountains (east of Parker), the Peach Spring Tuff, and post–Peach Spring Tuff volcanic deposits hosted in the Black Mountains (Fig. 7). Trace-element concentrations in dikes in the Chemehuevi Mountains are comparable to coeval regional plutonic and volcanic rocks, but differ from the Peach Spring Tuff ignimbrite (Pease, 1991; Bryant and Wooden, 2008; Pamukcu et al., 2013; McDowell et al., 2014; Gentry, 2015).

Dike intrusion in the Chemehuevi Mountains temporally overlapped extrusive volcanism and spanned the timing of extension. Some dikes predate hanging-wall tilting of the 18.8 Ma Peach Spring Tuff as indicated by U/Pb zircon ages of dacite dikes from 21.45 ± 0.19 Ma (mylonitic biotite dacite), to 20.94 ± 0.13 Ma and 19.2 ± 0.11 Ma (undeformed biotite, hornblende dacite, and biotite dacite, respectively) (LaForge et al., 2017). Post-detachment basalt, in thin north-striking dikes, plugs, and local flows dated at 11.1 ± 0.3 Ma (K-Ar whole-rock), intrudes and locally fuses cataclasites associated with detachment faulting (John, 1986, 1987a), implying the basalt locally flowed onto an erosional surface that truncated the central part of the Chemehuevi detachment fault system after slip ceased.

Structural constraints on the initiation angle of the detachment fault system exposed in the Chemehuevi Mountains are based on a wide variety of observations, including fault rock type and associated mineral deformation mechanisms, orientation and cross-cutting relations of syntectonic dikes and faults, and lack of change in metamorphic grade of footwall rocks to the regionally developed normal fault system. In each case, the initial dip of the fault is limited to <30°. Application of $^{40}Ar/^{39}Ar$ and fission-track thermochronology to rocks in the footwall of the fault system provides further constraints on the timing and initiation angle of regional detachment faulting. At the onset of extension ca. 23 Ma, granitic rocks now exposed in the southwestern and northeastern portions of the footwall were at <200 °C and >400 °C respectively, separated by a distance of ~23 km down the known slip direction. This gradual increase in temperature with distance is attributed to the gentle tilting and warping of an originally inclined depth section across horizontal isotherms. Assuming reasonable geothermal gradients, that inference constrains the exposed part of the Chemehuevi detachment fault to have had a regional dip initially less than 30° before warping (John and Foster, 1993).

A seismic profile southwest from the area of STOP 1-2 has been interpreted by Okaya and Frost as showing a series of fault blocks tilted southwest, riding above a regionally extensive Chemehuevi detachment fault (Frost and Okaya, 1986; Pridmore and Frost, 1992). Gans and Gentry's (2016) alternative model for the Whipple detachment fault has the westernmost part of that fault dipping steeply before it was domed to a gentler western dip.

Highlights on the Way to STOP 1-3

Continue on U.S. 95 northward for ~12.7 mi to Five Mile Road. The Chemehuevi detachment fault dips west off the back side of the core complex, and the multicolored hills include Proterozoic gneisses capped by the steeply dipping Miocene volcanic deposits we just visited, in the hanging wall to the fault system. En route, we summit Lobecks Pass, a narrow pass between the northern Chemehuevi and southern Sacramento Mountains ~7 mi from STOP 1-2.

Immediately after leaving the narrows (southwest of the South Needles gas compressor station), we drive over the culmination of the Colorado River gravity high. Here the peak of the gravity high is roughly 20 mGal above the background (Campbell and John, 1996). The Colorado River gravity high is a positive gravity anomaly coincident with the axis of the CREC. This gravity high, along with a subparallel magnetic high, extends along the zone of documented maximum mid-Tertiary extension for ~150 km alongside the Colorado River, having magnitudes of 10–20 mGal above the regional background (Simpson et al., 1990; Campbell and John, 1996). The elliptical gravity culmination here beside the Chemehuevi and Sacramento Mountains is ~10 km across, and is underlain by the small (~50 km^2) 19 Ma Sacram pluton, including mixed and mingled diorite/gabbro and hornblendite, with granodiorite and granite at the site of the peak of the gravity high. Miocene diorite has the highest measured densities in the area, and is interpreted to be the minor surface expression of a larger, deeper mafic source for the Colorado River gravity high, modeled as the top of the massive subvertical dike system. As noted above, the modeled magmatic inflation of this dike system would account for 5–18 km, 10%–20% of the total CREC extension (Campbell and John, 1996). As we continue downhill, to the north (left) we view the white 19 Ma "Sacram granite" and associated diorite exposed in the lowlands. Campbell-Stone et al. (2000) used the Miocene pluton's age and outcrop elongation, together with a cross-cutting Miocene dike swarm and other indicators of extension, to propose that three discrete magmatic episodes record rotation of the least principal stress direction, in the horizontal plane, from 055° to 015° azimuth between ca. 20 and 17 Ma.

Shortly after we pass through the last of the bedrock hills, look for a low, light-colored embankment crossing oblique to the highway. This is part of an extensive set of outcrops of fine-grained, greenish-colored siliciclastic Bouse deposits capped by thin Quaternary alluvial fan and terrace deposits; remnants of Bouse basal carbonate are draped on paleo-bedrock topography on the margins of the hills to the southwest.

Turn right on 5 Mile Road (Old Trails Highway), continue for 1.4 mi, and merge onto I-40 eastbound toward Kingman, Arizona. Swelling clays of Bouse Formation siliciclastic beds that underlie much of the next 5 mi of the interstate highway have necessitated expensive road repair. In 5.2 mi, take the Park Moabi exit, then turn left over the freeway, and proceed 0.5 mi on Park Moabi Road past a roadcut that exposes claystones of the Bouse Formation overlain by Chemehuevi Formation and interfingered angular locally derived gravels. Extensive exposures of thin beds of Bouse limestone in the area are draped on steep alluvial fan surfaces and locally interbedded with angular gravels higher on the piedmont to just north of I-40. Turn left on National Old Trails Road for 0.8 mi.

STOP 1-3. Park Moabi—Bouse Formation (34.7259° N, 114.5236° W)

The purpose of this stop is to examine deep-water siliciclastic Bouse beds that we interpret to have been deposited near the southern end of a giant lake in a basin (Mohave basin) distinct from the Blythe basin of STOP 1-1 (Fig. 16).

At this point we are in the southern end of the Mohave basin. The distribution of highest Bouse Formation shoreline gravels and high-standing deposits of travertine in Mohave Valley is found at comparable levels in Cottonwood Valley, the next valley to the north. This has led us to conclude that a large lake inundated both valleys to as deep as 365 m. Here, at the south end of the valley, we can view deepwater pro-delta deposits in the part of the Bouse Formation that Metzger (1968) called the interbedded unit. We see multiple fining-upward sand beds in a section that is primarily greenish mud. The sand beds likely are density current (turbidite) deposits emplaced in deep water in the distal part of the lake, and may have been related to flood events of the Colorado River entering the lake at its north end. A key point is that we are likely near the upstream face of a paleodivide that once separated Mohave-Cottonwood Valley from Chemehuevi Valley, and these deposits are from the distal part of the river delta that was at the head of the lake many miles upstream.

Figure 16. Resistant fining-upward tan sand beds in greenish-gray clay and silt deposits of the Bouse Formation near Park Moabi. The sand beds likely record prodelta turbidites deposited in deep water, with finer-grained deposits representing the gradual settling of suspended load (Turak, 2000; Pearthree and House, 2014). These types of deposits are present in the Bouse in each valley.

The Bouse Formation here in Mohave Valley has a stratigraphy similar to that in the Blythe basin (STOP 1-1), even though it occupied a hydrologically separate and presumably slightly older lake basin. Exposures of the Bouse Formation in the Park Moabi area include the basal carbonate draped over alluvial fan deposits, overlain by the thick pro-delta sequence of interbedded mudstone and fine sandstone. Small-displacement normal faults can be seen to cut Bouse Formation sediments at this site. Upper Pleistocene deposits from local tributaries and the Colorado River overlie the Bouse Formation here.

Highlights on the Way to STOP 1-4

Return eastward a short distance to Park Moabi Road and continue across it on National Old Trails Road for 1.4 mi to a site near the Colorado River and its bridges. See the "Topock Gorge Geologic River Guide" in the GSA Data Repository (see footnote 1).

STOP 1-4. Coarse Conglomerate Deposited by the Colorado River (34.7267° N, 114.4990° W)

Here are good exposures of a very coarse-grained Colorado River deposit that overlies the Bouse Formation and older fan deposits above an erosional unconformity. This coarse conglomerate (Metzger and Loeltz, 1973) may correlate to a thicker and higher boulder conglomerate found on the Arizona side of the river south of Topock. Both are mapped as the boulder conglomerate of Bat Cave Wash (Howard et al., 2013; Figs. 17, 18). Similar post-integration fluvial boulder conglomerates are exposed near Laughlin and along Topock Gorge (STOPS 2-3 and 2-5).

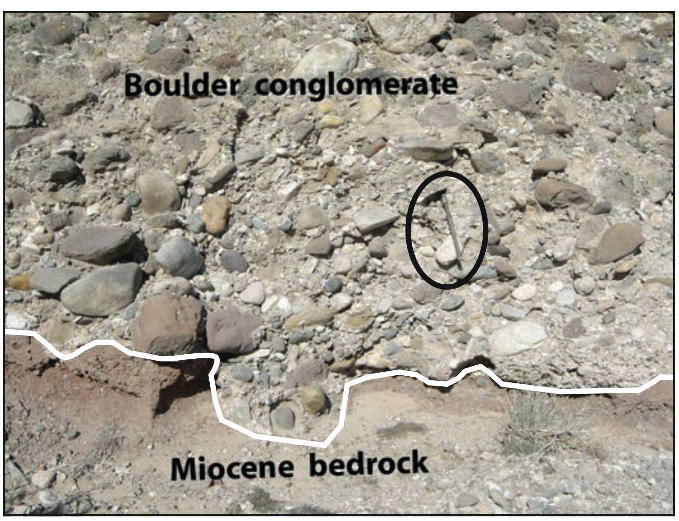

Figure 17. Coarse fluvial deposit, mapped as boulder conglomerate of Bat Cave Wash, 1.5 km SE of Topock on the Arizona side of the river (Howard et al., 2013). Boulders of gneiss and basalt are as large as 0.9 m across. Far-traveled rounded chert clasts are as wide as 0.2 m across. Current imbrication is toward the east-southeast (toward the camera). The trenching tool is 0.6 m long. The deposit here fills a channel cut into a substrate (at bottom) of red, poorly sorted, Middle Miocene alluvial-fan conglomerate (Howard and Malmon, 2011).

Together several of them outline an apparent N–S gradient 3× as steep as the modern river (Fig. 18), but exposures are insufficient to ascertain the full thickness and elevation range of the unit(s).

The coarse fluvial conglomerate here consists of rounded far-traveled Colorado River cobbles mixed with subrounded locally derived cobbles and small boulders. Boulders nearby in this deposit include vesicular basalt like that prominent in fans on the east flank of Mohave Valley, where they are derived from the Black Mountains. The clast assemblage may indicate that the fluvial boulder deposit scavenged clasts from alluvial fans on both sides of the river valley. The stratigraphic affinities of the coarse riverlaid conglomerates remain to be fully resolved, whether they represent the base of the Pliocene Bullhead Alluvium or younger inset riverlaid deposits or some of both.

Two much younger and unconsolidated rounded bouldery deposits occur in (post–70 ka) Riverside terraces 2 km downstream from STOP 1-4. They include rounded extra-local quartzite cobbles as large as 30 × 15 cm, as well as subrounded boulders derived more locally (Howard and Malmon, 2011).

The upper Pleistocene Chemehuevi Formation also crops out locally here, consisting mostly of sand and mud. The Chemehuevi Formation and the Bullhead Alluvium represent two major aggradational episodes by the river, respectively 100–150 m and 200–250 m thick.

A Holocene aggradation is also revealed, based on ^{14}C-dated riverlaid sediments drilled here for an engineering project to remediate contaminated groundwater (Fig. 19). The ^{14}C chronology indicates river aggradation between 9 and 6 ka (Howard et al., 2011). Near-zero ages in the upper 11 m of the section were interpreted to record a combination of the thickness of sediment disturbed by post–5 ka scouring (an inferred unconformity), overlain by sediment accumulated since 1938 in the upper reaches of Lake Havasu reservoir and by dredge spoils.

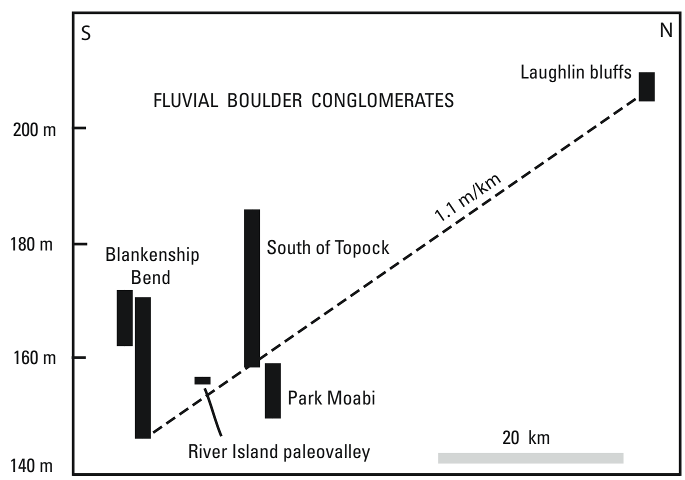

Figure 18. Longitudinal elevation profile of fluvial boulder conglomerates from north of Laughlin, Nevada (the conglomerate of Laughlin—House et al., 2005) south to Blankenship Bend (STOP 2-5). Distances are along the river.

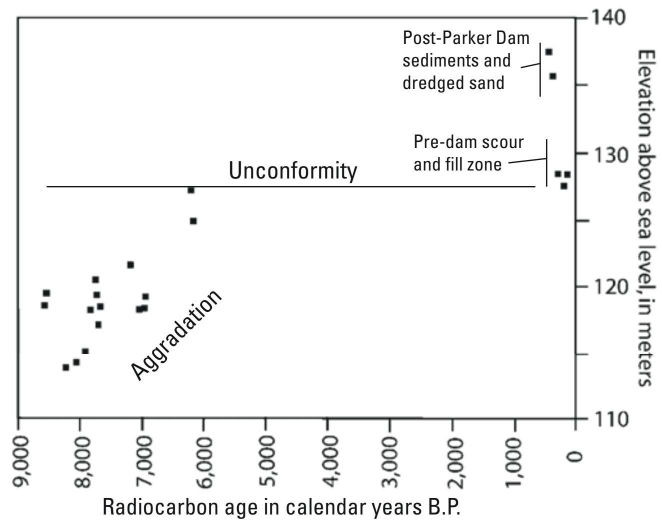

Figure 19. ^{14}C ages of Colorado River sediments drilled in six holes adjacent to the Colorado River near Topock, plotted against elevation (Howard et al., 2011).

Highlights on the Way to STOP 1-5

Return to I-40 and continue eastbound 1.8 mi across the river. The upstream end of Topock Gorge forms the rugged spectacle to the south, tomorrow's destination (Fig. 12). Spanning the river on the right (and now carrying a pipeline) is the Old Trails Arch Bridge (Fig. 20), which originally housed the roadbed of the legendary U.S. Route 66 featured in the film *The Grapes of Wrath* (1940), as well as the opening credits of *Easy Rider* (1969). The bridge is a brace-ribbed, hinged-arch bridge built in 1915–1916, and served as the highway bridge until 1948, when the Red Rock Bridge (formerly the railroad bridge) was modified for highway use. The pipeline that today uses the arch bridge carries natural gas to southern California.

Take the Topock exit 0.4 mi past the river crossing and turn left over I-40 onto AZ Route 10. Continue 5 mi along Arizona Route 10 past Topock Landing following the margin of the marsh. Before the river was dammed, its channel shifted often (Fig. 21) and summer high flows typically filled the wide floodplain. Aggradation in this area and flooding of Topock Marsh beside us resulted from impoundment of Lake Havasu downstream.

In 1 mile, we will cross the tamarisk-choked mouth of Sacramento Wash, a large ephemeral Arizona drainage. Gently to moderately tilted beds of Bullhead Alluvium are exposed along parts of the wash upstream (Howard et al., 2013). Beyond the wash, pass pink hills of Chemehuevi Formation. Five mi past I-40 at Golden Shores follow the traffic circle to County Route 1.

Continue north for 4.2 mi past roadcut exposures of cross-bedded sandstone of the Bullhead Alluvium adjacent to Topock Marsh. The highway merges with Courtwright Road at ~12.5 mi. Here an outcrop of the Chemehuevi Formation can be seen behind a small power plant. Near here, and at three other sites to the north between here and Hoover Dam, the Chemehuevi Formation contains the Monkey Rock tephra bed, tephro-correlated to ca. 70 ka (Malmon et al., 2011).

Continue west across the historical river floodplain for 3.7 mi (Fig. 21) and turn right at the stop sign onto Arizona 95 toward Bullhead City. The floodplain experienced many historical changes in appearance and in the position of the river and lakes before engineering development (e.g., Malmon et al., 2010). Continue north for 10.5 mi to Aztec Road, where we will turn left (west) and stair-step down a series of thin, post-Chemehuevi gravel terraces for 1.5 mi on our way to the floodplain. The terrace gravels sit atop Bullhead Alluvium in exposures along the river. For 1 mi, we will be crossing the historic floodplain of the Colorado River. Ahead of us, the Pliocene Bouse Formation

Figure 20. 1924 view upstream (north) at the National Old Trails Arch Bridge and the railway bridge upstream from it (LaRue, 1925). The river enters Topock Gorge to the right of this scene.

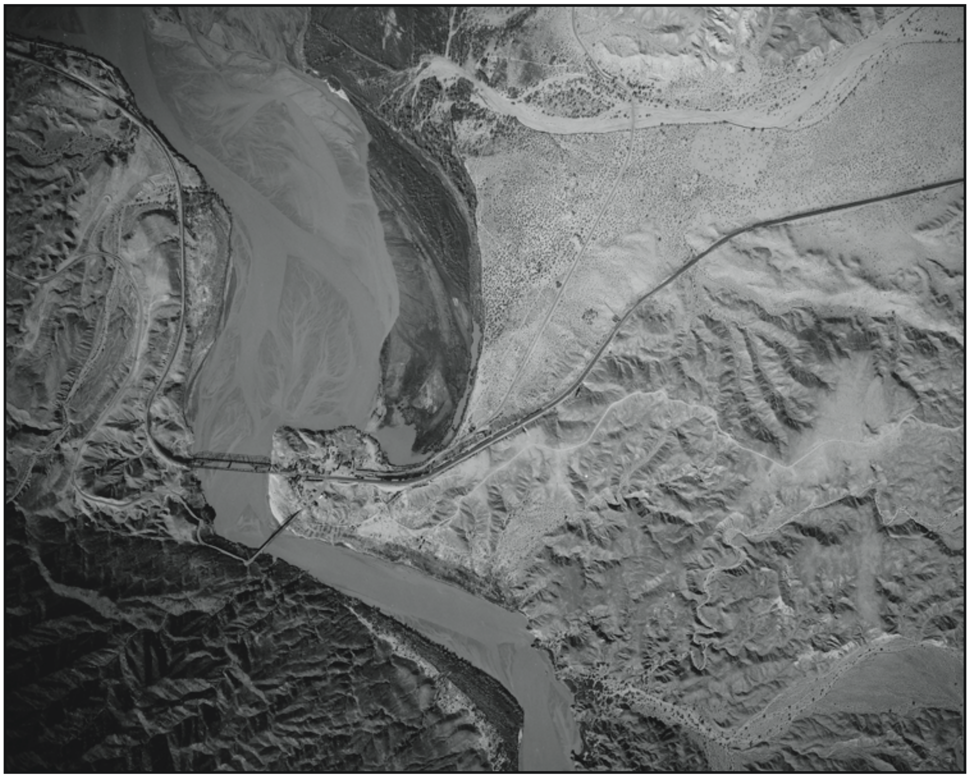

Figure 21. January 1936 aerial photograph of the Topock Crossing of the lower Colorado River, before the river downstream was dammed to form Lake Havasu reservoir. North at the top. Source: Fairchild Aerial Surveys, Flight C-3821A, commissioned by U.S. Dept. of the Interior.

banks up against the east flank of the Dead Mountains to Pliocene shoreline elevations as high as 560 m a.s.l., 390 m above the highway (House et al., 2005).

Continue along Aztec Road across the Colorado River into Nevada. Take a right at the stop sign and follow Aha Macav Parkway for 4.7 mi to its intersection with Needles Highway on the piedmont of the Dead Mountains. Turn right. Continue north for 4.4 mi, looking ahead to views of a pediment cut on granite, and at pre-Bouse upper Miocene fanglomerate that overlaps the pediment and buttresses against an erosional scarp at the lower end of the pediments (Fig. 22). Pass through roadcuts of this fanglomerate (cut by small faults). Past the roadcuts, carefully pull into a clearing on the opposite (west) side of the road before reaching a conspicuously brownish-red rock outcrop.

STOP 1-5. Perched Pediment, Mirage Pluton, and Newberry Fault (35.1233° N, 114.6394° W)

The purpose of this stop at the foot of the Newberry Mountains is to discuss how Mohave Valley became a low depocenter, and to view the Miocene Mirage pluton and a Miocene extensional fault that structurally superposes Proterozoic granite on it.

This area reveals evidence of continued basin lowering of Mohave Valley before and after Colorado River waters first found their way here in the early Pliocene. We are near the base of an erosional scarp that truncates a now-perched pediment above our heads that cuts across the middle Miocene Mirage pluton (Fig. 22). A fanglomerate that we just passed in roadcuts is in buttress unconformity against the scarp and pediment, and Bouse Formation overlies the fanglomerate. This represents a history in which a pediment formed sloping toward the axis of ancestral Mohave Valley after most of the Miocene extension. Subsequent valley lowering stranded the pediment above an erosional scarp, which then was overlapped by upper Miocene fanglomerate as the basin filled, and then by the Bouse Formation. Evidence of lowered Bouse and Bullhead formations encountered by drilling in the valley (Metzger and Loeltz, 1973) indicates that additional lowering occurred in the last 4 m.y. A Quaternary graben and a valley-side-down monocline deform Bullhead and younger sediments on the Arizona side of Mohave Valley (House et al., 2005; Pearthree et al., 2009). These features together implicate long continued subsidence as part of the reason that Mohave Valley was a low and subsiding depocenter when Colorado River water first arrived and began depositing the Bouse Formation.

A canyon at this stop is cut into faulted exposures of Mirage pluton, here a porphyritic sphene-biotite monzogranite. The pluton was dated as 16.0 ± 0.2 Ma and intrudes the larger 17–16 Ma Spirit Mountain pluton (Walker et al., 2007). Both plutons are synextensional. The alkali feldspar phenocrysts in this rock are commonly rimmed by plagioclase. The Mirage pluton here is in the footwall of the Newberry fault and is chopped by many smaller displacement faults (Mathis, 1982; House et al., 2004).

Walk 200 m north along the base of the outcrop to the exposed Newberry fault (Mathis, 1982). The fault dips gently east, and slickenside striae on polished surfaces of the fault strike east-northeast. This major fault places red, oxidized rocks of coarse-grained Proterozoic granite (Davis Dam granite of

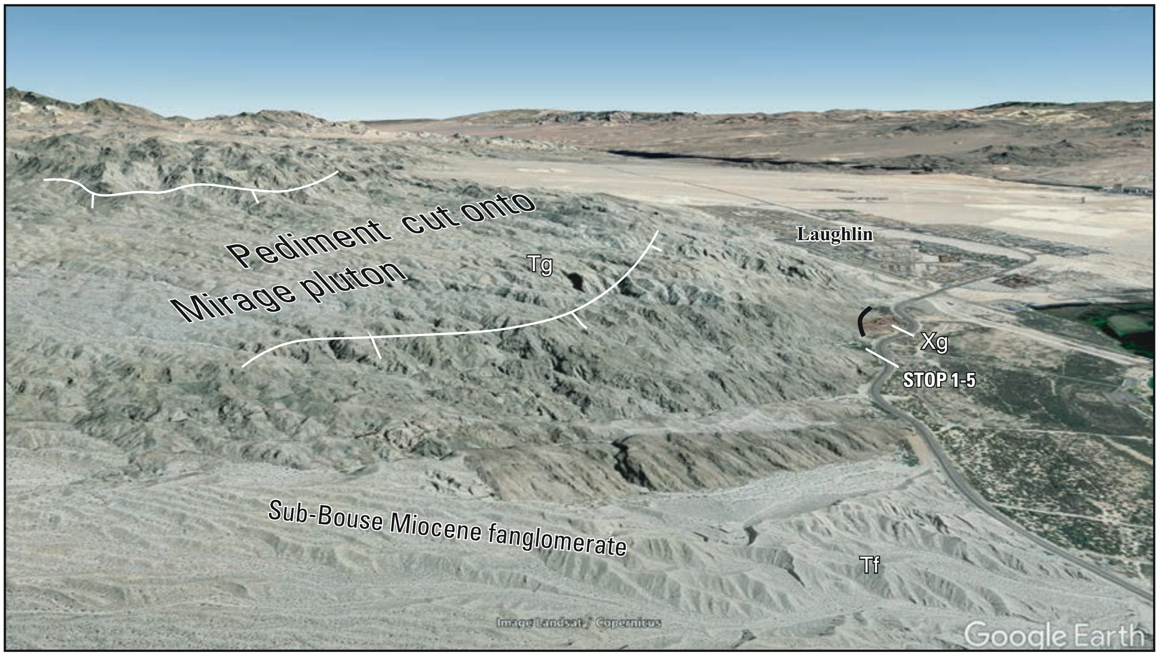

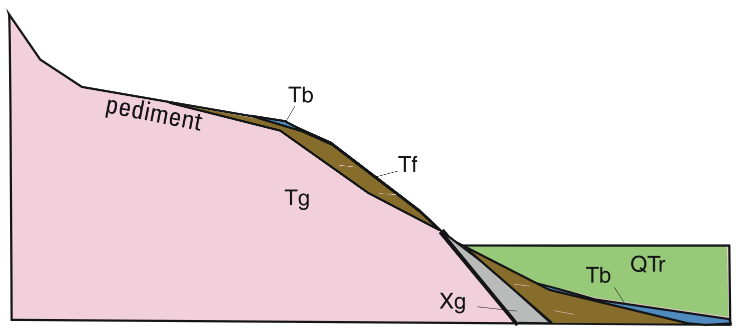

Figure 22. View NE of pediment cut onto the Mirage pluton. Tf—Miocene fanglomerate; Tg—Miocene granite; Xg—Proterozoic granite in hanging wall of Newberry fault. Erosional scarps shown with hachures. The fanglomerate buttresses depositionally against a scarp that truncates the pediment. Cross-section sketch vertically exaggerated to show relations; Tb—Bouse Formation (subvalley position inferred); QTr—Pliocene and younger Colorado River deposits.

Anderson and Bender, 1989) on the Mirage pluton. This superposition omits substantial crustal section and represents many kilometers of displacement (Frost and Martin, 1982). Later evidence showed that the Spirit Mountain and Mirage plutons tilted southwestward during extension (e.g., Faulds et al., 1992), as did the fault, which initially dipped more steeply.

Highlights on the Way to STOP 1-6

Continue northward on River Road (Needles Highway) 1 mile and turn right (east) on West Casino Drive. Follow West Casino Drive 4 mi, passing along the perimeter fence of the abandoned and mostly demolished Mohave generating station, which once burned coal from the Four Corners area. Exposures on that property include a Pleistocene Colorado River paleochannel and related deposits interbedded with tributary alluvium derived from the Black Mountains across the valley to the east. Upper Pleistocene terrace gravels are exposed on the south and east sides of the road. As the road bends to the north, we will surmount an island of Miocene fanglomerate derived from the Newberry Mountains to the west.

As we top the terrace, we will be crossing one of the highest Upper Pleistocene Riverside terraces, which record stages of late Pleistocene downcutting after deposition of the Chemehuevi Formation (Fig. 11).

At ~4 mi along Casino Drive, we will pull out along the east side of the road.

STOP 1-6. Panda Gulch, Nevada, and the Record of Downward Integration of the Colorado River (35.1408° N, 114.5790° W)

The purpose of this stop is to examine key stratigraphic evidence for downward integration of the Colorado River. See House et al. (2005) for a geologic map and more details about this site.

Here, we are at the north end of Mohave Valley just a few km south of the “Pyramid hills” (see Fig. 9), hills of Paleoproterozoic megacrystic granite (Davis Dam granite of Anderson and Bender, 1989) that separate Cottonwood Valley from Mohave Valley. We are standing on a broad and mostly flat Upper Pleistocene river terrace of the Colorado River that is part of the group of post–Chemehuevi Formation terraces (Fig. 11) that are included in the informally named Riverside alluvium[3]. The Upper Pleistocene sediments of this terrace bury a complex sequence of Pliocene and Pleistocene deposits that are exposed here at “Panda gulch” and along most of the river-facing bluffs. These key exposures are fortuitously preserved along the spine of a hill of locally derived Miocene alluvium and deposits related to the arrival of the Colorado River. The east side of the hill forms the bluffs (“Laughlin bluffs”) along the west bank of the Colorado River, and the west side is buried by Pliocene and Pleistocene Colorado River and Black Mountains–derived alluvial fan and channel deposits.

The exposures of upper Miocene to Pliocene strata in Panda gulch comprise a ‘golden section’ discovered in a geologic mapping campaign. This critical section just south of the casino strip of Laughlin, Nevada, reveals a model of the birth of the lower Colorado River through the following sequence (beginning at the bottom of the section):

1. Mohave Valley was an arid valley filling with locally derived sediment and building fans (Newberry fanglomerate, derived from the Newberry Mountains on the west) out into an axial valley that drained to a depocenter in southern Mohave Valley.
2. An abrupt increase in water entering Mohave Valley occurs from clear-water spillover (or leakage) through the Pyramid hills from a new lake that is forming just upstream in Cottonwood Valley. This new source of water cuts a series of channels transverse to the alluvial fan deposits (Newberry channel gravels). The overflow culminates in a large divide-breach flood as the lowering divide at the Pyramid hills fails. The monolithologic debris from the divide failure is conveyed in part through the Newberry channels, which are greatly enlarged or obliterated. A steep and incised boulder-laden debris fan builds at the head of the valley below the overtopped divide, with one or more channels extending farther south into the valley as the upstream lake continues to drain. One or more channels continue to deliver the ample runoff from the falling lake and debris from the initial debris fan (Pyramid gravel).
3. A beautifully blue, placid lake grows to fill both Mohave and Cottonwood Valleys, submerging the valley floors with 100’s of m of Colorado River water. Because the continuous input of exotic water is dammed at the south end of the valley, carbonate rains out of the water leaving a veneer of white limestone along the rising shoreline. The wind blows, waves form, gravel and sand swash along the beaches, and a delta and far-traveled bottomset beds of mostly fine siliciclastic deposits form from the growing delta at the head of the large new lake. All this constitutes the Bouse Formation.
4. The lake diminishes as incoming sediment at the head of the valley fills it, and the outlet through the Topock divide at the south end of Mohave Valley erodes. As the lake lowers and shrinks, the wedge of deltaic sediment is inferred to become deeply incised and regurgitated further downstream into Mohave Valley.
5. The grade of the nascent lower Colorado River must drop farther as downstream divides are lowered, and river deltas prograde through this and downstream water bodies in telescoping fashion, as incision continues until the Colorado River reaches the Gulf of California and establishes an even gradient to sea level (forming the base profile of the subsequent Bullhead Alluvium).
6. An increasingly energetic and sediment-laden river brings an immense and continuous slug of sediment into the valley and farther downstream, and aggrades the now integrated chain of valleys with 200–250 m of far-traveled sediment and interbedded tributary fan deposits, the Bullhead Alluvium. This stage represents a large braided river laden with far-traveled sand and gravel and spiked with large clasts plucked from local sources.

Each key member of the section is present here even though thin. Nearby outcrops expose thicker sections of the fluvial conglomerates and Bouse Formation (Fig. 23). Panda gulch is the only site where it is easy to see each stratum in succession: local fan gravel, overlying ‘Pyramid gravel,’ Bouse Formation marl and fine-grained sandstone, and finally Bullhead Alluvium overlying the other units on an erosional unconformity. The ‘Pyramid gravel’ is a mostly monolithologic boulder conglomerate dominated by dark gravel of megacrystic granite (Figs. 23, 24). This gravel was derived from Paleoproterozoic granite that makes up the Pyramid hills upstream at the site of Davis Dam a few miles north of Laughlin. The coarse gravel accumulated as an amalgamated 35 m stack of cross-bedded and massive, poorly sorted boulder conglomerate layers (Fig. 24). In some outcrops, the Pyramid gravel overlies and truncates distinctive, similarly southward-oriented channel forms in the underlying Miocene Newberry alluvial fan deposits, suggesting the occupation and modification of an axial channel system.

The Pyramid gravel is overlain by marl and fine calcareous sandstone of the Bouse Formation. This is evident as a thin zone of platey marl eroding out of the slope above the Pyramid gravel. The Bouse marl can be traced in several of the deep washes cut into the Laughlin bluffs. The Pyramid gravel records a catastrophic flood from the failure of a natural dam that held a lake upstream in Cottonwood Valley (House et al., 2008). The presence of the Bouse marl atop the flood deposits implies that a lake, dammed near Topock at the south end of the valley, then inundated this site and eventually both valleys.

[3]House et al. (2005) used the term Riverside ‘beds’ for a different stratum interpreted to underlie the Chemehuevi Formation. Subsequent mapping has brought that interpretation into question.

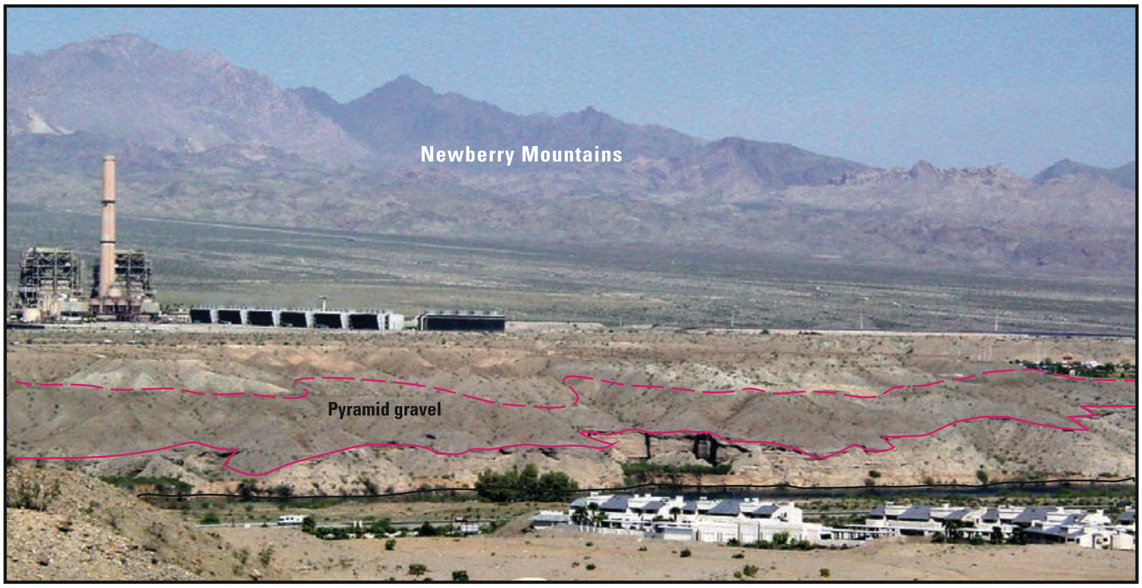

Figure 23. View from Bullhead City, Arizona, across the river to the "Laughlin bluffs," Nevada, below the abandoned (now demolished) power plant. Pyramid gravel forms the prominent dark band and overlies Miocene fanglomerate that forms steep light-toned cliffs at the base of the bluffs. Lighter-toned sediments evident near the surface of the terrace include Upper Pleistocene Colorado River deposits and piedmont alluvium.

Highlights on the Way to STOP 1-7

Continue north along Casino Drive 0.5 mi and turn left at the light onto Thomas Edison Drive. Follow Thomas Edison Drive for ~1.8 mi and turn right onto Highway 163. Roadcuts on this route show the Miocene Newberry Mountains–derived fanglomerate overlain by the conglomerate of Laughlin, another boulder-rich deposit containing large clasts of dark-colored Paleoproterozoic granite derived from the Pyramid hills (Faulds et al., 2004; House et al., 2005). This unit, like the Pyramid gravel, forms a dark band that is evident in many exposures around the perimeter

Figure 24. The Pyramid gravel as seen from river level.

of Laughlin (plotted on Fig. 18). The Laughlin unit, however, is mixed with a rich assortment of far-traveled gravel clasts of the Colorado River, making it distinct from the pre–Bouse Formation Pyramid gravel, which is entirely free of far-traveled Colorado River sediment. The Laughlin unit also contains a larger amount of light-colored boulders scavenged from fanglomerate derived from the Newberry Mountains. The age of the Laughlin unit is uncertain.

Continue ~1 mi and across the Colorado River into Arizona straight onto Bullhead Parkway. Follow the parkway for 5.1 mi. The parkway passes through Miocene to Pleistocene tributary gravels (including small outcrops of the Pyramid gravel and the Bouse Formation limestone, but these are easy to miss), and then passes through large road-cut exposures of cross-bedded sand and gravel of the Bullhead Alluvium. The Bullhead deposits are being actively mined for aggregate and some very thick exposures can be seen from the parkway. After 5.1 mi, turn left (east) on Silver Creek Road and proceed 4.7 mi to a small parking area. Silver Creek Wash is a large ephemeral wash that fed a large alluvial complex from the Black Mountains downslope to the late Miocene axis of Mohave Valley.

STOP 1-7. Bouse Formation at Silver Creek, Arizona, Overlooking Mohave Valley (35.0843° N, 114.4683° W)

The primary purposes of this stop are to (1) explore really interesting, extensive, and high exposures of the Bouse Formation and related tributary deposits (Fig. 25); (2) consider the deposits and processes associated with the Bouse lake margin as it approached the maximum level of filling and then began to recede; (3) consider the implications of high shoreline deposits of the Bouse Formation in Mohave and Cottonwood Valleys in a model for downward integration of the incipient Colorado River by overspilling; and (4) discuss the role of the Bullhead Alluvium as a record of subsequent river evolution and its implications for regional tectonics.

Looking eastward into the Black Mountains, we are peering into the remnants of the Silver Creek caldera (Fig. 8). The caldera was the source for the supereruption that produced the Miocene Peach Spring Tuff, one of the world's most extensive ash-flow tuffs.

There are numerous outcrops of Bouse Formation travertine-tufa on bedrock or colluvium in this area, including a large outcrop we will visit immediately north of Silver Creek Road. This outcrop encrusts a bedrock-cored paleo-hillslope, and has classic

Figure 25. Exposure of the Bouse Formation (thinly bedded) and overlying and underlying tributary gravel deposits at Silver Creek, Arizona, showing complex interbedding of limestone, sandstone, and local gravel deposits that record the interaction of lacustrine and tributary deposition up to the maximum lake highstand. The Bouse section is capped by tributary gravel, which can be traced basinward (to the left) into a complex set of coarse-grained fan and fan delta deposits that rest on an erosional surface cut into the interbedded facies of the Bouse Formation. These tributary gravel deposits likely record progradation of alluvial fans as the Bouse lake level began to recede after spillover of the lake outlet began. Unmanned aerial vehicle image by Brian Gootee, Arizona Geological Survey.

gently rounded or hemispherical forms and upward-radiating internal structures.

After observing the high travertine-tufa deposits, we will take a short hike down into and across Silver Creek Wash to view iconic Bouse Formation carbonate and tributary sediments. Most of the outcrop consists of delicate thin-bedded limestone and calcarenite draped over pebbles, cobbles, and boulders of alluvial fan surfaces. Sedimentary structures and paleocurrent indicators show that these fans were associated with smaller tributary washes sourced from the north or northeast. The lack of substantial reworking of the fan deposits and the thin, delicate bedding of the limestone suggest to us that the lake water rose rapidly over this area, and the limestone was deposited in quiet-water conditions. The contact of the limestone with overlying locally derived gravel deposits is erosional, with some spectacular small channel forms cut into and through the basal carbonate. Basal carbonate in the thicker, easternmost exposures consists of marl interbedded with locally derived, reworked gravel deposits suggestive of wave action. These eastern, stratigraphically higher deposits likely record interaction between paleo–Silver Creek and lacustrine deposition near the very highest level of lake filling. In the highest parts of the exposed sections, tributary deposits having fan-delta foreset beds cut into the marl indicate tributary floods interacting with the body of standing water, probably after the lake level had begun to recede after initial lake spillover. Subaerial fan deposits that bevel and offlap the marl indicate tributary fan progradation in response to dropping water level in the basin.

The highest limestone and calcarenite beds in the Silver Creek deposits are between 555 and 560 m a.s.l. Comparably high outcrops found up to 45 km north of here on both sides of Cottonwood Valley include shoreline gravel, travertine, and thin marl beds. Less extensive but likely Bouse carbonate deposits have been found up to 540 m a.s.l. 50 km south of Silver Creek, the southernmost Bouse outcrops in Mohave basin. These widely spaced, comparably high shoreline deposits record the highstand of paleolake Mohave, inferred to date just prior to initial spillover southward into Chemehuevi Valley. The Bouse deposits are traceable from relatively large outcrops to thin layers interbedded with local fanglomerate in several locations. Bouse highstand elevations of 540–560 m a.s.l. on this side of the valley over ~100 km north-south implies they have experienced little tilting; if post-Bouse uplift has occurred, it was notably uniform.

The Bullhead Alluvium outcrops that we passed on the way uphill, and will see again on the way downhill, represent the massive early Pliocene aggradation by the river shortly after it cut through its interbasin divides and fully integrated to the Gulf of California (House et al., 2008; Howard et al., 2015). In this part of Mohave Valley, Bullhead outcrops range in elevation from 150 m a.s.l. along the river to just over 400 m a.s.l. on the eastern piedmont, representing >250 m of aggradation. The distribution of Bullhead Alluvium exposures and their range of elevations along the river corridor indicate that the base of the Bullhead is locally subsided in some valleys (to below sea level in part of the Blythe basin), but otherwise mostly mimics the modern river valley. The maximum outcrop elevations outline a gradient from Lake Mead 100's of km downstream to near the river's delta, which is nearly identical to the gradient of the much younger late Pleistocene aggradation of the Chemehuevi Formation (Fig. 10). This correspondence is interpreted to indicate first, that the Bullhead has undergone little or no regional tilting since it was deposited (the last 3–4 m.y.), and second, that the river valley and its grade to Pliocene and modern sea levels have undergone little or no regional uplift in that time interval. The river has roughly reoccupied this grade multiple times in its history. Up-to-the-east displacements of the Bullhead and an older unit at faults in the Lake Mead area upstream from here (Fig. 10), along with differential incision rate estimates in that region, together indicate 100's of m of post-Miocene fault uplift of the western part of the Colorado Plateau, while the Colorado River valley downstream remained regionally tectonically stable (Crow et al., 2018b).

Return to Laughlin

To return to Laughlin, Nevada, for the evening, follow Silver Creek Road back to Bullhead Parkway, turn right onto the parkway, and then turn left on Casino Drive. Lodging at Edgewater Resort and Casino is on the left along the river (35.1614° N, 114.5714° W).

DAY 2. Topock Gorge Canoe Trip (!)

Today we will canoe downriver through Topock Gorge, straddling the California-Arizona border, and will explore riverside views of the CREC and features marking the evolution of the Colorado River. Topock Gorge is the crown jewel of the 37,515-acre Havasu National Wildlife Refuge, and one of the last remaining untouched natural portions of the lower Colorado River before it reaches the Gulf of California.

We will launch at the Topock Marina (34.7192°N, 114.4838°W). Travel will be self-powered by canoe on the calm waters of the Colorado River with no access to anything you don't bring with you. You will need to carry water, sunglasses, sunscreen, a hat, long-sleeved shirt (for sun and wind protection), and shoes that can get wet with you in the canoe. You will be reconnected with the vehicle and your luggage at the end of the day.

The purposes of the day are to explore both the history of extension in the Chemehuevi Mountains core complex and further evidence of the evolution of the Colorado River. See the Data Repository for the Topock Gorge Geologic River Guide (see footnote 1).

Canoeing Logistics

We will launch at Topock (34.7192°N, 114.4838°W) using canoes from a commercial outfitter from Bullhead City. If you are arranging this trip on your own, we suggest that you bring your own boat or arrange rental and shuttle services from outfitters in Lake Havasu City, Arizona; Bullhead City, Arizona; or Needles, California. Trip length is 17 miles along the river.

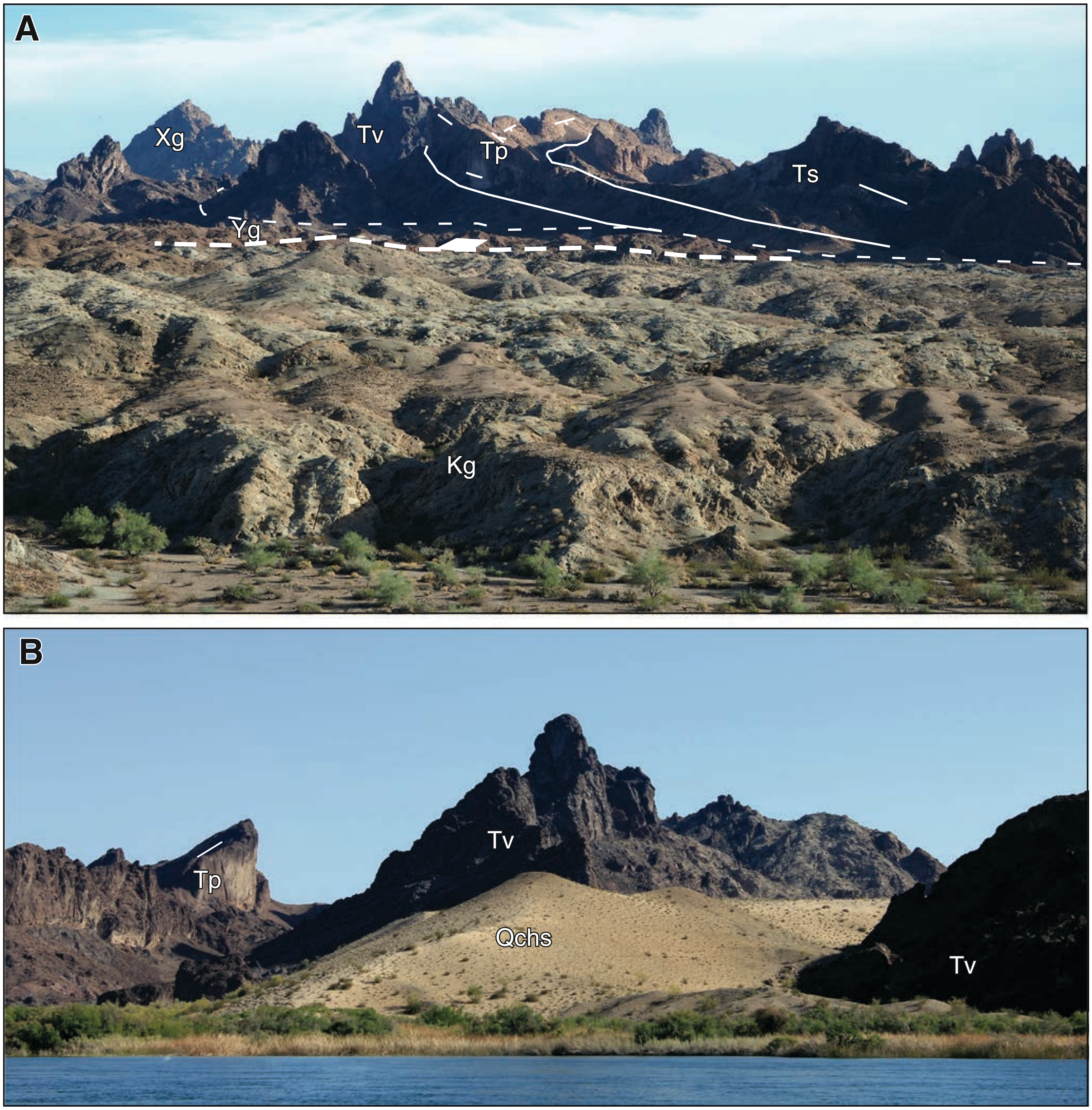

Figure 26. Topock Gorge. (A) View southward toward Gold Dome pinnacle in The Needles on the Arizona side of upper Topock Gorge; the Colorado River and STOP 2-1 are to the right of the field of view. Faults are highly generalized (dashed line with box on hanging wall). Tp—Peach Spring Tuff in west-plunging syncline; Ts—sedimentary conglomerate and breccia above the tuff; Tv—steeply dipping volcanics below the tuff; Yg and Xg—Proterozoic granite and gneiss, respectively, on which Tv is nonconformable; Kg—rocks of the Cretaceous Chemehuevi Mountains Plutonic Suite, structurally below the Devils Elbow fault and in part below the Chemehuevi detachment fault. (B) View upstream near STOP 2-3. Sand facies of the Chemehuevi Formation (Qchs), partly reworked by the wind, occupies paleovalley east of River Island.

Highlights on the Way to Topock

From Laughlin, proceed south 5.7 mi on S. Casino Drive to Needles Highway. Turn left and follow it southward for 22 mi. After 6–7 mi, as you cross into California, the Dead Mountains on the west (right) are another core complex exposure, consisting of the (light-toned) lower Miocene Avi granodiorite pluton and darker Proterozoic gneiss and mylonitic lower Miocene granodiorite gneiss.

Alluvial fans on the east side piedmont of the Dead Mountains locally cover thick deposits of deltaic Bouse Formation siliciclastic sediments. The basal carbonate is exposed primarily as drapes on bedrock hillslopes near the mountain front, commonly at the base of the sediments in deep exposures. Scattered rinds and rare, thick 'reefs' of shoreline Bouse travertine are found on the east front of the Dead Mountains at elevations ranging from 428 m to 525 m a.s.l., 35 m lower than the highest shoreline travertines and gravels on the east side of Mohave valley in Arizona. We suspect that a range of shoreline elevations is accounted for by fluctuating Bouse lake levels in the valley.

Seven mi into California, an extensional klippe of dark Miocene conglomerate can be seen on the right superposed on the gneissic rocks on the east flank of the Dead Mountains. The Dead Mountains area experienced deformation after the main phase of extensional mylonitization and faulting, including a N-S fault on the range's west flank, now in reverse-fault orientation, that juxtaposes 12 Ma basalt and conglomerate against the gneisses (Spencer, 1985). A monoclinal 90° downward bend of the crystalline rocks westward toward the fault, expressed in folded gneiss foliation, accounts for the reverse dip of an originally normal fault and indicates post–12 Ma contractile deformation. The tectonic significance of the monocline, and that of a parallel series of steep north-striking faults and lineaments in the Dead and Sacramento Mountains remain to be determined.

At 22 mi along Needles Highway (River Road), merge onto I-40 eastbound in Needles, and follow I-40 for 14.3 mi to cross the river again into Arizona, and then immediately take the Topock exit and cross over I-40. In 0.6 mi, enter the Topock launch site for a comfort stop and canoe launch. Consult Figures 5, 12, and 15 and the Topock Gorge Geologic River Guide (see footnote 1) to begin your one-way river trip.

Highlights on the Way to STOP 2-1

Pre-Bouse upper Miocene fanglomerate is exposed close to the launch site at river level. Older tilted, red middle-Miocene conglomerate is exposed on both sides of the river as the canoes pass under the highway and railway bridges. As we boat south along the river, ahead are The Needles (Fig. 26A), spectacular pinnacles of steeply southwest-tilted, synextensional volcanic, hypabyssal, and sedimentary rocks that lie structurally above the Chemehuevi detachment fault that we saw in the distance yesterday. The Colorado River in this location has incised into fractured rocks associated with the detachment fault as the fault curves around one of its two broad NE-trending antiformal corrugations in the Chemehuevi Mountains (to the right on the California side). Exposures to the west (right) are rocks in the footwall to the Chemehuevi detachment fault including altered and brecciated gneisses and granitic rocks of Proterozoic and Cretaceous age, hosting a greenish cast from characteristic chlorite-epidote-albite alteration of the footwall of the fault system. Deformed Miocene alluvial fan deposits on the left bank (east) lie in the hanging wall.

See if you can identify the view portrayed in the Ives report (Fig. 12). STOP 2-1 is 1.8 mi downstream from the I-80 bridge, by a gauging station on the east (Arizona) shore of the Colorado River (Fig. 5).

STOP 2-1. Chemehuevi Detachment Fault (34.6875° N, 114.4626° W)

The purpose of this stop is to examine the master Chemehuevi detachment fault, a CREC structure that accommodated a minimum of 18 km top-to-the-NE separation (Figs. 27, 28B).

Depending on the river level, it may be necessary to beach canoes on a small beach south of the wash (at the gauging station). Leave the canoes and climb over the small hill composed of Colorado River gravel, to descend into the main wash. Walk 0.2 mi up the main wash from the river. Climb the small dirt road on the left (north) side of the wash to exposures of the Chemehuevi detachment fault. The fault dips 12° east, and superposes biotite granodiorite (Late Cretaceous Chemehuevi Mountains Plutonic Suite) and numerous (presumed tilted) subhorizontal Miocene mafic dikes in the hanging wall, against a footwall of porphyritic, hornblende-biotite granodiorite (of the Chemehuevi Mountains Plutonic Suite). The fault is characterized by a zone of deformation up to 10's of m thick, hosting altered cataclasite and ultracataclasite derived from both the footwall and hanging wall (Fig. 27).

Highlights on the Way to STOP 2-2

Drink some water, then return to the canoes and continue 0.8 mi downstream, crossing the river to STOP 2-2 on the California side. It is best to land at the northern tip of the small peninsula just south of the sandbar, and to make your way through the salt cedar along small burro trails to the main wash.

STOP 2-2. Devils Elbow Fault (34.6770° N, 114.4572° W)

The purpose of this stop is to examine the Devils Elbow fault, an extensional fault that is structurally higher than the Chemehuevi detachment fault and the deeper Mohave Wash fault, and to discuss stratigraphic and structural features in its hanging wall.

From the west river bank, ***walk*** southwest 0.5 mi (0.8 km). Exposures on the right (north) include the Peach Spring Tuff above older mafic volcanic rocks. At the fork in the wash, ***keep left*** and follow the burro trail 0.3 mi (0.5 km) over the low saddle through Colorado River gravels that unconformably overlie altered and fractured granitic rocks in the hanging wall of the Chemehuevi detachment fault. Red rocks to the east include altered Miocene volcanic deposits, with interstratified sedimentary breccia and megabreccia deposits in the hanging wall (upper

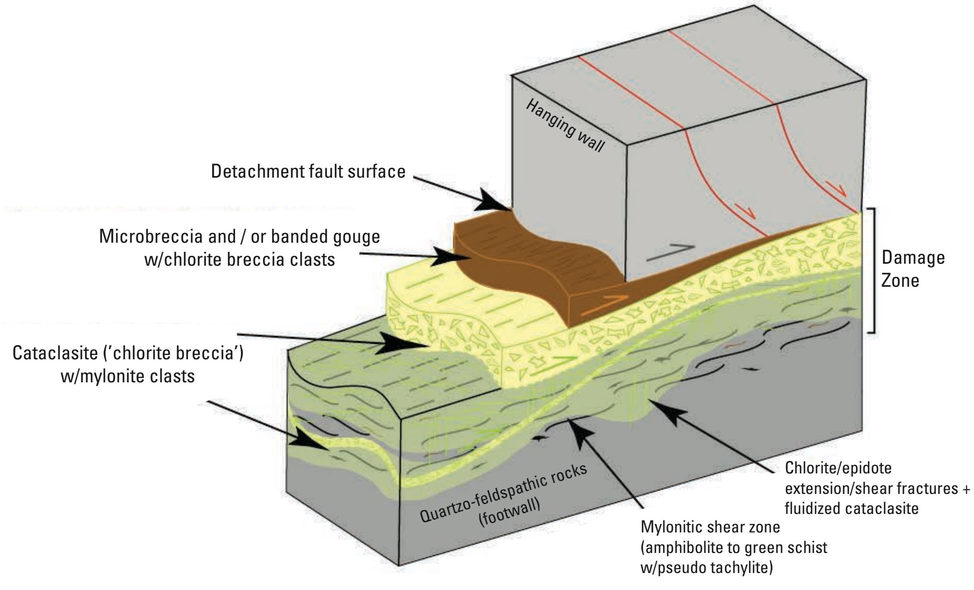

Figure 27. Architecture of a continental detachment fault system cutting isotropic quartzo-feldspathic basement. The fault zone comprises anastomosing low-angle normal-fault shear zones. Hydrothermal alteration of the footwall is concentrated in the damage zone, and varies from cm to 100's of m in thickness. Modified slightly from John and Cheadle (2010).

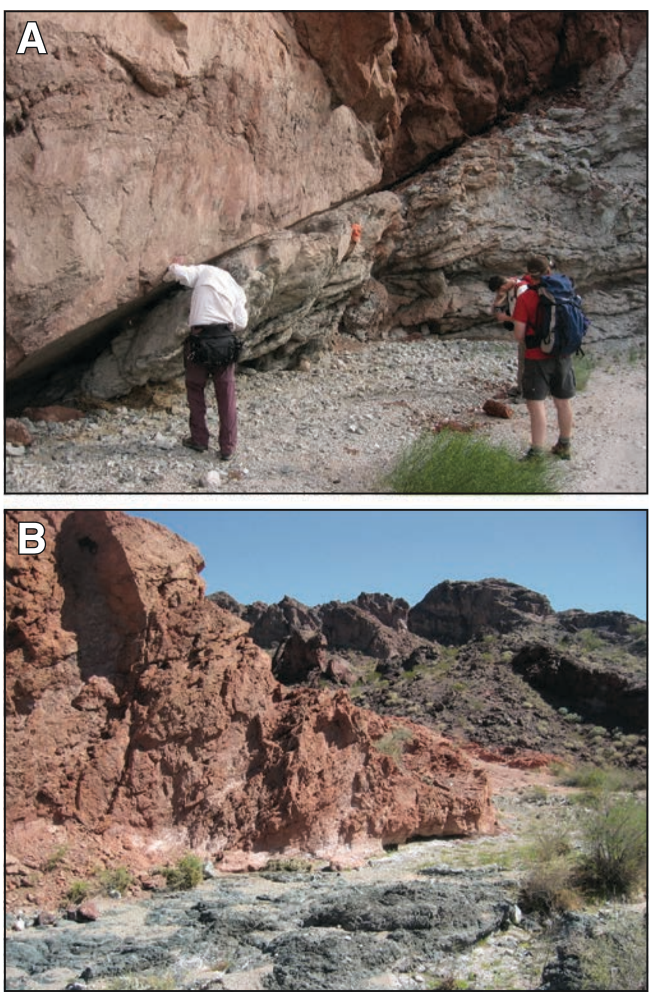

plate) of the Devils Elbow fault. The fault at this exposure dips 35° east with well-preserved slickenside striae plunging 33° downdip (Fig. 28A). Although poorly constrained, top-to-the-east-northeast slip on the Devils Elbow fault is several km (John, 1987a). Rocks in the footwall of this fault form the hanging wall to the Chemehuevi detachment fault, and are part of the Chemehuevi Mountains Plutonic Suite, with associated mafic and felsic dikes (now subhorizontal) derived from a footwall location ~18 km to the west-southwest.

Drink some water and return to the canoes. Before leaving the beach, look east across the river to the high peaks on the Arizona skyline. A tan-colored tuff dip-slope there is the 18.8 Ma Peach Spring Tuff, which served as the substrate to the syntectonic sedimentary succession. The tuff occupied a paleovalley here and thins northward to near zero thickness near STOP 2-1. Viewed from here, tan exposures of the tuff form a spectacular, well-defined syncline, plunging moderately toward the southwest (Figs. 5, 26A). The syncline is interpreted as a fault-related fold that formed during extension, where a steep, now-transverse fault, which bounds two steeply tilted blocks of basement rocks,

Figure 28. (A) Devils Elbow fault at STOP 2-2 juxtaposing reddish Miocene gneissic-clast landslide megabreccia deposits (Tgnm in the "Topock Gorge Geologic River Guide" [see footnote 1]), against a footwall of fractured and altered porphyritic hornblende-biotite granodiorite (Kgd). (B) Chemehuevi detachment fault at Devils Elbow between STOPS 2-2 and 2-3 (between River mi 5 and 6 in the Geologic River Guide), juxtaposing reddish Miocene crystalline-clast landslide megabreccia deposits (Tbx), against a greenish-gray footwall of fractured and highly altered Kgd.

propagated upward into the layered Miocene section (Figs. 29, 30; John and Howard, 1994; Howard and John, 1997). Deformation of the folded rocks is complex and includes bedding-plane faults and at least one small reverse fault (Howard et al., 2013; see the geologic river guide [see footnote 1]). The core of the syncline is filled with coarse sedimentary breccia and thick, irregular megabreccia deposits, made up of clasts of crystalline rocks (Miller and John, 1999).

Highlights on the Way to STOP 2-3

Continue downriver in the gorge as it cuts through moderately to steeply southwest-dipping volcanic and sedimentary rocks, cut by numerous high-angle and low-angle faults. The Miocene section lies nonconformably above light-colored Proterozoic gneisses and granites, all in the hanging walls of the Chemehuevi and Devils Elbow faults just seen. Rocks on the west shore (right) include a thick sequence of rock avalanche and crystalline megabreccia deposits >1 km long and a few 10's of m thick, wholly of cracked Proterozoic crystalline rocks interstratified in sedimentary breccia (Miller and John, 1999). At 1.2 mi past STOP 2-2, a small bay east of Pulpit Rock on the Arizona side at the river bend marks the bed of an old abandoned valley of the Colorado River that veers southeast into Arizona and bounds the east side of River Island (Lee, 1908; Howard et al., 2008). STOP 2-3 is at the south end of this abandoned valley.

Beyond a big bend in the river back to the left (Devils Elbow), rocks on the right (west) are dominantly the Peach Spring Tuff and the lower volcanic sequence, cut by numerous down-to-the-east normal faults. Rocks in the vertical walls along the east bank (left) include post–Peach Spring Tuff sedimentary breccia and megabreccia deposits.

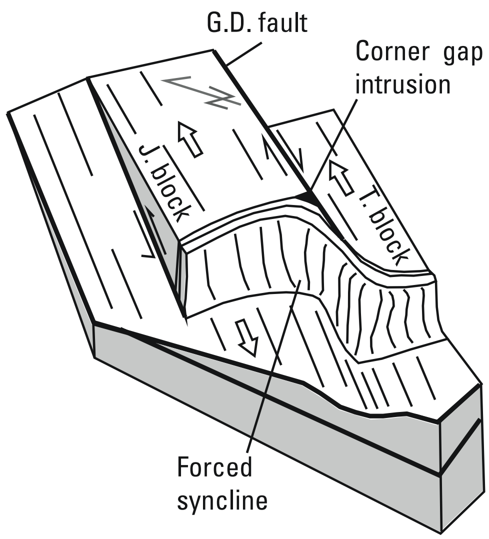

Figure 29. Cutaway diagram showing very simplistically how a forced syncline may form above a steep fault that separates two large blocks of basement rocks (Howard and John, 1997). The Gold Dome (G.D.) fault separates the steeply tilted Jackpot (J.) and Tumarion (T.) blocks of Proterozoic and Cretaceous basement rock. Where the Gold Dome fault cuts into the overlying Miocene section, the layered volcanic rocks are complexly deformed in a triangular zone including bedding-plane faulting, local reverse faulting, and an upward-propagated fold. A complex synformal Miocene intrusion mapped in the field grossly resembles, in shape and position, a corner gap portrayed in a laboratory experiment where a layered sequence unglued from two sliding rigid blocks at the tip of their fault boundary (Ameen, 1988; John and Howard, 1994; Howard et al., 2013). A higher (Powell Peak) plate (not shown) overrides the T. block.

STOP 2-3. River Island and Abandoned River Valley (34.6491° N, 114.4462° W)

The purposes of this stop are to examine the Peach Spring Tuff and to view the abandoned river valley, which contains both the Chemehuevi Formation and older fluvial boulder conglomerate.

At the southern end of River Island and east of a hogback of Peach Spring Tuff, boulder-rich fluvial conglomerate is inset into the deformed Miocene rocks as exposed in the abandoned river valley. The thalweg of the boulder-filled paleochannel is 10 m above the level of Lake Havasu. Subrounded boulders (as large as 1 m across) are estimated to be 70% gneiss, 20% volcanic rocks, and 10% Proterozoic and Mesozoic granite, rock types that are local. Extralocal quartzite, chert, and limestone clasts are abundant among the pebble and cobble fraction of the deposit.

The Upper Pleistocene Chemehuevi Formation viewed up the paleovalley is also inset into the Miocene lower volcanic sequence, and is partly wind reworked (Fig. 26B). Most of the full thickness of the Chemehuevi Formation here consists of sands. This supports a model that channel sands formed the bulk of the formation; peripheral overbank mudstones are preserved only along valley margins (Malmon et al., 2011). What caused the massive aggradation in the late Pleistocene? It remains perplexing.

Highlights on the Way to STOP 2-4

Leaving STOP 2-3 will offer a view from the river of the Chemehuevi Formation in the paleovalley (Fig. 26B). As we boat downriver 4 mi to STOP 2-4, we pass through a series of folds associated with the large, upended tilted blocks of crystalline rock, above the Chemehuevi fault system (similar to that viewed from a distance at STOP 2-2). The stratified rocks drape around the corners of adjoining basement blocks, forming the moderately to steeply plunging folds, interpreted as forced drape folds, with amplitudes as great as 2 km (John and Howard, 1994). The folds in the stratified rocks contrast with the simply tilted, monoclinal blocks of crystalline basement around which the strata drape. The drape folds here and elsewhere in the southern Basin and Range province demonstrate that major plunging folds can form during extensional tectonism (Howard and John, 1997), and not only during regional shortening deformation.

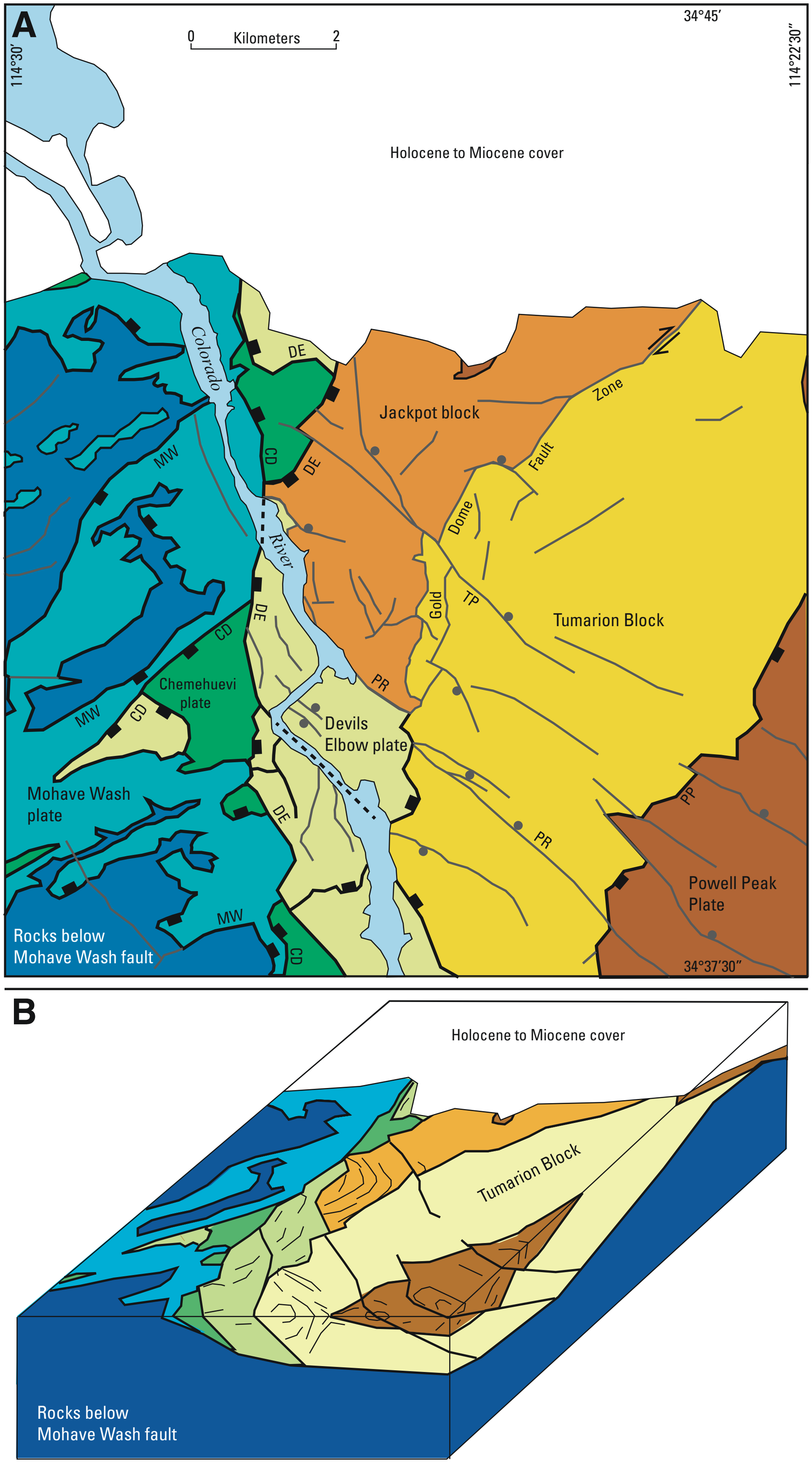

Figure 30. (A) Tectonic map of the Topock 7.5′ quadrangle showing (colored) structural blocks (slightly modified from Howard et al., 2013). Low-angle normal faults shown with thick black lines and other faults are shown with dark-gray, slightly thinner lines. Hanging walls are indicated for normal faults (ball) and low-angle normal faults (rectangles). The Mohave Wash fault (MW) carries the Mohave Wash plate over a deeper footwall. The structurally higher and younger large-displacement Chemehuevi detachment fault (CD) carries the Chemehuevi and higher plates. The Chemehuevi detachment fault truncates the higher Devils Elbow fault (DE), which carries the Devils Elbow plate. The dextral, mostly steep Gold Dome fault zone separates higher parts of that plate into the Jackpot and Tumarion tilt blocks. The Powell Peak fault (PP) carries the Powell Peak plate over the Tumarion block. The Tumarion Peak fault (TP) and Pulpit Rock fault (PR) cut the Tumarion and Jackpot blocks. (B) Interpretive tectonic block diagram of the quadrangle. Rocks that are in the Chemehuevi plate (green) and higher plates mostly are tilted steeply to the southwest. Thin form lines indicate layering in Miocene volcanic and sedimentary rocks.

STOP 2-4. Volcanic Rocks at Picture Rock (34.6242° N, 114.4382° W)

The purpose of this stop is to examine the older Miocene volcanics and related features.

STOP 2-4 is on the east side of the Colorado River near the lower end of Topock Gorge. A plaque placed here by the Mohave (Aha-Makaav) and Chemehuevi (Nüw) Tribes refers to this area of petroglyphs as Hum-Me-Chomp: "the [place] where the river once churned to make this place inaccessible to the living." This area is said to have once included a trading site between the nomadic Chemehuevi Indians who roamed the area west of the Colorado River, and the Mohave Indians who lived in the river valleys and along the east side of the river. The rocks are part of a south-dipping sequence of mafic and intermediate volcanic flows of the lower volcanic sequence, which locally overlies a very thin basal arkose resting directly on the Paleoproterozoic gneiss. The lavas are unconformably overlain locally by the Peach Spring Tuff, and younger syntectonic sedimentary rocks exposed in Trampas Wash directly to the west, and in Blankenship Wash to the south and east.

Highlights on the Way to STOP 2-5

Continue downstream past the mouth of Trampas Wash on river right at the site of an obvious outcrop of a tephra bed in Miocene rocks near the river. Near the mouth of the wash (not stopping there on this trip) is an exposure of a series of small paleochannels that cut transversely in a downstream direction across older dipping fanglomerates. These features are strongly reminiscent of the Newberry channels discussed at STOP 1-6. About 1.2 mi up Trampas Wash at a local tributary, there is an intriguing exposure of a paleochannel filled with a granodiorite boulder–rich conglomerate (Fig. 31). The paleochannel cuts across the depositional and structural grain of older strata, is reminiscent of the spillover-linked channels of the Pyramid gravel visited at STOP 1-6, and possibly could be linked to the early Pliocene spillover integration of Mohave-Cottonwood Valleys with Chemehuevi Valley. In other words, the boulder deposit may have resulted from flood breaching of the Topock divide by overflow from the Mohave paleolake as the incipient Colorado River began to find its path toward the sea.

At 1.3 mi downstream from Picture Rock, a small island of megabreccia near the east shore of the river, is Mohave Rock. It reputedly was used by steamship captains to winch their boats up the rapids described by Ives, before flooding in Lake Havasu when Parker Dam was built in the 1930s. Rowboats were sent upriver carrying the ship's anchor, which was attached to Mohave Rock and hauled in, moving the ship slowly up the rapids toward smoother water.

Continue downriver to the upstream curve of Blankenship Bend on the Arizona side of the Colorado River.

STOP 2-5. Blankenship Bend: Chemehuevi Formation and Older Sediments (34.5977° N, 114.4295° W)

The purposes of this stop are to view the Chemehuevi Formation and older fluvial boulder conglomerate.

The white cliff exposures along the east shore of the Colorado River at Blankenship Bend are part of an island-like peninsula underlain by gently dipping post-extension upper Miocene conglomerate derived from felsic members of the Chemehuevi Mountains Plutonic Suite to the west. The peninsula is bounded on the west by the modern Colorado River channel and on the east by a paleochannel filled with mud and sand of the Upper Pleistocene Chemehuevi Formation. Fluvial boulder conglomerate unconformably overlies the upper Miocene conglomerate, and in turn is overlain by pinkish sands and muds of the Upper Pleistocene Chemehuevi Formation. The boulders in the fluvial conglomerate are clearly winnowed from the underlying coarse alluvial-fan deposit by the ancient Colorado River (Fig. 32). Where exposed, the boulders are moderately to deeply weathered. Good exposures of the fluvial conglomerate reveal that it

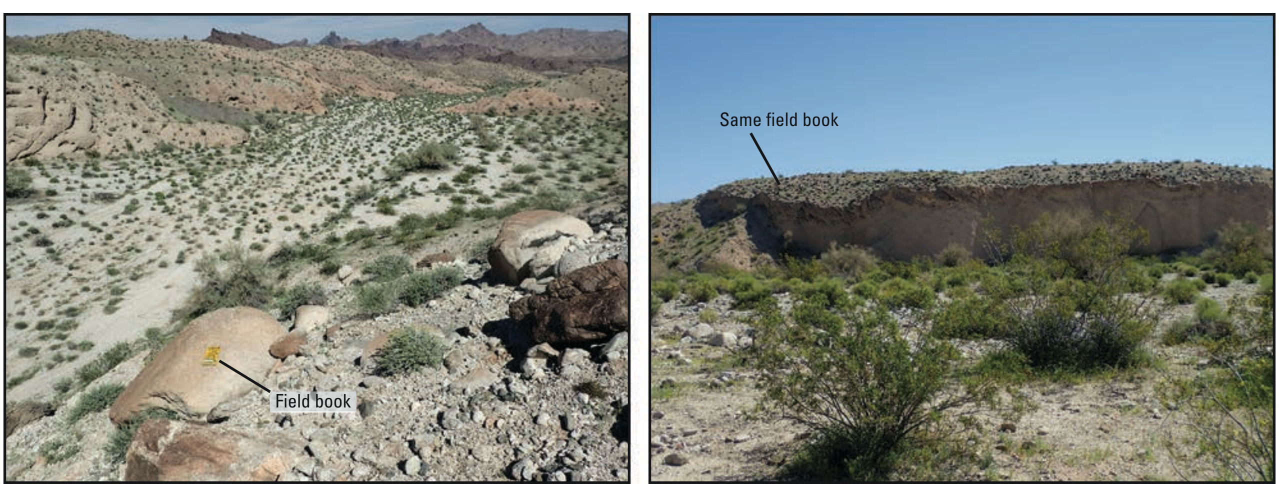

Figure 31. Two views of a boulder-filled paleochannel in Trampas Wash, 1.5 mi (2.4 km) upstream (southwest) of the Colorado River. This feature filled with locally derived and subrounded large boulders is reminiscent of the Pyramid gravel at STOP 1-6.

is a mix of coarse, far-traveled cobble gravel and locally derived river-sculpted boulders. This facies association of far-traveled cobbles and locally derived boulders is typical of ancient Colorado River flood deposits, and is particularly pronounced near the bases and margins of paleochannels cut into old alluvial fan deposits. The stratigraphic position of the boulder deposit is unresolved, whether part of the Bullhead Alluvium or younger, which clouds the significance of the flood it records. Is the boulder conglomerate the same one seen at River Island (STOP 2-3) and yesterday's STOP 1-4? And/or the conglomerate of Laughlin seen while traveling between STOPS 1-6 and 1-7?

The younger Chemehuevi Formation fills paleotopography including a Colorado River paleovalley cut through the boulder deposit and into underlying fanglomerate. The aggradation of the Chemehuevi Formation ca. 70 ka is second only to the Bullhead Alluvium in its volume and thickness (Malmon et al., 2011), making it an enigmatic singular event of the Quaternary, a period of time in which the Colorado River was apparently dominated by net incision into the thick fill packages of the Bouse Formation and Bullhead Alluvium. Did other Pleistocene aggradation events come and go as the river worked through its thick ancestral fill? Or does the Chemehuevi Formation record a particularly rare series of events in the river's Quaternary history?

Highlights on the Way to STOP 2-6

Along the west side of the Colorado River at Blankenship Bend, a gently dipping vesicular basalt flow records one of the last gasps of volcanism associated with extension in the area. It is interstratified within the upper part of the post–Peach Spring Tuff sedimentary section that makes up the Trampas Wash (California) and Blankenship (Arizona) basins. The basalt has been correlated on both sides of the river based on rare earth element chemistry, tying the two basins together at a late stage in their depositional history.

Downstream from Blankenship Bend, Chemehuevi Valley (Chemehuevi basin) opens up, and synextensional units are hidden below bluff exposures of upper Miocene fanglomerate (alluvium of Castle Rock), inset younger boulder conglomerate that may be lower Bullhead Alluvium, and pinkish mud and fine sands of the Chemehuevi Formation. Here, also, the river's delta at the head of the Lake Havasu reservoir becomes strongly apparent and the current of the river begins to wane. The primary channel is lined with vegetated marshes that form placid backwaters and intricate discontinuous channels. The delta has been accumulating here since the completion of Parker Dam in 1938. Owing to the sediment-trapping efficiency of Hoover Dam (completed in 1936) and Davis Dam (completed in 1950), the bulk of this delta is likely dominated by sediment recycled from the floodplains of Cottonwood and Mohave Valleys.

On our way to the takeout at Castle Rock, we pass extensive exposures of the Chemehuevi Formation on river left. The Chemehuevi deposits fill a paleochannel cut into the granite-rich fanglomerate and overlying Colorado River boulder conglomerate. The Chemehuevi Formation has a characteristic stratigraphy of a light-brown, slope-forming, sand-dominated facies atop a bluff and badland forming reddish-brown mud-dominated facies

Figure 32. River-sculpted and imbricated boulders, up to 1 m across, of Chemehuevi Peak Granodiorite (under field book) and other rocks in boulder conglomerate near the crest of Blankenship Bend peninsula.

(Malmon et al., 2011). The outcrops in the Blankenship Bend area sit at the northern end of a string of remnants that track a paleochannel position east of the present channel location. Well logs from a neighborhood built atop the Chemehuevi Formation indicate a channel depth of 15 m below the pre-reservoir river elevation (~20 m below the average lake elevation in this area) (House et al., 2018). Evidence from the Blankenship Bend area, and from sites upstream in Mohave and Cottonwood Valleys, indicates that the Chemehuevi Formation buries an eroded landscape having well-developed calcic soils on the slopes of erosional landforms.

Continue in the main Colorado River channel 3 mi beyond Blankenship Bend past heavily vegetated young delta bars and banks to the northern (upstream) end of The Island, toward the left. Paddle left (east) into the smaller channel (34.5655° N, 114.4044° W) and continue south to Castle Rock Bay, a large embayment in the cliffs to the east. The entrance to Castle Rock Bay is through a small channel at the very south (34.5621° N, 114.3962° W), just barely downstream from Castle Rock. The canoe takeout requires boating between patches of dense vegetation (and very shallow water) to Castle Rock on the left (east). Once we land, be sure to haul ***all*** equipment (paddles, canoes, personal flotation devices, shoes, water bottles, cameras, and any trash) to the parking lot roughly 250 m east past Castle Rock itself.

STOP 2-6. Castle Rock and Canoe Takeout (34.5641° N, 114.3938° W)

Castle Rock exposes cliffs of the pre–Bouse alluvium of Castle Rock. Pinkish fine sands of the Chemehuevi Formation overlie it and Chemehuevi Formation mud fills erosional niches in it. At the takeout, note how the contact between the Chemehuevi Formation sand facies and underlying mud facies coincides with a beveled surface on the alluvium of Castle Rock. What does this tell us about the age difference between the mud and sand facies here? Optically stimulated luminescence analyses from recently collected samples in this sequence are in progress.

Nearby exposures of the Bullhead Alluvium atop the bluffs of Castle Rock alluvium contain rip-up blocks of Bouse Formation marl, and in situ outcrops of the marl are found in close association with them (House et al., 2018). On the west side of the lake, flat to gently dipping outcrops of Bouse Formation limestone line the shoreline and extend into the lake.

We will travel by car to lodging in Lake Havasu City.

DAY 3. Mohave, Riverside, and Big Maria Mountains

Today, we again examine both the products of continental extension and of the subsequent integration of the Colorado River. In addition, we will address the pre-Cenozoic framework of the crust by viewing an area where Warren Hamilton identified the contorted Paleozoic stratigraphic sequence and its Proterozoic basement. The day begins in Lake Havasu City and ends en route to Blythe, California, and the return to Phoenix.

Highlights on the Way to STOP 3-1

Take McCulloch Boulevard north across London Bridge and proceed west 2.5 mi. Just beyond a sign on the left for Site 6, turn left into a wide gravel parking area and park near one of the small light beacons for a view west across Lake Havasu. The London Bridge was brought here by developer Robert P. McCulloch and reassembled piece-by-piece to span a water body dug to turn a pre-dam peninsula into an island.

STOP 3-1. Bouse Formation View (34.4554° N, 114.3752° W)

The purpose of this stop is to view the setting of the Bouse Formation and discuss its deposition in filling basins. From this vantage, we look westward into Chemehuevi Valley across Lake Havasu at the white band marking the basal carbonate rocks of the Bouse Formation. The basal limestone is draped over piedmont deposits that dip ~1.5 degrees to the northeast (generally toward us). We interpret this as a primary depositional dip of a transgressive unit, as the Bouse water surface rose as it filled the valley. Brown claystone and mudstone and orange sandstone form overlying siliciclastic members of the Bouse Formation.

The western part of Chemehuevi Valley exposes a mostly complete section of the Bouse Formation, including a likely delta-top facies of sandy channels and paleosol-bearing muds (Fig. 33). Textures indicative of nearshore deposition in the basal beds of the Bouse Formation at a range of elevations give evidence that the shoreline progressively climbed up the slope of the paleovalley as the valley filled with water (Fig. 34).

Highlights on the Way to STOP 3-2

Retrace McCulloch Boulevard 2.5 mi across London Bridge. A block beyond London Bridge, turn left for one block, then left another block, then turn right on Arizona Highway 95. Proceed northward for 2 mi to Kiowa Boulevard. Turn right on Kiowa Boulevard and proceed 4.2 mi up the alluvial fan through Lake Havasu City. Turn left on Bison Street. Proceed for 0.6 mi and park at the end of the pavement.

Hike up the prominent high hill to the east for a vista of the Mohave Mountains.

STOP 3-2. Mohave Mountains (34.5211° N, 114.2727° W)

The purpose of this stop is to view a huge block of the upper crust tilted during Miocene extension, and its relation to domed core complexes in the CREC.

From this hilltop vantage, we are standing on a lower Miocene intrusive-extrusive rhyolite unit that was mapped by Jane Nielson as part of a package of steeply SW-facing Miocene volcanics (Nielson and Beratan, 1995; Howard et al., 1999). Dips in the Miocene section fan upward, so that dip decreases with higher stratigraphic position. The base of the Miocene section, in low ground east of us, is marked by a thin vertical to overturned southwest-facing basal arkose unit nonconformably overlying Proterozoic basement gneisses, which make up most of the high Mohave Mountains mass in front of us, the Crossman block. This upturned block exposes a crustal section below the volcanic

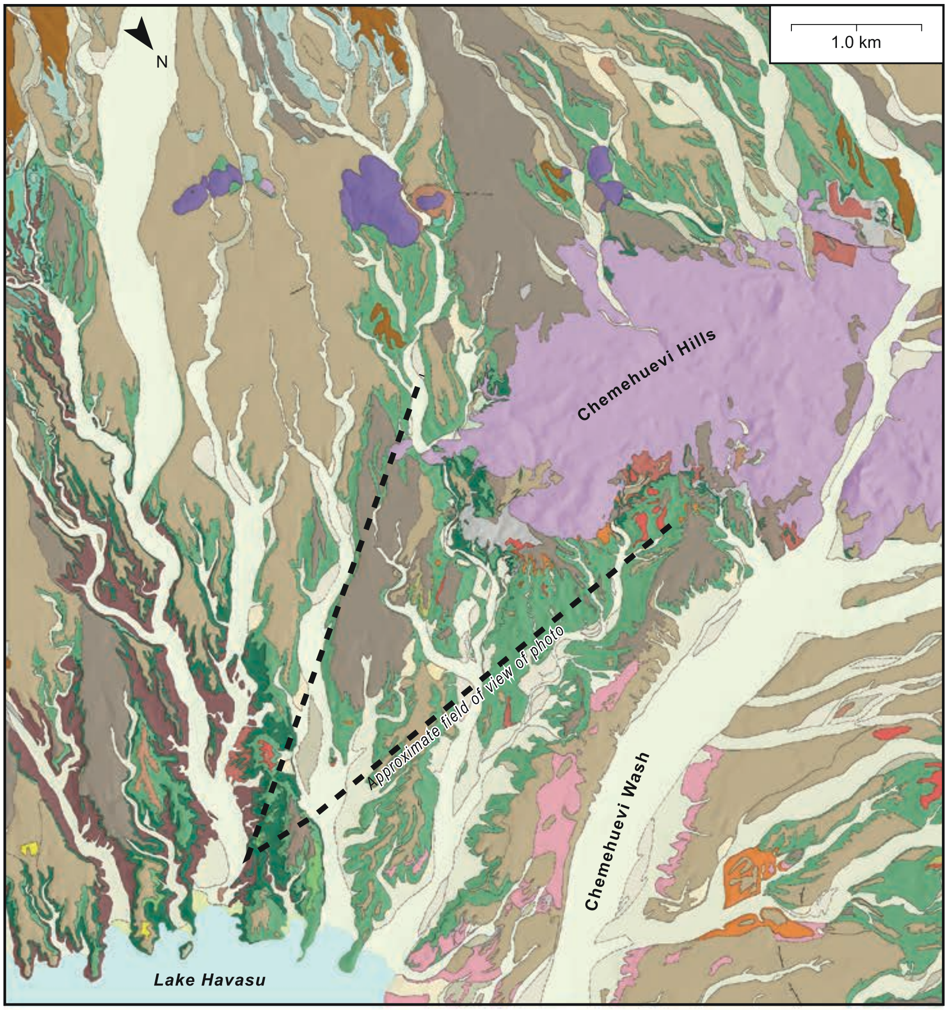

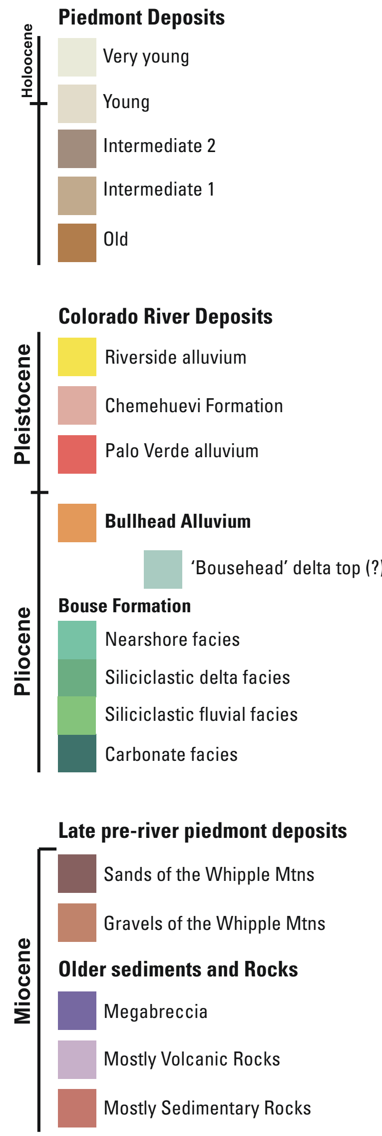

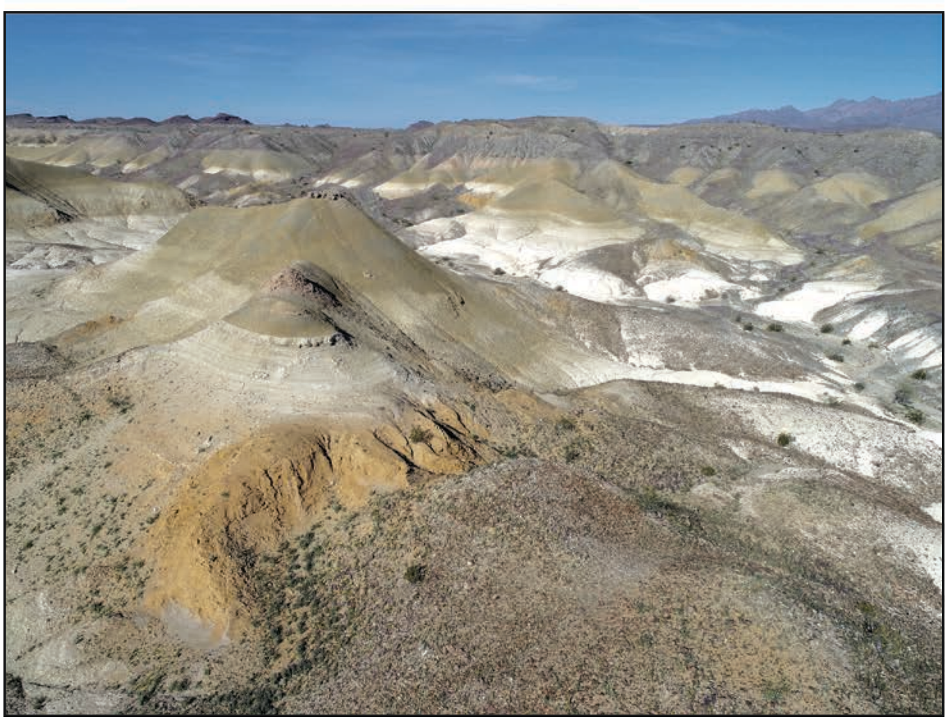

Figure 33. Geologic map of part of Chemehuevi Valley (above) and unmanned aerial vehicle view of Bouse Formation (below) in the direction indicated by the dashed lines on the map. Note that north is down to the right on the map. Gray unit on map is Proterozoic gneiss. In the photo, orange unit consists of deltaic(?) sand interlayered with white carbonates of the Bouse Formation; claystones (brown to green) of the Bouse interbedded facies overlie the carbonates.

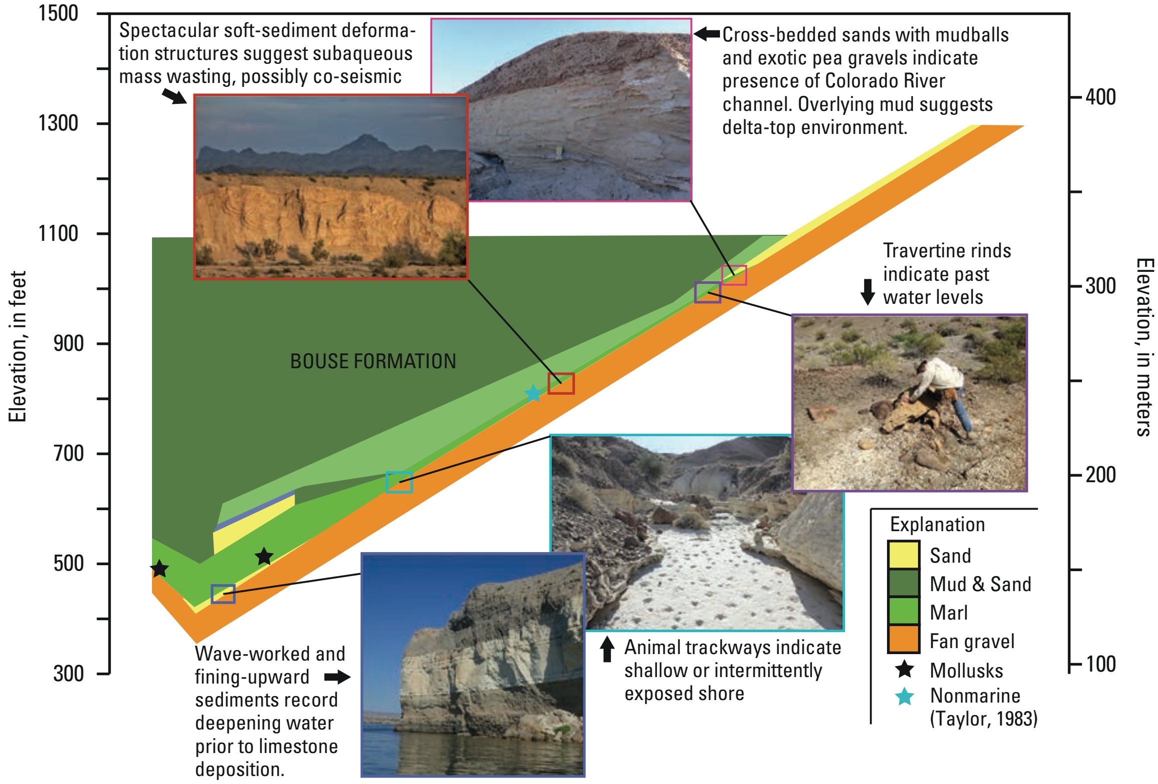

Figure 34. Schematic cross section of Bouse Formation in Chemehuevi Valley showing some features that indicate sequential deposition of wave-winnowed gravel, then limestone marl, then mud as water level deepened and the shoreline rose up the basin slope.

section that encompasses 13 km of Proterozoic gneiss and 2 km cumulative thickness of sheeted early Miocene dikes, totaling 15 km measured downward from the nonconformity. Most of the dikes dip moderately NE (Nakata, 1982). A paleomagnetic study concluded that the dikes were intruded partway through the progressive tilting of the block (Pease et al., 2005). Mesoproterozoic diabase sheets area are also scattered through the tilt block, and they maintain a uniform SW strike and subvertical dip parallel to the nonconformity at the base of the Miocene (Nakata, 1982). Like many other sites over an extensive region of the southwestern United States, this orientation shows that the sheets were originally subhorizontal, and confirms that this block of the Mohave Mountains tilted 90° down to the southwest as a homoclinal block during Miocene extension (Howard, 1991, 2011). In afternoon lighting, the mountain face northeast of us clearly reveals the Miocene dike swarm cutting bands of steeply dipping Proterozoic leucogranite gneiss and dark amphibolite (Fig. 35).

Looking back across the river to the west, Chemehuevi Valley is a conspicuous lowland between the domal Whipple metamorphic core complex to its south and the Chemehuevi metamorphic complex on the north. The Whipple and Chemehuevi detachment faults project under us and the allochthonous Crossman block. In your mind, picture the Crossman block restoring back to this Chemehuevi Valley lowland before extension and tilting. The block's steep upturned geometry seemingly requires that the underlying footwall on which it rides domed up as the block slid relatively northeastward away from a headwall in a rolling-hinge process.

Highlights on the Way to STOP 3-3

Retrace your route back down Bison Street, turn right on Kiowa Boulevard and proceed for 2 mi to Arizona Highway 95. Turn left on Arizona 95 and proceed for 4 mi. Turn right into the Lake Havasu Water Safety Center and then left to park near a low hill.

STOP 3-3. War Eagle Megabreccia (34.4519° N, 114.3227° W)

The purpose of this stop is to examine and discuss rock-avalanche breccia deposits that are common in the Basin and Range extensional province. The hillside exposes a brecciated granitic gneiss and microdiorite.

This megabreccia is part of a huge (~11 km^3) Middle Miocene megabreccia deposit widely exposed in a series of tilted fault blocks in the Aubrey Hills to the southeast and the Whipple Mountains and Chemehuevi Valley to the west (Fig. 33; Yin and Dunn, 1992; Dorsey and Becker, 1995; Forshee and Yin, 1995; Dorsey and Roberts, 1996; Howard et al., 1999). Megabreccias like this are widespread in the Basin and Range province and

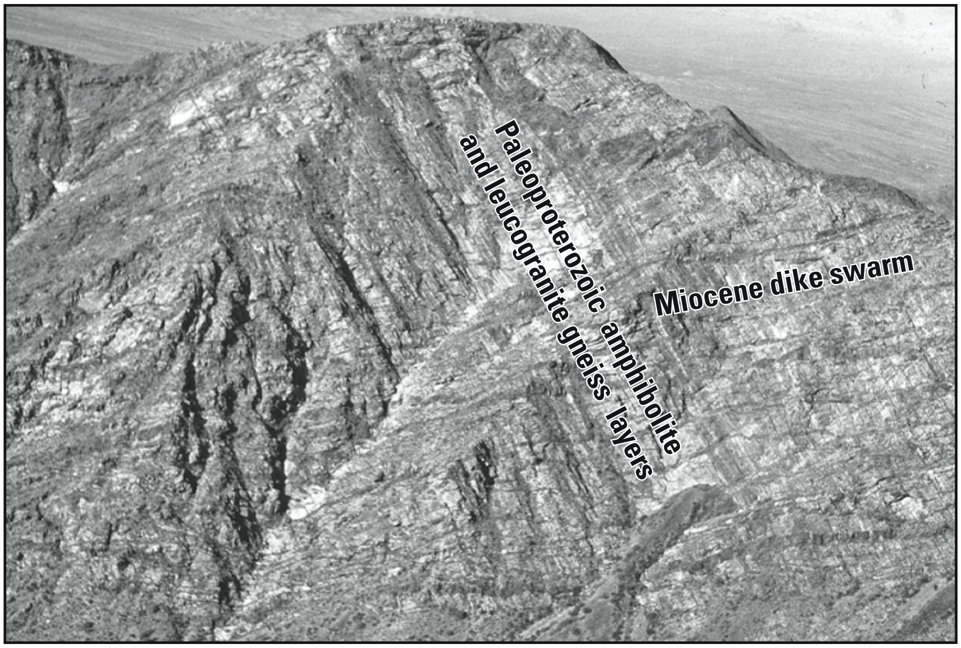

Figure 35. Face of the tilted Mohave Mountains Crossman block showing Miocene dike swarm (Nakata, 1982; photo is in public domain) cutting across Paleoproterozoic gneisses, including dark amphibolite layers, which outline part of the limb of a large Proterozoic antiform.

generally represent deposition into sedimentary basins by far-traveled, highly mobile rock avalanches (Yarnold, 1993). Imagine slope failures when earthquakes shook tectonically over-steepened slopes as the region extended. This particular breccia unit (War Eagle megabreccia) includes clasts as large as a city block. Not far from here, Miocene shale immediately beneath it is folded and grooved, showing a northeast direction of landsliding. The breccia unit dips southwestward and overlies a series of Miocene volcanic and sedimentary units, including basalt dated 14.5 ± 1.0 Ma (Dorsey and Becker, 1995). Clast composition traces the breccia's provenance to the War Eagle Mine area of the Whipple Mountains lower plate, 17 km west of us (Yin and Dunn, 1992). The breccia, now tilted and distended in fault blocks, records the earliest erosional unroofing of the Whipple Mountains core.

Highlights on the Way to STOP 3-4

Return to Arizona 95, turn right, and proceed 38 mi along a terrain of SW-tilted blocks of Proterozoic and overlying Miocene rocks in hanging-wall position above the Whipple detachment fault.

After 19 mi, we approach and cross the Bill Williams River arm of Lake Havasu. High mesas ahead overlooking the Bill Williams River expose 100's of m of post-extensional sedimentary rock and basalt (Sherrod, 1988). This upper Miocene section overlies the tilted rocks. Basalt capping lavas and as dikes date this section as 9–7 Ma (Spencer and Reynolds, 1989). These rocks experienced relatively minor faulting and tilting at the tail end of regional extension in the CREC. Their position and thickness here imply that they projected over some of the Whipple Mountains. Their presence raises the question of when and how canyons began eroding through them and making way for the subsequent integration of the Colorado River across the Whipple Mountains highland. The presence of Bouse Formation low in Chemehuevi Valley upstream and in Parker Valley downstream, both significantly lower than the mesa tops, indicates that those depressions somehow formed before any river arrived here. What happened to remove or lower the thick, now high, sections of upper Miocene alluvium and basalt?

The Bill Williams River. The Bill Williams River is a significant tributary to the lower Colorado River. It drains more than 13,500 km^2 of the rugged highlands of western Arizona, and is the largest drainage to enter the Colorado between Lake Mead and Yuma, Arizona, where the Gila meets the Colorado. The Bill Williams watershed drains rugged terrain up to the edge of the Colorado Plateau, making it susceptible to significant flood runoff from winter rain-on-snow events and regional-scale dissipating tropical storms. The much larger Gila River watershed has a complicated flood regime, but the largest floods have also occurred in fall or winter. Consequently, the flood regime of Colorado River changes somewhat below its junction with the Bill Williams, because these large tributaries have flood-runoff regimes that differ significantly from that of the bulk of the mainstem river, which gets most of its water from late spring snowmelt in the Rocky Mountains.

Storage in Lake Havasu above Parker Dam began on 1 July 1938. Fourteen months later, a historic series of three tropical storms entered the southwestern United States in September, dropping 230–250 mm (~9–10 in.) of rain in this region and even more in other parts of the Southwest (Gatewood et al., 1946). An ensuing large flood (~2100–2850 m^3s^{-1}) on the Bill Williams contributed to a 2 m increase in the level of Lake Havasu in less than 3 days (Gatewood et al., 1946). The flood entered the reservoir when its capacity was fortuitously low, which helped avert a significant flood event downstream. In part owing to the obvious problems of floods down the Bill Williams compromising dam operations, Alamo Dam was eventually built in 1968. This drastically decreased peak flood discharges to no more than 200 m^3s^{-1} and detained essentially all of the sediment from the upper 90% of the Bill Williams watershed. This limited outflow capacity reduces peak discharges up to 90%, but protracted low discharge outflows are required to then manage the water behind Alamo Dam. This can result in weeks- to months-long flat hydrographs, which transport a continuous stream of water and reworked sediment to near the intakes for the Central Arizona Project Canal, which delivers Colorado River water to Phoenix and Tucson. Managing rivers is complicated. Much of the sediment in the Bill Williams River delta in southern Lake Havasu is composed of 'legacy' sediment from its now overfit valley bottom below the dam. AZ Highway 95 crosses the Bill Williams delta marsh where it sits near Parker Dam at the south end of Lake Havasu. Thus, there is a novel situation in which there are modern river deltas at each end of Lake Havasu—each recording the progressive effects of flow regulation upstream on sediment discharge. Certainly there are interesting things to be learned in those delta sediments.

Continue south on Arizona 95 for another 19 mi through tilted Miocene strata and Proterozoic crystalline rocks in hanging-wall blocks to the Whipple detachment fault. Here we are in the Parker Strip following the canyon. Many roadcuts on this route offer nice exposures through the rugged mountains and beside the crystal-clear river flowing in the canyon. We pass through a low-lying, abandoned bedrock channel of the Colorado River at River Island State Park, and pass scattered exposures of the Bullhead Alluvium overlying sandy deposits correlative to the Osborn Wash Formation of Davis et al. (1980), interbedded with basalt flows and unconformably overlain by the Bullhead Alluvium at Lakeside Boulevard (Spencer et al., 2015). Across the river on the upper piedmont of the Whipple Mountains are isolated deposits of Bullhead Alluvium eroding out of a paleochannel that was carved in high-standing remnants of upper Miocene fanglomerate (Fig. 36; Spencer et al., 2015).

In Parker, turn left (southeast) at a traffic light to follow Arizona 95 for 1 mile. Turn right on Tribal Highway 1 (Mohave Road) toward Blythe. Proceed through Colorado River Indian Tribal land in Parker Valley for 10.6 mi. Turn right at a flashing orange light onto Agnes Wilson Road. In 2 mi, cross the Colorado River into California and view metamorphic rocks in the Riverside Mountains ahead, lower plate to the Whipple Mountains detachment fault (Carr and Dickey, 1980). In 2 more mi, we climb out of the floodplain through bluffs that expose Upper Pleistocene Colorado River sands and gravels, and surmount a terrace surface on the lower piedmont of the Riverside Mountains. In another mile at the stop sign, carefully cross U.S. 95 and proceed 0.35 mi on a graded gravel road. Follow the fork in the road that veers to the left (southwest), and follow it up the alluvial fan surface for 0.65 mi and park.

STOP 3-4. Bouse Formation at the Foot of the Riverside Mountains (34.0403° N, 114.4953° W)

The purpose of this stop is to further examine the Bouse Formation and to consider whether it records the filling of the Blythe Basin by sedimentation in a brackish lake dammed at the downstream end of the valley or an estuary connected to the marine waters of the Gulf of California. The interbedded valley-fill facies of the Bouse Formation is exposed here, and these siliciclastic deposits overlie a carbonate-cemented tributary gravel that may be a bottomset of the coarse-grained fan delta sequence emanating from the narrow tributary canyon (Fig. 37). There is a prominent bathtub ring of nearshore Bouse tufa on bedrock just above the top of the fill sequence. A challenging hike down into a slot canyon would reveal a spectacular fan delta complex of the Bouse Formation that forms the substrate for a 70-m-thick sequence of the valley-fill facies of the Bouse Formation.

The valley-fill facies fragment that we see here is extensively exposed to our east on the far side of the valley. There, it forms the likely substrate of much of the Cactus Plain dune field (Pearthree et al., 2014). Similar stratified sediments of the Bouse are also exposed extensively off the north flank of the Riverside Mountains. In the latter location, evidence for subaerial exposure, including mudcracks and paleosols interbedded with erosive cross-bedded Colorado River sands, are present in the Bouse sequence. This suggests the possibility that this part of the fill sequence is part of the river's delta plain near the head of Parker Valley. If so, did this feature once extend upstream into Chemehuevi Valley, where paleosols and erosive fluvial sand deposits are also found high in the section?

Highlights on the Way to STOP 3-5

Retrace the gravel road downhill a mile and turn right (south) on U.S. 95. Once back on the highway, travel south toward the Big Maria Mountains. On our way, we will get an excellent view of the Big Maria sand sheet, a large blanket of windblown sand that ramps up the northwest side of the Big Marias. In contrast to the dunes of the Cactus Plain that are sourced from Colorado River sediment, the Big Maria sand sheet is sourced from the Mojave Desert (Zimbelman and Williams, 2002; Muhs et al., 2003). This striking contrast over such a short distance is interpreted as evidence that it is hard to blow significant amounts of sand across a wide valley of a large perennial river (Pease and Tchakerian, 2003).

Proceed 18.3 mi along the river valley and turn right off the highway toward Blythe Intaglios. Follow the gravel road 1 mile to the second parking area.

STOP 3-5. Blythe Intaglios, Big Maria Mountains, and Warren Hamilton Tribute (33.7991° N, 114.5390° W)

The purposes of this final stop are to appreciate some of the prehistory of the region and to honor the work and career of Warren Hamilton. The Blythe intaglios, geoglyph images as long as 52 m of people and animals scraped out of desert pavement, were noticed by a pilot in 1931 (Fig. 38). They are among hundreds of intaglios in the Colorado Desert. Although local indigenous

Figure 36. Channel filling remnants of the Bullhead Alluvium high on the Whipple Mountain piedmont west of the river. Photo shows bouldery local base of the unit (hat for scale), where it cuts into mildly deformed upper Miocene sediments.

people knew of them, their original purpose and their sculptors are unknown.

The Big Maria Mountains rising above us were mapped long ago by Warren Hamilton (Fig. 39). His long-time collaborator Brad Myers remarked proudly that Hamilton's mapping of the Big Maria Mountains area was "full of squiggly lines—and Warren isn't a squiggly-line person!" (1981, oral commun. with K.A. Howard). Warren deeply appreciated field geologic observations and integrated them with geophysics into big new innovative earth science ideas.

Figure 37. View into the Riverside Mountains from STOP 3-4. Horizontal siliciclastic beds of the Bouse Formation (Tbos) overlie fan and fan-delta deposits with interbeds of Bouse travertine and marl (Tbogm). Both are in buttress unconformity against metamorphic bedrock. A relatively thin rind of travertine encrusts the bedrock just above the siliciclastic sediments (Tbot). The narrow gorge beginning near the base of the flat-bedded Bouse sediments contains good exposures of interbedded tributary and Bouse strata.

Figure 38. Some of the Blythe intaglios. Fence enclosures (the larger one here is 30 m long) protect the features from vehicle tracks, such as those seen around and partly over the intaglios. Google Earth image.

Hamilton demonstrated that the metamorphosed strata in the Big Maria Mountains correlate directly to the succession of Paleozoic continental platform rocks displayed in Grand Canyon, here intricately deformed and convoluted, so that locally the whole succession and each formation are thinned in places to an astounding 1% of original thickness. The metamorphosed Cambrian Tapeats Sandstone at the base of this succession rests on Proterozoic basement rocks. At the top, metamorphosed Mesozoic strata overlie the Permian Kaibab Limestone, now marble. Hamilton proposed that the strata were deformed in the Mesozoic between rising domes of the Proterozoic basement and Jurassic intrusions, then subjected to Cretaceous contractional tectonics, and then to Cenozoic extensional and dextral faulting (Hamilton, 1964, 1982, 1987a, 1987b; Hamilton et al., 1987).

Hamilton's mapping carefully depicted the highly complex, contorted bedrock of the Big Maria Mountains, and also conveyed a keen grasp of the geomorphology of the piedmont and the river's contortions evident on its scroll-bar floodplain (Fig. 39; Hamilton, 1964, 1987a). His early perception of what later became known as the Bouse Formation effectively captures today's concepts and ongoing controversies, as contained in the following passage from his 1960 contribution titled "Pliocene(?) Sediments of Salt Water Origin near Blythe, Southeastern California":

> Either the Gulf of California previously extended into this area, or else a huge saline lake existed here. Such a lake might have been dammed by the rising of the Chocolate Mountains, 50 mi to the south, across the Colorado River, but if so, the mountains have since been lowered by subsidence as well as by erosion. (Hamilton, 1960)

The scope of Warren Hamilton's huge contributions in his more than four decades in the U.S. Geological Survey rivals any since G.K. Gilbert's. Hamilton's big-picture contributions in continental mobility and plate tectonics were typically contrarian

Figure 39. Warren Hamilton in the Riverside Mountains in 1980. Note the scroll bars and sweeping meander loop that ornament the Colorado River floodplain (Blythe Alluvium) in the background. Photo by Robert Simpson; used with permission.

and well ahead of their time. His perspectives expanded further, in his following two decades at the Colorado School of Mines, into a series of insightful and iconoclastic new interpretations of the evolution of early Earth and the terrestrial planets (e.g., Hamilton, 2019).

Highlights on the Way Back to Phoenix

Return to U.S. 95, turn right and follow U.S. 95 for 16 mi to Blythe. Turn onto I-10 eastbound toward Phoenix (150 mi).

As we pass through and eastward from Blythe, California, toward Ehrenberg, Arizona, the palimpsest patterns of the once mighty and mighty variable Colorado River are mostly impossible to see beneath the dense patchwork of agricultural land. However, this transect of the floodplain has been rendered in maps by Ives expedition cartographer Friedrich von Egloffstein and by Willis T. Lee, an early geologic investigator in this region. Those historical maps combined with a chronology of aerial photos dating to 1930 (pre–Hoover Dam) are helping to develop a detailed geologic map of this section of the floodplain (Fig. 40).

Past Ehrenberg, we climb the piedmont of the Dome Rock Mountains, where outcrops of the Chemehuevi Formation and various aged alluvial fan deposits are well exposed. Small outcrops of Bouse travertine and shoreline gravels have been identified in bedrock niches south of Interstate-10. Once across the Dome Rock Mountain summit, we will pass through the colorful town of Quartzsite, Arizona. Look for the intriguing profile of the Kofa Mountains to the southeast as we enter the heart of the southern Basin and Range. Quartzsite sits in the middle of the

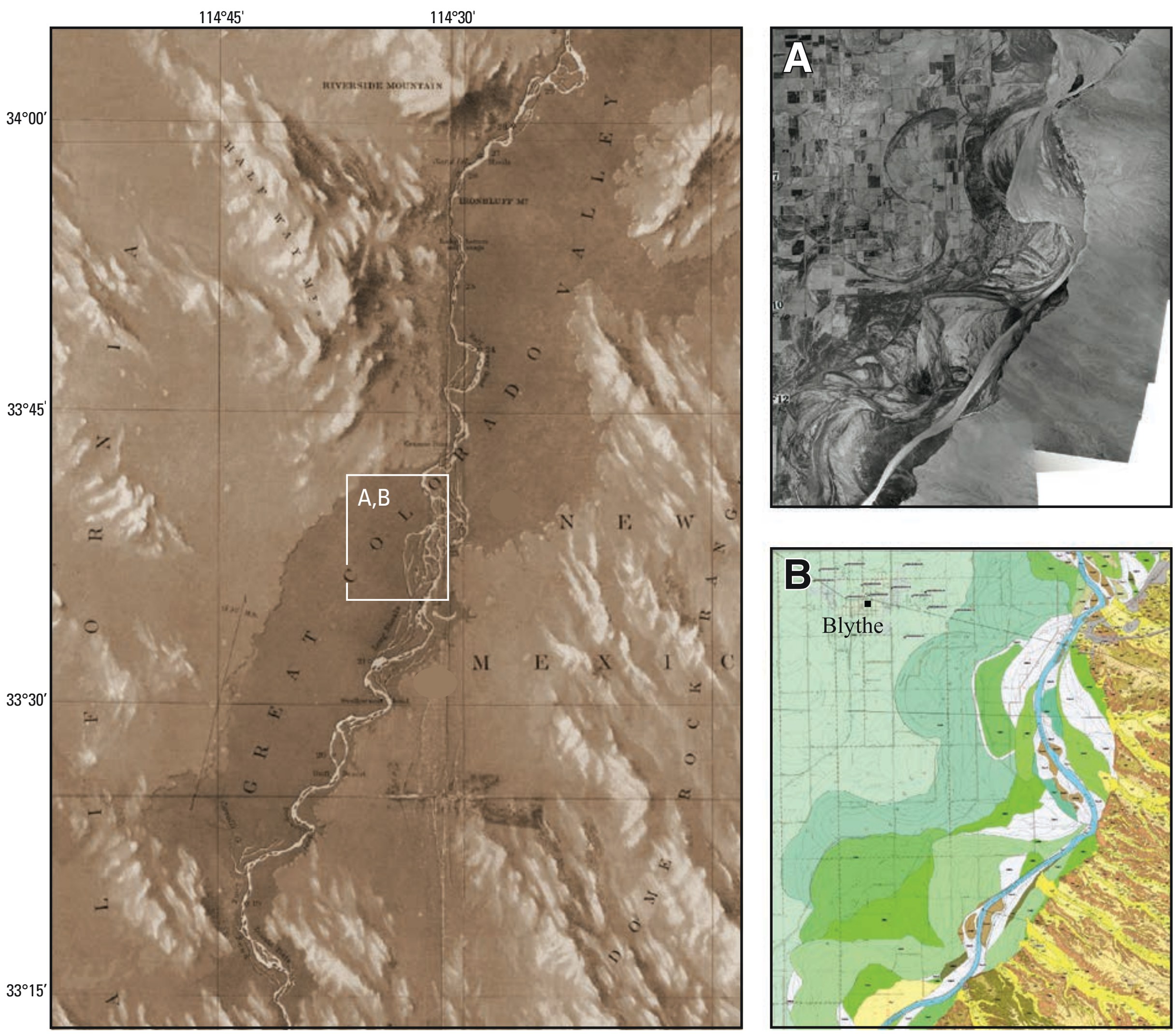

Figure 40. Selected map renditions of the Blythe, California, area in the Great Colorado Valley. Main map is excerpt from “Geological Map No. 1” prepared by J.S. Newberry and drawn by F.W. von Egloffstein for the Ives expedition, showing most of the Great Valley of the Colorado as mapped in 1858 (Ives, 1861). (Inset A) Mosaic of aerial photographs dating to 1930 showing the area of the Blythe 7.5′ quadrangle. Source: Fairchild Aerial Surveys, Flight C-1050, commissioned by U.S. Dept. of the Interior. (Inset B) Draft geologic map of the Blythe 7.5′ quadrangle (Block et al., 2018).

La Posa Plain, a broad and relatively flat valley drained by Tyson Wash, a large wash that drains to the Colorado River floodplain north of Blythe. The La Posa Plain also hosts a large amount of eolian sediment, particularly along its east side and north end (Fig. 13). The Bullhead Alluvium and Bouse Formation underlie parts of the La Posa valley.

Near the rest area at mile 55, we are in the headwaters of Bouse Wash and will cross into the divide of the Gila River, which drains more than 115,000 km^2 of central and southern Arizona and a small part of southwestern New Mexico.

ACKNOWLEDGMENTS

We thank Scott Bennett and Jon Spencer for very helpful reviews and suggestions that improved the manuscript. Brian Gootee, Larry Hamilton, and Bob Simpson graciously provided photographic images. Debra Block helped with several of the figures.

REFERENCES CITED

Allen, C.M., Wooden, J.L., Howard, K.A., Foster, D.A., and Tosdal, R.M., 1995, Sources of the Early Cretaceous plutons in the Turtle and West Riverside Mountains, California: Anomalous Cordilleran Interior plutons: Journal of Petrology, v. 36, p. 1675–1700.

Ameen, M.S., 1988, Folding of Layered Cover Due to Dip-Slip Basement Faulting [Ph.D. thesis]: London, University of London, Imperial College of Technology, 210 p.

Anderson, E.M., 1951, The Mechanics of Faulting and Dyke Formation with Applications to Britain: Edinburgh, Oliver and Boyd, 206 p.

Anderson R.E., 1969, Notes on the Geology and Paleohydrology of the Boulder City pluton, southern Nevada: U.S. Geological Survey Professional Paper 650-B, p. 35–40.

Anderson, J.L., 1988, Core complexes of the Mojave-Sonoran Desert; Conditions of plutonism, mylonitization, and decompression, *in* Ernst, W.G., ed., Metamorphism and Crustal Evolution of the Western United States (Rubey Volume 7): Englewood Cliffs, New Jersey, Prentice-Hall, p. 502–525.

Anderson, J.L., and Bender, E.E., 1989, Nature and origin of Proterozoic A-type granitic magmatism in the southwestern United States: Lithos, v. 23, p. 19–52, https://doi.org/10.1016/0024-4937(89)90021-2.

Anderson, J.L., and Cullers, R.L., 1990, Middle to upper crustal plutonic construction of a magmatic arc; An example from the Whipple Mountains metamorphic core complex, *in* Anderson, J.L., ed., The Nature and Origin of Cordilleran Magmatism: Geological Society of America Memoir 174, https://doi.org/10.1130/MEM174-p47, p. 47–69.

Anderson, R.E., 1971, Thin-skin distension in Tertiary rocks of southeastern Nevada: Geological Society of America Bulletin, v. 82, p. 43–58, https://doi.org/10.1130/0016-7606(1971)82[43:TSDITR]2.0.CO;2.

Anderson, R.E., Longwell, C.R., Armstrong, R.L., and Marvin, R.F., 1972, Significance of K-Ar ages of Tertiary rocks from the Lake Mead region, Nevada-Arizona: Geological Society of America Bulletin, v. 83, p. 273–288, https://doi.org/10.1130/0016-7606(1972)83[273:SOKAOT]2.0.CO;2.

Armstrong, R.L., and Ward, P., 1991, Evolving geographic patterns of Cenozoic magmatism in the North American Cordillera; The temporal and spatial association of magmatism and metamorphic core complexes: Journal of Geophysical Research. Solid Earth, v. 96, no. B8, p. 13,201–13,224, https://doi.org/10.1029/91JB00412.

Atwater, T., and Stock, J., 1998, Pacific–North America plate tectonics of the Neogene southwestern United States: An update: International Geology Review, v. 40, no. 5, p. 375–402, https://doi.org/10.1080/00206819809465216.

Bennett, S.E.K., Oskin, M.E., and Iriondo, A., 2013, Transtensional rifting in the proto–Gulf of California near Bahía Kino, Sonora, México: Geological Society of America Bulletin, v. 125, no. 11–12, p. 1752–1782, https://doi.org/10.1130/B30676.1.

Bennett, S.E.K., Darin, M.H., Dorsey, R.J., Skinner, L.A., Umhoefer, P.A., and Oskin, M.J., 2016a, Animated tectonic reconstruction of the lower Colorado River region: Implications for late Miocene to Present deformation, *in* Reynolds, R.E., ed., Going LOCO: Investigations along the Lower Colorado River—2016 Desert Symposium Field Guide and Proceedings: Northridge, California State University Desert Studies Center, p. 73–86.

Bennett, S.E.K., Oskin, M.E., Iriondo, A., and Kunk, M.J., 2016b, Slip history of the La Cruz fault: Development of a late Miocene transform in response to increased rift obliquity in the northern Gulf of California: Tectonophysics, v. 693, p. 409–435, https://doi.org/10.1016/j.tecto.2016.06.013.

Bergland, E., 1876, Appendix B. Preliminary report upon the operations of Party No. 3, California Section, season of 1875–1876, with a view to determine the feasibility of diverting the Colorado River for purposes of irrigation, *in* Wheeler, G.M., ed., Annual report upon the geographical surveys west of the one hundredth meridian in California, Nevada, Utah, Colorado, Wyoming, New Mexico, Arizona, and Montana: Being Appendix JJ of the Annual Report of the Chief of Engineers for 1876: Washington, D.C., Government Printing Office, p. 124–125.

Block, D., House, P.K., and Gootee, B., 2018, The 'Blythe Alluvium': Holocene to modern floodplain and channel deposits of the lower Colorado River, Arizona, Nevada, and California: Geological Society of America Abstracts with Programs, v. 50, no. 5, https://doi.org/10.1130/abs/2018RM-314093.

Block, D., Gootee, B.F., House, P.K., and Pearthree, P.A., 2019, Geologic Map of the Blythe 7.5′ Quadrangle, La Paz County, Arizona, and Riverside County, California: Arizona Geological Survey DGM-XX19, scale 1:24,000 (in review).

Block, L., and Royden, L.H., 1990, Core complex geometries and regional scale flow in the lower crust: Tectonics, v. 9, no. 4, https://doi.org/10.1029/TC009i004p00557.

Bradshaw, T.K., Hawksworth, C.J., and Gallagher, T., 1993, Basaltic volcanism in the southern Basin and Range: No role for a mantle plume: Earth and Planetary Science Letters, v. 116, p. 45–62, https://doi.org/10.1016/0012-821X(93)90044-A.

Bright, J., Cohen, A.S., Dettman, D.L., Pearthree, P.A., Dorsey, R.J. and Homan, M.B., 2016, Did a catastrophic lake spillover integrate the late Miocene early Pliocene Colorado River and the Gulf of California?: Microfaunal and stable isotope evidence from Blythe Basin, California-Arizona, USA: Palaios, v. 31, no. 3, p. 81–91, https://doi.org/10.2110/palo.2015.035.

Brun, J.P., Sokoutis, D., and Van Den Driessche, J., 1994, Analogue modeling of detachment fault systems and core complexes: Geology, v. 22, p. 319–322, https://doi.org/10.1130/0091-7613(1994)022<0319:AMODFS>2.3.CO;2.

Burchfiel, B.C., and Davis, G.A., 1975, Nature and controls of Cordilleran orogenesis, western United States; extensions of an earlier synthesis: American Journal of Science, v. 275-A, p. 97–118, https://eurekamag.com/research/019/499/019499430.php.

Bryant, B., and Wooden, J.L.,1989, Lower-plate rocks of the Buckskin Mountains, Arizona: A progress report, *in* Spencer, J.E., and Reynolds, S.J., eds., Geology and Mineral Resources of the Buckskin and Rawhide Mountains, West-Central Arizona: Arizona Geological Survey Bulletin, v. 198, p. 47–50.

Bryant, B., and Wooden, J.L., 2008, Geology of the Northern Part of the Harcuvar Complex, Western Arizona: U.S. Geological Survey Professional Paper 1752, 51 p.

Buck, W.R., 1988, Flexural rotation of normal faults: Tectonics, v. 7, p. 959–973, https://doi.org/10.1029/TC007i005p00959.

Buising, A.V., 1990, The Bouse Formation and bracketing units, southeastern California and western Arizona; Implications for the evolution of the proto–Gulf of California and the lower Colorado River: Journal of Geophysical Research, v. 95, no. B, p. 21,111–20,132.

Campbell, E.A., and John, B.E., 1996, Constraints on extension-related plutonism from modeling of the Colorado River gravity high: Geological Society of America Bulletin, v. 108, p. 1242–1255, https://doi.org/10.1130/0016-7606(1996)108<1242:COERPF>2.3.CO;2.

Campbell-Stone, E., and John, B.E., 2002, Temporal changes in deformation mode: From failure to flow in the Colorado River extensional corridor: International Geology Review, v. 44, p. 512–527, https://doi.org/10.2747/0020-6814.44.6.512.

Campbell-Stone, E.A., John, B.E., Foster, D.A., Geissman, J.W., and Livaccari, R.F., 2000, Mechanisms for accommodation of Miocene extension—Low-angle normal faulting, magmatism, and secondary breakaway faulting in the southern Sacramento Mountains, southeastern California: Tectonics, v. 19, p. 566–587, https://doi.org/10.1029/1999TC001133.

Carl, B.S., and Miller, C.F., 1991, Western Old Woman Mountains shear zone: Evidence for late ductile extension in the Cordilleran orogenic belt: Geology, v. 19, p. 893–896, https://doi.org/10.1130/00917613(1991)019<0893:WOWMSZ>2.2.CO:2.

Carr, W.J., 1991, A Contribution to the Structural History of the Vidal-Parker Region, California and Arizona: U.S. Geological Survey Professional Paper 1430, 40 p.

Carr, W.J., and Dickey, D.D., 1980, Geologic Map of the Vidal, California and Parker SW, California–Arizona quadrangles: U.S. Geological Survey Miscellaneous Investigations Map I-1125, scale 1:24,000.

Carr, W.J., Dickey, D.D., and Quinlan, W.D., 1980, Geologic Map of the Vidal NW, Vidal Junction and Parts of the Savahia Peak SW and Savahia Peak Quadrangles, San Bernardino County, California: U.S. Geological Survey Miscellaneous Investigations Map I-1126, scale 1:24,000.

Chapman, J.B., Dafov, M.N., Gehrels, G., Ducea, M.N., Valley, J.W., and Ishida, A., 2018, Lithospheric architecture and tectonic evolution of the southwestern U.S. Cordillera: Constraints from zircon Hf and O isotopic data: Geological Society of America Bulletin, v. 130, p. 2031–2046, https://doi.org/10.1130/B31937.1.

Crossey, L.J., Karlstrom, K.E., Dorsey, R.J., Pearce, J., Van Wijk, J.W., Beard, L.S., Asmerom, Y., Polyak, V.J., Crow, R.S., Cohen, A., Bright, J., and Pecha, M.E., 2015, Importance of groundwater in propagating downward integration of the 6–5 Ma Colorado River system: Geochemistry of springs, travertines, and lacustrine carbonates of the Grand Canyon region over the past 12 Ma: Geosphere, v. 11, no. 3, p. 660–682, https://doi.org/10.1130/GES01073.1.

Crow, R.S., Block, D., Felger, T.J., House, P.K., Pearthree, P.A., Gootee, B.F., Youberg, A.M., Howard, K.A., and Beard, L.S., 2018a, The Colorado River and Its Deposits Downstream from Grand Canyon in Arizona, California, and Nevada: U.S. Geological Survey Open-File Report 2018–1005, 6 p., https://doi.org/10.3133/ofr20181005.

Crow, R., Howard, K.A., Beard, L.S., Pearthree, P.A., House, P.K., Karlstrom, K., Peters, L., McIntosh, W., Cassidy, C.E., and Block, D., 2018b, Plio-Pleistocene deformation in the Lake Mead region and uplift of the Colorado Plateau: Geological Society of America Abstracts with Programs, v. 50, no. 5, abstract 64-3, https://doi.org/10.1130/abs/2018RM-314096.

Crow, R., Pearthree, P., House, P.K., Stelten, M., Heizler, M., Schwing, J., Champion, D., Howard, K., and Hillhouse, J., 2018c, Geochronologic study of pre-Colorado-River deposits in Cottonwood Valley, AZ: Implications for the timing of river integration: Geological Society of America Abstracts with Programs, v. 50, no. 5, https://doi.org/10.1130/abs/2018RM-314086.

Crow, R., Schwing, J., Karlstrom, K., Heizler, M., Pearthree, P.A., House, P.K., Stelten, M., Dulin, S., and Crossey, L., 2019, Redefining the age of the Colorado River: New geochronologic constraints on its integration to the Gulf of California: Geological Society of America Abstracts with Programs, v. 51, no. XX (in press).

Davis, G.A., 1988, Rapid upward transport of mid-crustal mylonitic gneisses in the footwall of a Miocene detachment fault, Whipple Mountains, southeastern California: Geologische Rundschau, v. 77, p. 191–209.

Davis, G.A., and Lister, G.S., 1988, Detachment faulting in continental extension: Perspectives from the southwestern U.S. Cordillera, *in* Clark, S.P., Jr., Burchfiel, B.C., and Suppe, J., eds., Processes in Continental Lithospheric Deformation: Geological Society of America Special Paper 218, John Rodgers Symposium Volume, p. 133–159, https://doi.org/10.1130/SPE218-p133.

Davis, G.A., Anderson, J.L., Frost, E.G., and Shackelford, T.J., 1980, Mylonitization and detachment faulting in the Whipple-Buckskin-Rawhide Mountains terrane, southeastern California and Arizona, *in* Crittenden, M.D., Jr., Coney, P.J., and Davis, G.H. eds., Cordilleran Metamorphic Core Complexes: Geological Society of America Memoir 153, p. 79–130, https://doi.org/10.1130/MEM153-p79.

Davis, G.A., Anderson, J.L., Martin, D.L., Krummenacher, D., Frost, E.G., and Armstrong, R.L., 1982, Geologic and geochronologic relations in the lower plate of the Whipple detachment fault, Whipple Mountains, southeastern California; A progress report, *in* Frost, E.G., and Martin, D.L., eds., Mesozoic-Cenozoic Tectonic Evolution of the Colorado River Region, California, Arizona, and Nevada (Anderson-Hamilton Volume): San Diego, California, Cordilleran Publishers, p. 409–432.

DeCelles, P.G., 2004, Late Jurassic to Eocene evolution of the Cordilleran thrust belt and foreland basin system, western U.S.A.: American Journal of Science, v. 304, p. 105–168, https://doi.org/10.2475/ajs.304.2.105.

Dickinson, W.R., and Snyder, W.S., 1979, Geometry of subducted slabs related to San Andreas transform: The Journal of Geology, v. 87, p. 609–627, https://doi.org/10.1086/628456.

Dorsey, R.J., and Becker, U., 1995, Evolution of a large Miocene growth structure in the upper plate of the Whipple detachment fault, northeastern Whipple Mountains, California: Basin Research, v. 7, p. 151–163, https://doi.org/10.1111/j.1365-2117.1995.tb00101.x.

Dorsey, R.J., and Roberts, P., 1996, Evolution of the Miocene north Whipple basin in the Aubrey Hills, western Arizona, upper plate of the Whipple detachment fault, *in* Beratan, K.K., ed., Reconstructing the History of Basin and Range Extension Using Sedimentology and Stratigraphy: Geological Society of America Special Paper 303, p. 127–146, https://doi.org/10.1130/0-8137-2303-5.127.

Dorsey, R.J., Fluette, A., McDougall, K., Housen, B.A., Janecke, S.U., Axen, G.J., and Shirvell, C.R., 2007, Chronology of Miocene–Pliocene deposits at Split Mountain Gorge, southern California: A record of regional tectonics and Colorado River evolution: Geology, v. 35, no. 1, p. 57–60, https://doi.org/10.1130/G23139A.1.

Dorsey, R.J., Housen, B.A., Janecke, S.U., Fanning, C.M., and Spears, A.L., 2011, Stratigraphic record of basin development within the San Andreas fault system: Late Cenozoic Fish Creek–Vallecito basin, southern California: Geological Society of America Bulletin, v. 123, no. 5–6, p. 771–793, https://doi.org/10.1130/B30168.1.

Dorsey, R.J., O'Connell, B., Homan, M.B., and Bennett, S.E.K., 2017, Influence of the eastern California shear zone on deposition of the Mio-Pliocene Bouse Formation: Insights from the Cibola area, Arizona, *in* Reynolds, R.E., ed., Going LOCO: Investigations along the Lower Colorado River—2016 Desert Symposium Field Guide and Proceedings: Northridge, California State University Desert Studies Center, p. 150–157.

Elston, D.P., and Young, R.A., 1991, Cretaceous-Eocene (Laramide) landscape development and Oligocene-Pliocene drainage reorganization of transition zone and Colorado Plateau, Arizona: Journal of Geophysical Research, v. 96, no. B7, p. 12,389–12,406, https://doi.org/10.1029/90JB01978.

Faulds, J.E., Geissman, J.W., and Mawer, C.K., 1990, Structural development of a major extensional accommodation zone in the Basin and Range Province, northwestern Arizona and southern Nevada; Implications for kinematic models of continental extension, *in* Wernicke, B.P., ed., Basin and Range Extensional Tectonics near the Latitude of Las Vegas, Nevada: Geological Society of America Memoir 176, p. 37–76, https://doi.org/10.1130/MEM176-p37.

Faulds, J.E., Geissman, J.W., and Shafiqullah, M., 1992, Implications of paleomagnetic data on Miocene extension near a major accommodation zone in the Basin and Range province, northwestern Arizona and southern Nevada: Tectonics, v. 11, p. 204–227, https://doi.org/10.1029/91TC00869.

Faulds, J.E., Smith, E.I., and Gans, P., 1999, Spatial and temporal patterns of magmatism and extension in the northern Colorado River extensional corridor, Nevada and Arizona: A preliminary report: Nevada Petroleum Society Guidebook, p. 171–183.

Faulds, J.E., House, P.K., Pearthree, P.A., Bell, J.W., and Ramelli, A.R., 2004, Preliminary Geologic Map of the Davis Dam Quadrangle and Eastern Part of the Bridge Canyon Quadrangle, Clark County, Nevada, and Mohave County, Arizona: Nevada Bureau of Mines and Geology Open-File Report 2003–05, scale 1:24,000.

Faulds, J.E., Schreiber, B.C., Langenheim, V.E., Hinz, N.H., Shaw, T.H., Heizler, M.T., Perkins, M.E., El Tabakh, M., and Kunk, M.J., 2016, Paleogeographic implications of late Miocene lacustrine and nonmarine evaporite deposits in the Lake Mead region: Immediate precursors to the Colorado River: Geosphere, v. 12, p. 721–767, https://doi.org/10.1130/GES01143.1.

Ferguson, C.A., McIntosh, W.C., and Miller, C.F., 2013, Silver Creek caldera—The tectonically dismembered source of the Peach Spring Tuff: Geology, v. 41, p. 3–6, https://doi.org/10.1130/G33551.1.

Feuerbach, D.L., Smith, E.I., Walker, J.D., and Tangeman, J.A., 1993, The role of the mantle during crustal extension: Constraints from geochemistry of volcanic rocks in the Lake Mead area, Nevada and Arizona: Geological Society of America Bulletin, v. 105, p. 1561–1575, https://doi.org/10.1130/0016-7606(1993)105<1561:TROTMD>2.3.CO;2.

Fletcher, J.M., and Karlstrom, K.E., 1990, Late Cretaceous ductile deformation, metamorphism and plutonism in the Piute Mountains, eastern Mojave

Desert: Journal of Geophysical Research. Solid Earth, v. 95, no. B1, https://doi.org/10.1029/JB095iB01p00487.

Forshee, E.J., and Yin, A., 1995, Evolution of monolithologic breccia in supradetachment basins, Whipple Mountains, California: Basin Research, v. 7, p. 181–197, https://doi.org/10.1111/j.1365-2117.1995.tb00103.x.

Foster, D.A., and John, B.E., 1999, Quantifying tectonic exhumation in an extensional orogen with thermochronology: Examples from the southern Basin and Range Province, *in* Ring, U., Brandon, M., Lister, G.S., and Willett, S.D., eds., Exhumation Processes: Normal Faulting, Ductile Flow, and Erosion: Geological Society, London, Special Publication 154, p. 356–378, https://doi.org/10.1144/GSL.SP.1999.154.01.16.

Foster, D.A., Miller, D.S., and Miller, C.F., 1991, Tertiary extension in the Old Woman Mountains area, California: Evidence from apatite fission track analysis: Tectonics, v. 10, p. 875–886, https://doi.org/10.1029/91TC00865.

Foster, D.A., Miller, C.F., Harrison, T.M., and Hoisch, T.D., 1992, ^{40}Ar/^{39}Ar thermochronology and thermobarometry of metamorphism, plutonism, and tectonic denudation in the Old Woman Mountains area, California: Geological Society of America Bulletin, v. 104, p. 176–191, https://doi.org/10.1130/0016-7606(1992)104<0176:AATATO>2.3.CO;2.

Frost, E.G., and Martin, D.L., 1982, Comparison of Mesozoic compressional tectonics with mid-Tertiary detachment faulting in the Colorado River area, California, Arizona, and Nevada, *in* Cooper, J.D., compiler, Geologic Excursions in the California Desert: Geological Society of America Cordilleran Section, 78th Annual Meeting, Anaheim, California, April 19–21, p. 113–159.

Frost, E.G., and Okaya, D.A., 1986, Application of seismic reflection profiles to tectonic analysis in mineral exploration: Arizona Geological Society Digest, v. 16, p. 137–156.

Gans, P.B., 1987, An open-system, two-layer crustal stretching model for the Eastern Great Basin: Tectonics, v. 6, no. 1, https://doi.org/10.1029/TC006i001p00001.

Gans, P.B., and Bohrson, W.A., 1998, Suppression of volcanism during rapid extension in the Basin and Range Province, United States: Science, v. 279, no. 5347, p. 66–68, https://doi.org/10.1126/science.279.5347.66.

Gans, P.B., and Gentry, B.J., 2016, Dike emplacement, footwall rotation, and transition from magmatic to tectonic extension in the Whipple Mountains metamorphic core complex, southeastern California: Tectonics, v. 35, p. 2564–2608, https://doi.org/10.1002/2016TC004215.

Gans, P.B., Mahood, G.A., and Schermer, E., 1989, Synextensional Magmatism in the Basin and Range Province: A Case Study from the Eastern Great Basin: Geological Society of America Special Paper 233, 55 p., https://doi.org/10.1130/SPE233-p1.

Gatewood, J.S., Shrader, F.F., and Stackpole, M.R., 1946, Notable local floods of 1939, Part 1. Floods of September 1939 in Colorado River Basin below Boulder Dam: U.S. Geological Survey Water-Supply Paper 967, p. 1–39.

Gentry, B.J., 2015, Tectonic Significance of the Chambers Well Dike Swarm Whipple Mountains Metamorphic Core Complex, CA [M.S. thesis]: Santa Barbara, University of California Santa Barbara, 59 p.

Glazner, A.F., and Bartley, J.M., 1984, Timing and tectonic setting of Tertiary low-angle normal faulting and associated magmatism in the southwestern United States: Tectonics, v. 3, p. 385–396, https://doi.org/10.1029/TC003i003p00385.

Glazner, A.F., and Supplee, J.A., 1982, Migration of Tertiary volcanism in the southwestern United States and subduction of the Mendocino fracture zone: Earth and Planetary Science Letters, v. 60, p. 429–436, https://doi.org/10.1016/0012-821X(82)90078-4.

Goodge, J.W., and Vervoort, J.D., 2006, Origin of Mesoproterozoic A-type granites in Laurentia; Hf isotope evidence: Earth and Planetary Science Letters, v. 243, p. 711–731, https://doi.org/10.1016/j.epsl.2006.01.040.

Hamilton, W., 1960, Pliocene(?) sediments of salt water origin near Blythe, southeastern California, *in* Geological Survey Research 1960; Short Papers in the Geological Sciences: U.S. Geological Survey Professional Paper 400-B, p. 276–277.

Hamilton, W., 1964, Geologic Map of the Big Maria Mountains NE quadrangle, Riverside County, California, Yuma County, Arizona: U.S. Geological Survey Geologic Quadrangle Map GQ-350, scale 1:24,000.

Hamilton, W., 1982, Structural evolution of the Big Maria Mountains, northeastern Riverside County, southeastern California, *in* Frost, E.G., and Martin, D., eds., Mesozoic-Cenozoic Tectonic Evolution of the Colorado River Region, California, Arizona, and Nevada: San Diego, California, Cordilleran Publishers, p. 1–27.

Hamilton, W., 1984, Generalized Geologic Map of the Big Maria Mountains Region, Northeastern Riverside County, Southeastern California: U.S. Geological Survey Open-File Report 84–407, scale 1:48,000.

Hamilton, W., 1987a, Mesozoic geology and tectonics of the Big Maria Mountains region, southeastern California: Arizona Geological Society Digest, v. 18, p. 33–47.

Hamilton, W., 1987b, Crustal extension in the Basin and Range province, southwestern United States, *in* Coward, M.P., Dewey, J.F., and Hancock, P.L., eds., Continental Extensional Tectonics: Geological Society, London, Special Publication 28, p. 155–176, https://doi.org/10.1144/GSL.SP.1987.028.01.12.

Hamilton, W.B., 1988, Detachment faulting in the Death Valley region, California and Nevada, *in* Carr, M.D., and Yount, J.C., eds., Geologic and Hydrologic Investigations of a Potential Nuclear Waste Disposal Site at Yucca Mountain, Southern Nevada: U.S. Geological Survey Bulletin 1790, p. 51–85.

Hamilton, W.B., 2019, Toward a myth-free geodynamic history of Earth and its neighbors: Earth-Science Reviews (in press).

Hamilton, W.B., and Myers, W.B., 1966, Cenozoic tectonics of the western United States: Reviews of Geophysics, v. 4, p. 509–549, https://doi.org/10.1029/RG004i004p00509.

Hamilton, W., and Myers, W.B., 1967, The Nature of Batholiths: U.S. Geological Survey Professional Paper 554-C, 30 p.

Hamilton, W., Tosdal, R.M., Stone, P., and Haxel, G.B., 1987, Mesozoic tectonics of southeastern California, *in* Davis, G.H., and VandenDolder, E.M., eds., Geologic Diversity of Arizona and Its Margins—Excursions to Choice Areas: Arizona Geological Survey Special Paper 5, p. 337–350.

Hammond, J.G., 1990, Middle Proterozoic diabase intrusions in the southwestern U.S.A. as indicators of limited extensional tectonism, *in* Gower, C.F., Rivers, T., and Ryan, B., eds., Mid-Proterozoic Laurentia-Baltica: Geological Association of Canada Special Paper 38, p. 517–531.

Harvey, J.C., 2014, Zircon age and oxygen isotopic correlations between Bouse Formation tephra and the Lawlor Tuff: Geosphere, v. 10, p. 221–232, https://doi.org/10.1130/GES00904.1.

Hazlett, R.W., 1990, Extension-related Miocene volcanism in the Mopah Range volcanic field, southeastern California, *in* Anderson, J.L., ed., The Nature and Origin of Cordilleran Magmatism: Geological Society of America Memoir 174, p. 133–146, https://doi.org/10.1130/MEM174-p133.

Hillhouse, J.W., and Wells, R.E., 1991, Magnetic fabric, flow directions, and source area of the lower Miocene Peach Springs Tuff in Arizona, California, and Nevada: Journal of Geophysical Research, v. 96, no. B7, p. 12,443–12,460, https://doi.org/10.1029/90JB02257.

Holland, M.E., Karlstrom, K.E., Gehrels, G., Shufildt, O.P., Begg, G., Griffin, W., and Belousova, E., 2018, Paleoproterozoic Vishnu basin in southwestern Laurentia: Implications for supercontinent reconstructions, crustal growth, and the origin of the Mojave crustal province: Precambrian Research, v. 308, p. 1–17, https://doi.org/10.1016/j.precamres.2018.02.001.

House, P.K., 2016, The LOCO Strata: New observations, mapping, discoveries, and ideas about key geologic deposits chronicling the inception and evolution of the lower Colorado River from the Pliocene to the present, *in* Reynolds, R.E., Going LOCO: Investigations along the Lower Colorado River—2016 Desert Symposium Field Guide and Proceedings: Northridge, California State University Desert Studies Center, p. 65–72.

House, P.K., Howard, K.A., Pearthree, P.A., and Bell, J.W., 2004, Preliminary Geologic Map of the Nevada and Arizona Parts of the Mount Manchester Quadrangle: Nevada Bureau of Mines and Geology Open-File Report 04–4, scale 1:24,000, http://pubs.nbmg.unr.edu/Geol-map-Mt-Manchester-quad-p/of2004-04.htm.

House, P.K., Pearthree, P.A., Howard, K.A., Bell, J.W., Perkins, M.E., Faulds, J.E., and Brock, A.L., 2005, Birth of the lower Colorado River—Stratigraphic and geomorphic evidence for its inception near the conjunction of Nevada, Arizona, and California, *in* Pederson, J., and Dehler, C.M., eds., Interior Western United States: Geological Society of America Field Guide 6, p. 357–387, https://doi.org/10.1130/2005.fld006(17).

House, P.K., Pearthree, P.A., and Perkins, M.E., 2008, Stratigraphic evidence for the role of lake spillover in the inception of the lower Colorado River in southern Nevada and western Arizona, *in* Reheis, M.C., Herschler, R., and Miller, D.M., eds., Late Cenozoic Drainage History of the Southwestern Great Basin and Lower Colorado River Region—Geologic and Biotic Perspectives: Geological Society of America Special Paper 439, p. 335–353, https://doi.org/10.1130/2008.2439(15).

House, P.K., John, B.E., Malmon, D.V., Block, D., Beard, S.L., Felger, T.J., Crow, R., Schwing, J., and Cassidy, C.E., 2018, Geologic Map of the Castle Rock 7.5′ Quadrangle, Arizona and California: U.S. Geological Survey Scientific Investigations Map 3411, scale 1:24,000, https://doi.org/10.3133/sim3411.

Howard, J.L., 1996, Paleocene to Holocene paleodeltas of ancestral Colorado River offset by the San Andreas fault system, southern California: Geology, v. 24, p. 783–786, https://doi.org/10.1130/0091-7613(1996)024<0783:PTHPOA>2.3.CO;2.

Howard, K.A., 1991, Intrusion of horizontal dikes: Tectonic significance of Middle Proterozoic diabase sheets widespread in the upper crust of the southwestern United States: Journal of Geophysical Research, v. 96, p. 12,461–12,478.

Howard, K.A., 1993, Volcanic history of the Colorado River extensional corridor: Active or passive rifting?: Geological Society of America Abstracts with Programs, v. 25, no. 5, p. 54.

Howard, K.A., 2011, The upper crust on its side—Steeply tilted slabs in the Basin and Range, *in* Steininger, R., and Pennell, B., eds., Great Basin Evolution and Metallogeny: Geological Society of Nevada 2010 Symposium: Reno, Geological Society of Nevada, v. 1, p. 289–298.

Howard, K.A., and Bohannon, R.G., 2001, Lower Colorado River: Framework, Neogene deposits, incision, and evolution, *in* Young, R.A., and Spamer, E.E., eds., The Colorado River: Origin and Evolution: Grand Canyon, Arizona, Grand Canyon Association, p. 101–106.

Howard, K.A., and John, B.E., 1987, Crustal extension along a rooted system of imbricate low-angle faults: Colorado River extensional corridor, California and Arizona, *in* Coward, M.P., Dewey, J.F., and Hancock, P.L., eds., Continental Extensional Tectonics: Geological Society, London, Special Publication 28, p. 299–311, https://doi.org/10.1144/GSL.SP.1987.028.01.19.

Howard, K.A., and John, B.E., 1997, Fault-related folding during extension: Plunging basement-cored folds in the Basin and Range: Geology, v. 25, p. 223–226, https://doi.org/10.1130/0091-7613(1997)025<0223:FRFDEP>2.3.CO;2.

Howard, K.A., and Malmon, D.V., 2011, Boulders deposited by Pliocene and Pleistocene floods on the lower Colorado River, *in* Beard, L.S., Karlstrom, K.E., Young, R.A., and Billingsley, G.H., eds., CREvolution 2—Origin and Evolution of the Colorado River System, Workshop Abstracts: U.S. Geological Survey Open-File Report 2011–1210, p. 145–150, http://pubs.usgs.gov/of/2011/1210/.

Howard, K.A., Goodge, J.W., and John, B.E., 1982, Detached crystalline rocks of the Mohave, Buck, and Bill Williams Mountains, western Arizona, *in* Frost, E.G., and Martin, D.L., eds., Mesozoic-Cenozoic Tectonic Evolution of the Colorado River Region, California, Arizona, and Nevada (Anderson-Hamilton Volume): San Diego, California, Cordilleran Publishers, p. 377–392.

Howard, K.A., John, B.E., and Miller, C.F., 1987, Metamorphic core complexes, Mesozoic ductile thrusts, and Cenozoic detachments: Old Woman Mountains–Chemehuevi Mountains transect, California and Arizona, *in* Davis, G.H., and Vandendolder, E.M., eds., Geologic Diversity of Arizona and Its Margins: Excursions to Choice Areas: Arizona Bureau of Geology and Mineral Technology Special Paper 5, p. 365–382.

Howard, K.A., John, B.E., Davis, G.A., Anderson, J.L., and Gans, P.B., 1994, A Guide to Miocene Extension and Magmatism in the Lower Colorado River Region, Nevada, Arizona, and California: U.S. Geological Survey Open-File Report 94–246, 54 p., https://doi.org/10.3133/ofr94246.

Howard, K.A., McCaffrey, K.J.W., Wooden, J.L., Foster, D.A., and Shaw, S.E., 1995, Jurassic thrusting of Precambrian basement over Paleozoic cover in the Clipper Mountains, southeastern California, *in* Miller, D.M., and Busby, C., eds., Jurassic Magmatism and Tectonics of the North American Cordillera: Geological Society America Special Paper 299, p. 375–392, https://doi.org/10.1130/SPE299-p375.

Howard, K.A., Nielson, J.E., Wilshire, H.G., Nakata, J.K., Goodge, J.W., Reneau, S.L., John, B.E., and Hansen, V.L., 1999, Geologic Map of the Mohave Mountains area, Mohave County, Western Arizona: U.S. Geological Survey, Miscellaneous Investigations Map I-2308, scale 1:48,000.

Howard, K.A., Lundstrom, S.C., Malmon, D.V., and Hook, S.J., 2008, Age, distribution, and formation of late Cenozoic paleovalleys of the lower Colorado River and their relation to river aggradation and degradation, *in* Reheis, M.C., Herschler, R., and Miller, D.M., eds., Late Cenozoic Drainage History of the Southwestern Great Basin and Lower Colorado River Region: Geologic and Biotic Perspectives: Geological Society of America Special Paper 439, p. 391–410, https://doi.org/10.1130/2008.2439(18).

Howard, K.A., Malmon, D.V., McGeehin, J.P., and Martin, P., 2011, Holocene aggradation of the lower Colorado River in Mohave Valley, California and Arizona, *in* Beard, L.S., Karlstrom, K.E., Young, R.A., and Billingsley, G.H., eds., CREvolution 2—Origin and Evolution of the Colorado River System, Workshop Abstracts: U.S. Geological Survey Open-File Report 2011–1210, p. 151–152, http://pubs.usgs.gov/of/2011/1210/.

Howard, K.A., John, B.E., Nielson, J.E., Miller, J.M.G., and Wooden, J.L., 2013, Geologic Map of the Topock 7.5-Minute Quadrangle, Arizona and California: U.S. Geological Survey Scientific Investigations Map 3236, scale 1:24,000 + 60-p. pamphlet.

Howard, K.A., House, P.K., Dorsey, R.J., and Pearthree, P.A., 2015, River-evolution and tectonic implications of a major Pliocene aggradation on the lower Colorado River: The Bullhead Alluvium: Geosphere, v. 11, p. 1–30, https://doi.org/10.1130/GES01059.1.

Ives, J.C., 1861, Geological Report upon the Colorado River of the West, Explored in 1857 and 1858 by Lieutenant Joseph C. Ives, Corps of Topographical Engineers, under the Direction of the Office of Explorations and Surveys, A.A. Humphreys, Captain Topographical Engineer, in Charge: Government Printing Office, U.S. Senate Executive Document #90, 36th Congress, 5 parts. Also available as a 2002 digital archive edited by K.C. McKinney, U.S. Geological Survey Open-File Report 02–25, version 1.0.

John, B.E., 1986, Structrural and Intrusive History of the Chemehuevi Mountains Area, Southeastern California and Western Arizona [Ph.D. diss.]: Santa Barbara, California, University of California, 295 p.

John, B.E., 1987a, Geometry and evolution of a mid-crustal extensional fault system: Chemehuevi Mountains southeastern California, *in* Coward, M.P., Dewey, J.F., and Hancock, P.L., eds., Continental Extensional Tectonics: Geological Society, London, Special Publication 28, p. 313–335, https://doi.org/10.1144/GSL.SP.1987.028.01.20.

John, B.E., 1987b, Geologic Map of the Chemehuevi Mountains Area, San Bernardino County, California, and Mohave County, Arizona: U.S. Geological Survey Open-File Report 87–666, scale l:24,000 + explanation.

John, B.E., 1988, Structural reconstruction and zonation of a tilted mid-crustal magma chamber: The felsic Chemehuevi Mountains plutonic suite: Geology, v. 16, p. 613–617, https://doi.org/10.1130/0091-7613(1988)016<0613:SRAZOA>2.3.CO;2.

John, B.E., and Cheadle, M.J., 2010, Deformation and alteration associated with oceanic and continental detachment fault systems: Are they similar? *in* Rona, P.A., Devey, C.W., Dyment, J., and Murton, B.J., eds., Diversity of Hydrothermal Systems on Slow Spreading Ocean Ridges: American Geophysical Union, Geophysical Monograph Series 188, p. 175–205, https://doi.org/10.1029/2008GM000772.

John, B.E., and Foster, D.A., 1993, Structural and thermal constraints on the initiation angle of detachment faulting in the southern Basin and Range: The Chemehuevi Mountains case study: Geological Society of America Bulletin, v. 105, p. 1091–1108, https://doi.org/10.1130/0016-7606(1993)105<1091:SATCOT>2.3.CO;2.

John, B.E., and Howard, K.A., 1994, Drape folds in the highly attenuated Colorado River extensional corridor, California and Arizona, *in* McGill, S.F., and Ross, T.M., eds., Geological Investigations of an Active Margin: 27th Annual Meeting of the Geological Society of America Cordilleran Section, Guidebook, San Bernardino, California, March 21–23, 1994: San Bernardino, California, San Bernardino County Museum Association, p. 94–106.

John, B.E., and Mukasa, S.B., 1990, Footwall rocks to the mid-Tertiary Chemehuevi detachment fault: A window into the middle crust in the Southern Cordillera: Journal of Geophysical Research, v. 95, p. 463–485, https://doi.org/10.1029/JB095iB01p00463.

John, B.E., and Wooden, J.L., 1990, Petrology and geochemistry of the metaluminous to peraluminous Chemehuevi Mountains Plutonic Suite, southeastern California, *in* Anderson, J.L., ed., The Nature and Origin of Cordilleran Magmatism: Geological Society of America Memoir 174, p. 71–98, https://doi.org/10.1130/MEM174-p71.

Karlstrom, K.E., Crow, R., Crossey, L.J., Coblentz, D., and Van Wijk, J.W., 2008, Model for tectonically driven incision of the younger than 6 Ma Grand Canyon: Geology, v. 36, p. 835–838, https://doi.org/10.1130/G25032A.1.

Karlstrom, K.E., Lee, J.P., Kelley, S.A., Crow, R.S., Crossey, L.J., Young, R.A., Lazear, G., Beard, L.S., Ricketts, J.W., Fox, M., and Shuster, D.L., 2014, Formation of the Grand Canyon 5 to 6 million years ago through integration of older paleocanyons: Nature Geoscience, v. 7, p. 239–244, https://doi.org/10.1038/ngeo2065.

Karlstrom, K.E., Liu, L., Zhou, Q., Crossey, L.J., Crow, R., and Beard, L.S., 2017, Mechanisms for post-Bouse (post–5 Ma) deformation in the lower Colorado River region, *in* Reynolds, R.E., ed., Going LOCO: Investigations along the Lower Colorado River—2016 Desert Symposium Field Guide and Proceedings: Northridge, California State University Desert Studies Center, p. 145–149.

Kreemer, C., Blewitt, G., and Hammond, W.C., 2010, Evidence for an active shear zone in southern Nevada linking the Wasatch fault to the Eastern California Shear Zone: Geology, v. 38, p. 475–478, https://doi.org/10.1130/G30477.1.

Lachenbruch, A.H., Sass, J.H., and Morgan, P., 1994, Thermal regime of the southern Basin and Range province: 2. Implications of heat flow for regional extension and metamorphic core complexes: Journal of Geophysical Research, v. 99, B11, p. 22,121–22,133, https://doi.org/10.1029/94JB01890.

LaForge, J.S., John, B.E., and Grimes, C.B., 2017, Synextensional dike emplacement across the footwall of a continental core complex, Chemehuevi Mountains, southeastern California: Geosphere, v. 13, no. 6, p. 1867–1886, https://doi.org/10.1130/GES01402.1.

LaRue, E.C., 1925, Water Power and Flood Control of Colorado River below Green River, Utah: U.S. Geological Survey Water-Supply Paper 556, 176 p.

Lee, W.T., 1908, Geologic reconnaissance of a part of western Arizona: U.S. Geological Survey Bulletin, v. 252, p. 41–45.

Lister, G.S., and Baldwin, S.L., 1993, Plutonism and the origin of metamorphic core complexes: Geology, v. 21, p. 607–610, https://doi.org/10.1130/0091-7613(1993)021<0607:PATOOM>2.3.CO;2.

Lister, G.S., and Davis, G.A., 1989, The origin of metamorphic core complexes and detachment faults formed during Tertiary continental extension in the northern Colorado river region, USA: Journal of Structural Geology, v. 11, p. 65–94, https://doi.org/10.1016/0191-8141(89)90036-9.

Lucchitta, I., 1979, Late Cenozoic uplift of the southwestern Colorado Plateau and adjacent lower Colorado River region: Tectonophysics, v. 61, p. 63–95, https://doi.org/10.1016/0040-1951(79)90292-0.

MacKin, J.H., 1950, The down-structure method of viewing geologic maps: The Journal of Geology, v. 58, p. 55–72, https://doi.org/10.1086/625695.

Malmon, D.V., Felger, T.J., and Howard, K.A., 2010, Geologic considerations for the placement and design of backwater restoration sites along the lower Colorado River, *in* Melis, T.S., Hamill, J.F., Coggins, L.G., Jr., Grams, P.E., Kennedy, T.A., Kubly, D.M., and Ralston, B.E., eds., Proceedings of the Colorado River Basin Science and Resource Management Symposium, November 18–20, 2008, Scottsdale, Arizona: U.S. Geological Survey Scientific Investigations Report 2010–5135, p. 307–315. http://pubs.usgs.gov/sir/2010/5135/.

Malmon, D.V., Howard, K.A., House, P.K., Pearthree, P., Lundstrom, S.C., Sarna-Wojcicki, A., Wan, E., and Wahl, D., 2011, Stratigraphy and Depositional Environments of the Upper Pleistocene Chemehuevi Formation along the Lower Colorado River: U.S. Geological Survey Professional Paper 1786, 95 p., https://doi.org/10.3133/pp1786.

Mathis, R.S., 1982, Mid-Tertiary detachment faulting in the southeastern Newberry Mountains, Clark County, Nevada, *in* Frost, E.G., and Martin, D.L., eds., Mesozoic-Cenozoic Tectonic Evolution of the Colorado River Region, California, Arizona, and Nevada (Anderson-Hamilton volume): San Diego, California, Cordillerar Publishers, p. 326–340.

McCarthy, J., Larkin, S.P., Fuis, G.S., Simpson, R.W., and Howard, K.A., 1991, Anatomy of a metamorphic core complex: Seismic refraction wide-angle reflection profiling in southeastern California and western Arizona: Journal Geophysical Research, v. 96, p. 12,259–12,291, https://doi.org/10.1029/91JB01004.

McDougall, K., 2008, Late Neogene marine incursions and the ancestral Gulf of California, *in* Reheis, M.C., Hershler, R., and Miller, D.M., eds., Late Cenozoic Drainage History of the Southwestern Great Basin and Lower Colorado River Region: Geologic and Biotic Perspectives: Geological Society of America Special Paper 439, p. 355–373, https://doi.org/10.1130/2008.2439(16).

McDougall, K., and Miranda-Martinez, A.Y., 2014, Evidence for a marine incursion along the lower Colorado River corridor: Geosphere, v. 10, p. 842–869, https://doi.org/10.1130/GES00975.1.

McDowell, S.M., Miller, C.F., Mundil, R., Ferguson, C.A., and Wooden, J.L., 2014, Zircon evidence for a ~200 k.y. supereruption-related thermal flare-up in the Miocene Black Mountains, western Arizona, USA: Contributions to Mineralogy and Petrology, v. 168, 1031, https://doi.org/10.1007/s00410-014-1031-5.

McKenzie, D., 1978, Some remarks on the development of sedimentary basins: Earth and Planetary Science Letters, v. 40, p. 25–32.

Metzger, D.G., 1968, The Bouse Formation (Pliocene) of the Parker-Blythe-Cibola area, Arizona and California: U.S. Geological Survey Professional Paper 600-D, p. D126–D136.

Metzger, D.G., and Loeltz, O.J., 1973, Geohydrology of the Needles Area, Arizona, California, and Nevada: U.S. Geological Survey Professional Paper 486-J, 54 p., https://doi.org/10.3133/pp486J.

Metzger, D.G., Loeltz, O.J., and Irelna, B., 1973, Geohydrology of the Parker-Blythe-Cibola Area, Arizona and California: U.S. Geological Survey Professional Paper 486-G, 130 p., https://doi.org/10.3133/pp486G.

Mickus, K.L., and James, W.C., 1991, Regional gravity studies in southeastern California, western Arizona, and southern Nevada: Journal of Geophysical Research: Solid Earth, v. 96, no. B7, p. 12,333–12,350, https://doi.org/10.1029/91JB00840.

Miller, C.F., Howard, K.A., and Hoisch, T.D., 1982, Mesozoic thrusting, metamorphism, and plutonism, Old Woman–Piute Range, southeastern California, *in* Frost, E.G., and Martin, D.L., eds., Mesozoic-Cenozoic Tectonic Evolution of the Colorado River Region, California, Arizona, and Nevada (Anderson-Hamilton Volume): San Diego, California, Cordilleran Publishers, p. 561–581.

Miller, D.M., Reynolds, R.E., Bright, J.E., and Starratt, S.W., 2014, Bouse Formation in the Bristol basin near Amboy, California, USA: Geosphere, v. 10, no. 3, p. 462–475, https://doi.org/10.1130/GES00934.1.

Miller, J.M.G., and John, B.E., 1988, Detached strata in a Tertiary low-angle normal fault terrane, southeastern California: A sedimentary record of unroofing, breaching and continued slip: Geology, v. 16, p. 645–648, https://doi.org/10.1130/0091-7613(1988)016<0645:DSIATL>2.3.CO;2.

Miller, J.M.G., and John, B.E., 1999, Sedimentation patterns support seismogenic low-angle normal faulting, southeastern California and western Arizona: Geological Society of America Bulletin, v. 111, p. 1350–1370, https://doi.org/10.1130/0016-7606(1999)111<1350:SPSSLA>2.3.CO;2.

Muhs, D.R., Reynolds, R.L., Been, J., and Skipp, G., 2003, Eolian sand transport pathways in the southwestern United States: Importance of the Colorado River and local sources: Quaternary International, v. 104, p. 3–18, https://doi.org/10.1016/S1040-6182(02)00131-3.

Nakata, J.K., 1982, Preliminary report on diking events in the Mohave Mountains, Arizona, *in* Frost, E.G., and Martin, D.L., eds., Mesozoic-Cenozoic Tectonic Evolution of the Colorado River Region, California, Arizona, and Nevada (Anderson-Hamilton Volume): San Diego, California, Cordilleran Publishers, p. 85–90.

Nakata, J.K., Pernokas, M.A., Howard, K.A., Nielson, J.E., and Shannon, J.R., 1990, K-Ar and fission-track ages (dates) of volcanic, intrusive, altered, and metamorphic rocks in the Mohave Mountains area, west-central Arizona: Isochron-West, no. 56, p. 8–20.

Nichols, K.K., Bierman, P.R., Eppes, M.C., Caffee, M., Finkel, R., and Larsen, J., 2005, Late Quaternary history of the Chemehuevi Mountain piedmont, Mojave desert, deciphered using ^{10}Be and ^{26}Al: American Journal of Science, v. 305, p. 345–368, https://doi.org/10.2475/ajs.305.5.345.

Nielson, J.E., and Beratan, K.K., 1995, Stratigraphic and structural synthesis of a Miocene extensional terrane, southeast California and west-central Arizona: Geological Society of America Bulletin, v. 107, p. 241–252, https://doi.org/10.1130/0016-7606(1995)107<0241:SASSOA>2.3.CO;2.

Nielson, J.E., and Turner, R.D., 1986, Miocene rocks of the northern Turtle Mountains, San Bernardino County, California, *in* Cenozoic Stratigraphy, Structure and Mineralization in the Mojave Desert: Geological Society of America Cordilleran Section Guidebook and Volume, Trips 4 and 5, p. 25–32.

O'Connell, B., Dorsey, R.J., and Humphreys, E.D., 2017, Tidal rhythmites in the southern Bouse Formation as evidence of post-Miocene uplift of the lower Colorado River corridor: Geology, v. 45, p. 99–102, https://doi.org/10.1130/G38608.1.

Olmstead, F.H., Loeltz, O.J., and Irelan, B., 1973 Geohydrology of the Yuma Area: U.S. Geological Survey Professional Paper 486-H, 226 p.

Oskin, M., and Stock, J., 2003, Marine incursion synchronous with plate-boundary localization in the Gulf of California: Geology, v. 31, no. 1, p. 23–26, https://doi.org/10.1130/0091-7613(2003)031<0023:MISWPB>2.0.CO;2.

Pamukcu, A.S., Carley, T.L., Gualda, G.A.R., Miller, C.F., and Ferguson, C.A., 2013, The evolution of the Peach Spring giant magma body; Evidence from accessory mineral textures and compositions, bulk pumice and glass geochemistry, and rhyolite MELTS modeling: Journal of Petrology, v. 54, p. 1109–1148, https://doi.org/10.1093/petrology/egt007.

Parsons, T., and Thompson, G.A., 1991, The role of magma overpressure in suppressing earthquakes and topography: World-wide examples: Science, v. 253, p. 1399–1402, https://doi.org/10.1126/science.253.5026.1399.

Parsons, T., and Thompson, G.A., 1993, Does magmatism influence low-angle normal faulting?: Geology, v. 21, p. 247–250, https://doi.org/10.1130/0091-7613(1993)021<0247:DMILAN>2.3.CO;2.

Pearthree, P.A., and House, P.K., 2014, Paleogeomorphology and evolution of the early Colorado River inferred from relationships in Mohave and Cottonwood Valleys, Arizona, California, and Nevada: Geosphere, v. 10, p. 1139–1160, https://doi.org/10.1130/GES00988.1.

Pearthree, P.A., Ferguson, C.A., Johnson, B.J., and Guynn, J., 2009, Geologic Map and Report for the Proposed State Route 95 Realignment Corridor, Mohave County, Arizona: Arizona Geological Survey Digital Geologic Map DGM-65, 44 p., scale 1:24,000.

Pearthree, P.A., Spencer, J.E., Youberg, Ann, and House, P.K., 2014, Geologic Map of the Black Peak and Bobs Well 7.5 Quadrangles, La Paz County, Arizona: Arizona Geological Survey Digital Geologic Map DGM-108 v1, scale 1:24,000.

Pearthree, P.A., House, P.K., Crow, R., and Gootee, B.F., 2018, Paleolandscapes preserved beneath the Bouse Formation provide insights into the development of the lower Colorado River and latest Miocene and younger deformation: Geological Society of America Abstracts with Programs, v. 50, no. 5, https://doi.org/10.1130/abs/2018RM-313873.

Pease, P.P., and Tchakerian, V.P., 2003, Geochemistry of sediments from Quaternary sand ramps in the southeastern Mojave Desert, California: Quaternary International, v. 104, p. 19–29, https://doi.org/10.1016/S1040-6182(02)00132-5.

Pease, V.L., 1991, The Miocene Dike Swarm of the Mohave Mountains, Arizona: Petrography, Geochemistry, Geochronology, and Paleomagnetism [M.S. thesis]: San Jose, California, San Jose State University, 166 p.

Pease, V., Foster, D., Wooden, J., O'Sullivan, P., Argent, J., and Fanning, C., 1999, The northern Sacramento Mountains, southwest United States. Part II: Exhumation history and detachment faulting, *in* Mac Niocaill, C., and Ryan, P.D., eds., Continental Tectonics: Geological Society, London, Special Publication, p. 199–238, https://doi.org/10.1144/GSL.SP.1999.164.01.11.

Pease, V., Hillhouse, J.W., and Wells, R.E., 2005, Paleomagnetic quantification of upper-plate deformation during Miocene detachment faulting in the Mohave Mountains, Arizona: Geochemistry Geophysics Geosystems, v. 6, no. 9, 20 p., Q09004, https://doi.org/10.1029/2005GC000972.

Poulson, S.R., and John, B.E., 2003, Stable isotope and trace-element geochemistry of the basal Bouse Formation carbonate, southwestern USA: Implications for the Pliocene uplift history of the Colorado Plateau: Geological Society of America Bulletin, v. 115, p. 434–444, https://doi.org/10.1130/0016-7606(2003)115<0434:SIATEG>2.0.CO;2.

Pridmore, C.L., and Frost, E.G., 1992, Detachment faults, California's extended past: California Geology, January/February, p. 3–17, and March/April errata, p. 62.

Proffett, J.M., 1977, Cenozoic geology of the Yerington District, Nevada, and its implications for the nature of Basin and Range faulting: Geological Society of America Bulletin, v. 88, p. 247–266, https://doi.org/10.1130/0016-7606(1977)88<247:CGOTYD>2.0.CO;2.

Reynolds, R.E., Howard, K.A., Wake, T., Smith, G.R., and Roeder, M.A., 2016, A Blancan fauna from the deposits of Santa Fe Railroad, Bullhead Alluvium sequence at Sacramento Wash, Arizona, *in* Reynolds, R.E., ed., Going LOCO: Investigations along the Lower Colorado River—2016 Desert Symposium Field Guide and Proceedings: Northridge, California State University Desert Studies Center, p. 48–51.

Saleeby, J., 2003, Segmentation of the Laramide slab—Evidence from the southern Sierra Nevada region: Geological Society of America Bulletin, v. 115, p. 655–668, https://doi.org/10.1130/0016-7606(2003)115<0655:SOTLSF>2.0.CO;2.

Sarna-Wojcicki, A.M., Deino, A.L., Fleck, R.J., McLaughlin, R.J., Wagner, D., Wan, E., Wahl, D, Hillhouse, J.W., and Perkins, M., 2011, Age, composition, and areal distribution of the Pliocene Lawlor Tuff, and three younger Pliocene tuffs, California and Nevada: Geosphere, v. 7, p. 599–628, https://doi.org/10.1130/GES00609.1.

Seiler, C., Fletcher, J.M., Quigley, M.C., Gleadow, A.J., and Kohn, B.P., 2010, Neogene structural evolution of the Sierra San Felipe, Baja California: Evidence for proto-gulf transtension in the Gulf Extensional Province?: Tectonophysics, v. 488, no. 1–4, p. 87–109, https://doi.org/10.1016/j.tecto.2009.09.026.

Severinghaus, J., and Atwater, T., 1990, Cenozoic geometry and thermal state of the subducting slabs beneath western North America, *in* Wernicke, B.P., ed., Basin and Range Extensional Tectonics near the Latitude of Las Vegas, Nevada: Geological Society of America Memoir 176, p. 1–22, https://doi.org/10.1130/MEM176-p1.

Sherrod, D.R., 1988, Preliminary Geologic Map of the Monkeys Head Quadrangle, Mohave and LaPaz Counties, Arizona: U.S. Geological Survey Open-File Report 88–597, scale 1:24,000, 7 p.

Sherrod, D.R., and Nielson, J.E., eds., 1993, Tertiary Stratigraphy of Highly Extended Terranes, California, Arizona, and Nevada: U.S. Geological Survey Bulletin 2053, 250 p.

Shulaker, D.Z., Grove, M., Hourigan, J.K., Van Buer, N., Sharman, G., Howard, K., Miller, J., and Barth, A.P., 2019, Detrital K-feldspar Pb isotopic evaluation of extraregional sediment transported through an Eocene tectonic breach of southern California's Cretaceous batholith: Earth and Planetary Sciences Letters, v. 508, p. 4–17, https://doi.org/10.1016j.epsl.2018.11.040.

Simpson, R.W., Howard, K.A., Jachens, R.C., and Mariano, J., 1990, A positive gravity anomaly along the Colorado River extensional corridor: Evidence for new crustal material?: Eos (Transactions, American Geophysical Union), v. 71, p. 1594.

Singleton, J.S., 2015, The transition from large-magnitude extension to distributed dextral faulting in the Buckskin-Rawhide metamorphic core complex, west-central Arizona: Tectonics, v. 34, p. 1685–1708, https://doi.org/10.1002/2014TC003786.

Smith, E.I., Feuerbach, D.L., Naumann, T.R., and Mills, J.G., 1990, Mid-Miocene volcanic and plutonic rocks in the Lake Mead area of Nevada and Arizona; Production of intermediate igneous rocks in an extensional environment, *in* Anderson, J.L., ed., The Nature and Origin of Cordilleran Magmatism: Geological Society of America Memoir 174, p. 169–194, https://doi.org/10.1130/MEM174-p169.

Smith, P.B., 1970, New evidence for a Pliocene marine embayment along the lower Colorado River area, California and Arizona: Geological Society of America Bulletin, v. 81, p. 1411–1420, https://doi.org/10.1130/0016-7606(1970)81[1411:NEFAPM]2.0.CO;2.

Spencer, J.E., 1984, Role of tectonic denudation in uplift and warping of low-angle normal faults: Geology, v. 12, p. 95–98, https://doi.org/10.1130/0091-7613(1984)12<95:ROTDIW>2.0.CO;2.

Spencer, J.E., 1985, Miocene low-angle normal faulting and dike emplacement, Homer Mountain and surrounding areas, southeastern California and southernmost Nevada: Geological Society of America Bulletin, v. 96, p. 1140–1155, https://doi.org/10.1130/0016-7606(1985)96<1140:MLNFAD>2.0.CO;2.

Spencer, J.E., and Patchett, J.P., 1997, Sr isotope evidence for a lacustrine origin for the upper Miocene to Pliocene Bouse Formation, lower Colorado River trough, and implications for timing of Colorado Plateau uplift: Geological Society of America Bulletin,v. 109, p.767–778, https://doi.org/10.1130/0016-7606(1997)109<0767:SIEFAL>2.3.CO;2.

Spencer, J.E., and Reynolds, S.J., 1989, Tertiary structure, stratigraphy, and tectonics of the Buckskin Mountains, *in* Spencer, J.E., and Reynolds, S.J., eds., Geology and Mineral Resources of the Buckskin and Rawhide Mountains, West-Central Arizona: Arizona Geological Survey Bulletin 198, p. 103–167.

Spencer, J.E., and Reynolds, S.J., 1991, Tectonics of mid-Tertiary extension along a transect through west central Arizona: Tectonics, v. 10, p. 1204–1221.

Spencer, J.E., Patchett, P.J., Pearthree, P.A., House, P.K., Sarna-Wojcicki, A.M., Wan, E., Roskowski, J.A., and Faulds, J.E., 2013, Review and analysis of the age and origin of the Bouse Formation, lower Colorado River Valley, southwestern USA: Geosphere, v. 9, p. 444–459, https://doi.org/10.1130/GES00896.1.

Spencer, J.E., Youberg, A., Love, D.S., Pearthree, P.A., Steinke, T.R., and Reynolds, S.J., 2014, Geologic Map of the Bouse and Ibex Peak 7.5′ Quadrangle, La Paz County, Arizona: Arizona Geological Survey Digital Geologic Map DGM-107, v. 2.0, scale 1:24,000.

Spencer, J.E., Pearthree, P.A., House, P.K., and Reynolds, S.J., 2015, Geologic Map of the Cross Roads 7 1/2′ Quadrangle and the Southern Part of the Gene Wash 7.5′ Quadrangle, La Paz County, Arizona and San Bernardino County, California. Arizona Geological Survey Digital Geologic Map

DGM-111, scale 1:24,000; http://repository.azgs.az.gov/uri_gin/azgs/dlio/1660 IP-094141.

Stone, P., Howard, K.A., and Hamilton, W., 1983, Correlation of metamorphosed Paleozoic strata of the southern Mojave Desert region, California and Arizona: Geological Society of America Bulletin, v. 94, no. 10, p. 1135–1147, https://doi.org/10.1130/0016-7606(1983)94<1135:COMPSO>2.0.CO;2.

Suneson, N., and Lucchitta, I., 1983, Origin of bimodal volcanism, southern Basin and Range province, west-central Arizona: Geological Society of America Bulletin, v. 94, p. 1005–1019, https://doi.org/10.1130/0016-7606(1983)94<1005:OOBVSB>2.0.CO;2.

Taylor, D.W., 1983, Late Tertiary mollusks from the lower Colorado River valley, *in* Smith, G.R., ed., Contributions from the Museum of Paleontology: Ann, Arbor, Michigan, University of Michigan, v. 26, no. 13. p. 289–298.

Thacker, J.O., Karlstrom, K.E., Crossey, L.J., Crow, R., Beard, L.S., and Dorsey, R.J., 2017, Hypothesis for post-Bouse distributed deformation of the lower Colorado River corridor, *in* Reynold, R.E., ed., Going LOCO: Investigations along the Lower Colorado River—2016 Desert Symposium Field Guide and Proceedings: Northridge, California State University Desert Studies Center, p. 158–164.

Thacker, J., Karlstrom, K., Crossey, J., Crow, R., Cassidy, C., and Beard, S., 2018, Syn- and post-6 Ma deformation of the Bouse Formation: Implications for lower Colorado River tectonism and Bouse deposition: Geological Society of America Abstracts with Programs, v. 50, no. 5, https://doi.org/10.1130/abs/2018RM-313695.

Tidball, E.C., 2004, Soldier-Artist of the Great Reconnaissance, John C. Tidball and the 35th Parallel Pacific Railroad Survey: Tucson, Arizona, University of Arizona Press, 226 p.

Tosdal, R.M., 1990, Tectonics of the Mule Mountains thrust system, southeast California and southwest Arizona: Journal of Geophysical Research, v. 95, p. 20,025–20,048, https://doi.org/10.1029/JB095iB12p20025.

Tosdal, R.M., and Wooden, J.L., 2015, Construction of the Jurassic magmatic arc, southeast California and southwest Arizona, *in* Anderson, T.H., ed., Late Jurassic Margin of Laurasia—A Record of Faulting Accommodating Plate Rotation: Geological Society of America Special Paper 513, p. 189–221, https://doi.org/10.1130/2015.2513(04).

Turak, J., 2000, Re-evaluation of the Miocene/Pliocene Depositional History of the Bouse Formation, Colorado River Trough, Southern Basin and Range (CA, NV, and AZ) [M.S. thesis]: Laramie, University of Wyoming, 96 p.

Walker, B.A., Jr., Miller, C.F., Claiborne, L.L., Wooden, J.L., and Miller, J.S., 2007, Geology and geochronology of the Spirit Mountain batholith, southern Nevada: Implications for timescales and physical processes of batholith construction: Journal of Volcanology and Geothermal Research, v. 167, p. 239–262, https://doi.org/10.1016/j.jvolgeores.2006.12.008.

Ward, P.L., 1991, On plate tectonics and the geologic evolution of southwestern North America: Journal of Geophysical Research, v. 96, no. B7, p. 12,479–12,496, https://doi.org/10.1029/91JB00606.

Wells, M.L., and Hoisch, T.D., 2008, The role of mantle delamination in widespread Late Cretaceous extension and magmatism in the Cordilleran orogen, western United States: Geological Society of America Bulletin, v. 120, p. 515–530, https://doi.org/10.1130/B26006.1.

Wells, R.E., and Hillhouse, J.W., 1989, Paleomagnetism and tectonic rotation of the lower Miocene Peach Springs Tuff—Colorado Plateau to Barstow, California: Geological Society of America Bulletin, v. 101, p. 846–863, https://doi.org/10.1130/0016-7606(1989)101<0846:PATROT>2.3.CO;2.

Wernicke, B., 1985, Uniform-sense simple shear of the continental lithosphere: Canadian Journal of Earth Sciences, v. 22, p. 108–125, https://doi.org/10.1139/e85-009.

Wernicke, B., 1992, Cenozoic extensional tectonics of the U.S. Cordillera, *in* Burchfiel, B.C., Lipman, P.W., and Zoback, M.L., eds., The Cordilleran Orogen: Conterminous U.S.: Boulder, Colorado, Geological Society of America, Geology of North America, v. G-3, p. 553–582.

Wernicke, B., and Axen, G.J., 1988, On the role of isostasy in the evolution of normal fault systems: Geology, v. 16, p. 848–851, https://doi.org/10.1130/0091-7613(1988)016<0848:OTROII>2.3.CO;2.

Wernicke, B., Walker, J.D., and Beaufait, M.S., 1985, Structural discordance between Neogene detachments and frontal Sevier thrusts, central Mormon Mountains, southern Nevada: Tectonics, v. 4, no. 2, p. 213–246, https://doi.org/10.1029/TC004i002p00213.

Wernicke, B., Axen, G.J., and Snow, J.K., 1988, Basin and Range extensional tectonics at the latitude of Las Vegas, Nevada: Geological Society of America Bulletin, v. 100, p. 1738–1757, https://doi.org/10.1130/0016-7606(1988)100<1738:BARETA>2.3.CO;2.

Wilson, J.M., McCarthy, J., Johnson, R.A., and Howard, K.A., 1991, An axial view of a metamorphic core complex: Crustal structure of the Whipple and Chemehuevi Mountains, southeastern California: Journal of Geophysical Research, v. 96, no. B7, p. 12,293–12,311, https://doi.org/10.1029/91JB01003.

Wooden, J.L., and Miller, D.M., 1990, Chronologic and isotopic framework for Early Proterozoic crustal evolution in the eastern Mojave Desert region, SE California: Journal of Geophysical Research, v. 95, no. B12, p. 20,133–20,146, https://doi.org/10.1029/JB095iB12p20133.

Wooden, J.L., Barth, A.P., and Mueller, P.A., 2012, Crustal growth and tectonic evolution of the Mojave crustal province: Insights from hafnium isotope systematics in zircons: Lithosphere, v. 5, p. 17–28, https://doi.org/10.1130/L218.1.

Wright, J.E., Howard, K.A., and Anderson, J.L., 1987, Isotopic systematics of zircons from Late Cretaceous intrusive rocks, southeastern California; Implications for a vertically stratified crustal column: Geological Society of America Abstracts with Programs, v. 19, p. 898.

Yarnold, J.C., 1993, Rock-avalanche characteristics in dry climates and the effect of flow into lakes: Insights from mid-Tertiary sedimentary breccias near Artillery Peak, Arizona: Geological Society of America Bulletin, v. 105, no. 3, p. 345–360, https://doi.org/10.1130/0016-7606(1993)105<0345:RACIDC>2.3.CO;2.

Yin, A., and Dunn, J.F., 1992, Structural and stratigraphic development of the Whipple-Chemehuevi detachment fault system, southeastern California: Implications for the geometrical evolution of domal and basinal low-angle faults: Geological Society of America Bulletin, v. 104, p. 659–674, https://doi.org/10.1130/0016-7606(1992)104<0659:SASDOT>2.3.CO;2.

Zimbelman, J.R., and Williams, S.H., 2002, Geochemical indicators of separate sources for eolian sands in the eastern Mojave Desert, California, and western Arizona: Geological Society of America Bulletin, v. 114, no. 4, p. 490–496, https://doi.org/10.1130/0016-7606(2002)114<0490:GIOSSF>2.0.CO;2.

Manuscript Accepted by the Society 4 June 2019

Printed in the USA